Role of Rab GTPase proteins in cell wall deposition and potential use of *rabA* mutants in bioenergy crops

Daniel Lunn BSc MRes

Thesis submitted to the University of Nottingham for the degree of Doctor of Philosophy

August 2013

Abstract

It has long been known that fossil fuels are a finite source of energy. With this in mind research has turned to the development of renewable energy sources. One solution is the conversion of biomass to useable energy sources. These resources are located in the cell walls of currently available agronomic crops in the form of complex biopolymers, lignocelluloses, which are highly recalcitrant. In the following thesis I explore the novel mechanism of impacting cell wall composition using mutants involved in trafficking to the cell wall. The following work shows that Rab GTPase mutants impact on cell wall deposition, with specific sub-clades impacting particular cell wall polymers. I then go on to show these mutants have significant effect on recalcitrance and thus increase saccharification of the biomass, without impacting on agronomic properties. Finally I go on to show the same impact on cell wall composition in a presumed orthogolous Rab in tomato. These findings all have significant implications in the fields of intracellular trafficking, cell wall biology and bioenergy.

Acknowledgements

I would like to thank both my supervisors, Dr Grantley Lycett and Professor Gregory Tucker for giving me this excellent opportunity to study trafficking processes in cell wall deposition, with the added bonus of dealing with a topic of global economic importance. Their knowledge and skills have been vital in guiding me through this crucial period of my early career.

I give my thanks to all the members of both Tucker and Lycett group who have provided me with essential technical and intellectual knowledge throughout this period.

I would also like thank my wife for all the emotional support she has given me during the ups and downs of associated with studentship.

Finally I would thank the University Of Nottingham and BBSRC for providing the infrastructure and funding for the following project.

Contents

Figures

Key abbreviations

Arf GTPase =ADP ribosylation factor

AIS = Acetone insoluble solid

CDTA = 1,2-cyclohexanediaminetetraacetic acid

EtOH = Ethanol

FT-IR = Flouier transform infrared spectroscopy

G4 antisense = Antisense line developed for inhibition of Rab11a

HPAEC = High performance anion exchange chromatography

HPLC = High performance liquid chromatography

KOH = Posstium hydroxide

Na_2CO_3 = Sodium Carbonate

Rab GTPase = Ras like binding protein

RT = Room temperature

T-DNA = Transfer DNA

1 Introduction

1.1 Bioenergy current position, prospective and challenges

An increasing demand globally for finite fossil fuels and concern over greenhouse gas emissions from their combustion has led to justification of increased bioenergy research. In particular, bioenergy is seen as an alternative to petroleum, for road transport networks. Traditionally bioenergy was considered expensive and uneconomical; however ever rising oil prices have moved the balance of this debate in favour of bioenergy (Pauly and Keegstra 2008). This argument is particularly popular in Europe where bioenergy is seen a route to reduce CO_2 emissions, while increasing energy supply security through decreasing oil dependency (IEA 2009). Bioenergy is defined as renewable energy produced from biological sources. There are currently three main fuels in bioenergy, bioethanol, biogas and biodiesel, which are referred to as the bioenergy platforms. Currently biofuel falls into two generations. The 1st generation focuses on biofuel production from sugars, starch and vegetable oil, while the 2nd generation focuses on production of biofuel from lignocellulosic material (Sims *et al., 2010)*.

1.1.1 1st Generation biofuel

In the production of 1st generation biofuel, feedstocks are used to create three types of liquid biofuel, biogas, biodiesel and bioethanol. The production of biogas is through the fermentation of waste products using various biological organisms, biodiesel is the production of fuels through the mixture of oil from plant seeds and diesel and bioethanol is produced through the fermentation of starch and sugars. Bioethanol is the dominant form of bioenergy in the USA and Brazil produced from corn and sugar cane respectively and account for 75% of their biofuel. In Europe however biodiesel is the dominant biofuel, with Europe producing 54% of the worlds' total produced mainly from oil seed rape. The technical details of production of these resources are extensive, with Yuan *et al* (2008) giving a comprehensive review of the process. The production of 1st generation biofuel in particular in the US and Brazil is set to rise with an expected 45% increase in production from 2009-2014 (IEA 2009). Combined with 2nd generation methods (discussed below) biomass is expected to comprise around 10% of the global energy share by 2050 (IEA 2012). Despite this however the sustainability of 1st generation biofuel has been brought into question. There are three main problems with 1st generation biofuels the main argument being that bioenergy crops occupy land which is crucially required for food security (Gnansounou 2010). Many authorities agree with the argument, despite bioenergy feedstocks accounting for only 2% of global arable land. It is also

13

thought that some 1st generation biofuels have been the major contributor to increases in world commodity prices although literature values are disputed with estimates ranging from 15-25% of total food increase (Chakrabortty 2008). Another area of debate is the effect 1st generation biofuels have on CO_2 emissions. In Brazil in particular bioethanol production has been considered a major factor in transforming petroleum based economies to sustainable environment-friendly economies (Yuan *et al.*, 2008), however recent reports such as that from the OCED (2008) have brought these claims into dispute by giving a varied net greenhouse gas emission once land use change has been factored into account. Regardless of these uncertainties it appears 1st generation biofuel production will increase however with the EU imposing a limit of 5% of energy production from 1st generation bioenergy by 2020 (European Commission 2013), alternative biomass sources must be found.

1.1.2 2nd Generation biofuel

Mounting concerns about the sustainability of bioenergy crops and food security have stimulated focus on using non-food biomass. These 2nd generation feedstocks focus on using lignocellulosic biomass to create biofuel (Somerville 2007). Production of 2nd generation biofuel targets the rich vein of resources contained in the plant cell wall. Currently 2nd generation bioenergy crops are not deployed due to two reasons. The plant cell wall is a strong and

rigid structure and is inherently resistant to deconstruction. Second this causes the requirement for an energy intensive pre-treatment to allow access to hemicellulosess and cellulose before the enzyme hydrolysis step in the production process (McCann and Carpita 2008). Also the high level of enzyme required for this saccharification is also economically prohibitive, with the enzymes required to depolymerase cellulose and hemicelluloses to fermentable sugars costing between 40-100 times more than those required to convert starch into sugar (Merino and Cherry 2007). One focus of 2nd generation bioenergy I research is on cell wall manipulation and pre-treatment. The goals of cell wall manipulation are the alteration of the wall to allow hydrolysis of the resources contained within, with the ultimate objective of engineering a wall which can be hydrolysed without requirement for any pre-treatment (Li *et al.,* 2010; Brown *et al.,* 2011; Halpin *et al.,* 2011). Another line of research focuses on the pre-treatments themselves and their optimisation. This research requires balancing of their optimisation with the cost of production, to retain economic viability (Ibblet *et al.,* 2010; Greenham *et al.,* 2012). Plant cell walls contain the most abundant renewable biopolymers on the planet. Currently only 2% of this resource is used by humans (Pauly and Keegstra 2010). The plant cell wall contains cellulose and hemicellulosess which contribute between 40.6-51.2% and 28.5-37.2% of the cell wall respectively (Pauly and Keegstra 2008). The difficulty arises from the complex fibrils which cellulose forms, which are surrounded by the matrix of other cell wall components (Carpita and McCann 2008). Despite the multitude

of cell wall types present throughout the organism, the main components remain the same and the machinery to build them is often highly conserved (Suzuki *et al.*, 2006), further entrenching their perspective use as feedstock. However, the exact compositional percentages do greatly differ depending on the original feedstock. For example the primary and secondary cell wall vary greatly in percentage composition and in the predominant monomers used in their creation of their polymeric compounds (Carpita and Gibeaut 1993; Brett and Waldron 1996). The potential of 2nd generation biofuel could certainly aid the overall strategy of CO_2 emission reduction and provide the alternative to non-renewable fuels. However, the technology is still in its infancy and many difficulties must be overcome, before an economically viable 2nd generation biofuel is in production.

1.1.3 Breaking down the wall

A key objective for 2nd generation bioenergy is making a cell wall which could undergo hydrolysis without the need of pre-treatment, or at least with reduced severity of that pre-treatment. This has sparked interest in altering the highly conserved pathways for cell wall synthesis and improving the efficiency of pre-treatment methodologies. Research has attempted to reach this objective through alteration of deposition and through increasing solubility of cell wall components, using the addition of expansins and the altering of pectin and hemicellulosess side chains being prominent examples.

16

Expansins are thought to disrupt the cellulose microfibrils to allow for better cellulase access (Cosgrove 2001a and b). In the case of pectin, glycanases have been altered to increase the number of side chains allowing increased water binding to increase hydrolysis (Ulvskov *et al* 2005). A similar method has been reported with hemicellulosess, whereby the addition of side chains causes a decrease in hydrogen bonding, thus lowering the structural rigidity of the cell wall (Fry *et al* 1992). The challenge however with use of genetic manipulation, is that much is still to be learned about the cell wall and this knowledge underpins the concept of cell wall alteration for increased hydrolysis. Added to these arguments are the problems inherent with genetic manipulation. Through the natural world organisms have developed in such a way which allows for survival and the cell wall is far from an exception to this rule. The cell wall alteration will have to allow for better access to the cell wall material, while maintaining cell wall function. The cell wall structure and composition have evolved with two main functions; to protect the organism from attack by microbes and to provide mechanical strength and allow for growth (Sarkar *et al.*, 2009). Due to these crucial biological functions, genetic manipulation leading to biochemical alteration in the cell wall will have to be subtle enough to maintain biological function, while altering structure in such a way as to increase hydrolysis.

From an economic stand point, the biggest challenge to overcome is that 2nd generation bioenergy feedstocks require pre-treatment to allow access to the

sugar components, thus greatly increasing production cost (Yang and Wyman 2008). There are four different types of pre-treatment currently classified into biological, physical, chemical and physiochemical. Efforts in biological pre-treatments are usually centred on the use of different cellulase enzymes and the engineering of an optimal enzyme with which hydrolysis can be conducted (Kumar and Wyman 2009). With physical pre-treatment milling, mixing and heating are all used to create an optimum based around energy conversion through the process. Use of physical pre-treatment is often discarded because energy outputs are often less than the energy input required (Brodeur *et al.*, 2011). With chemical and physiochemical pre-treatments the situation becomes more complicated with both having a sub set of methods. Chemical pre-treatments mostly focus around acid and alkaline incubation steps. Alkaline pre-treatment involves incubating biomass with a particular base and incubating at an optimum temperature for a specific time period. The alkaline degrades the ester and glycosidic side chains altering the structure of lignin and causing partial decrystallisation of cellulose (McIntosh and Vancov 2010). The near complete removal of lignin allows more efficient enzyme hydrolysis, for example in wheat straw sodium hydroxide pre-treatment for 144 hours and 20°C resulted in 60% lignin and 40% hemicelluloses release from the biomass (Sun *et al.*, 2005). Alkali pre-treatment methods are often expensive, which has led to the use of lime as an alkali. The advantage of lime over other alkali pre-treatments is that lime costs are much lower in comparison to other alkalis and can be recovered through precipitation. Acid pre-treatment uses

18

dilute acids prior to hydrolysis. The key advantage of acid pre-treatment is that often fermentable sugars from hemicelluloses can be yielded from the pre-treatment (Carrasco *et al* 1994). There are two main physiochemical pre-treatments used, steam explosion and liquid hot water. Steam explosion uses high pressure and temperatures for a short period of time, disrupting the structure of fibrils. A few key advantage of this method are that relatively large particle sizes of biomass can yield high amounts of sugar concentrations and importantly removing the requirement of expensive physical treatment such as milling prior to the chemical pre-treatment. Another advantage of steam explosion is the method can be mixed with chemical pre-treatments, most commonly acids or alkali to make a two-step process. This two-step approach is the basis for the second most commonly used physiochemical pre-treatment, liquid hot water (LHW). This process aims to completely solubilise the hemicellulosess fraction, producing a hemicellulosess rich liquor and cellulose rich residue. This process aids hydrolysis by turning the matrix, hemicellulosess and lignin component into a solute, which can then be removed (Yano *et al* 2010). The advantage of this method is reduction in enzyme required and time taken in the hydrolysis step.

Both genetic engineering and pre-treatment optimisation are crucial to the economic viability of 2nd generation biofuel. However, it is unlikely that a single solution will be found. For these reasons development, and the combination of, biochemical manipulation, through genetic engineering and a

specific pre-treatment, are going to be needed for a roadmap for conversion of a specific feedstock to be formulated.

1.2 Cell wall composition and biosynthesis

1.2.1 Cell wall function

Cell wall composition and structure has evolved to fit specific roles and functions through the diverse plant kingdom. The evolution of the cell wall in plants is a literature review in itself and will only be briefly covered here. A comprehensive review has been conducted by Sarkar *et al* 2009. The plant cell wall is believed to have evolved to defend from herbivory. The sessile nature of plants requires them to have strong defence mechanisms, to deal with animal, fungal, bacterial and viral attack. It was originally thought that the cell wall was originally designed to deal with autotrophic life. Thus as the plant increased their uptake of hypotonic solutions, so this would lead to increased osmotic pressure, which in turn would threaten cell integrity. However, through the formation of a polysaccharide rigid wall, mechanical support is provided and prevents cell rupture (Raven *et al* 2005; Taiz and Zeiger 2006). The next step in the evolution of the wall, came from the movement from water to a land environment, this coupled to an increase in height, led to a position in which some parts were without either sufficient water, or

atmospheric gases (Duchese and Larson 1989). This led to the establishment of a vascular system. In terms of cell wall evolution this was coupled with the formation of a primary and secondary cell wall. These two layers are both functionally and biochemically different. The primary cell wall has a role in stability during the cell growth periods, whereas the secondary cell wall is deposited after growth and provides mechanical strength (Harris *et al* 2005). The differences between various hemicelluloses and pectin epitopes are most profound between primary and secondary cell wall and this is also true for quantity (Popper and Fry 2004). The increase of hemicelluloses particularly in the secondary cell wall is said to be indicative of their function in mechanical support (Harris *et al.*, 2005). However, two groups have shown that disrupting hemicelluloses biosynthesis has produced plants with only minor phenotypic alterations (Brown *et al.*, 2005; Cavalier *et al.*, 2008), questioning hemicelluloses roles in mechanical strength. The evolution to flowering again diversified the nature of cell wall composition. This gave rise to specific types of wall, reflecting the diverse tissue composition. All flowering plants have cellulose microfibrils with xylan and pectin epitopes however the lignin of angiosperms differs from that of gymnosperms. Gymnosperm secondary cell walls differ in regards to lignin composition only containing guaiacyl, while angiosperms contain guaiacyl and syringyl units with both containing p-hydroxyphenyl. Fruits and flowers do not have secondary cell walls. However, they do contain high levels of pectin, which is thought to be because they can be more easily modified during maturation (Rose *et al.*, 2003). Flowering

plants also can have silica components in their cell walls, in the forms of trichomes, spines and thorns which are effective in deterring herbivores (Raven 2005). The cell wall structure of grass is very different from that of angiosperms and lower plants. Unlike taller tree plants, grasses focus of rapid growth, over mechanical strength for this end they do not require high amounts of xyloglucan in the primary wall (Sarkar *et al* 2008). From this brief overview it is clear, that cell walls have increased in complexity with evolutionary distance, importantly giving an adapted cell wall fit for specific environments and tissue types.

Despite the dynamic nature of the wall, biochemically it is compositionally basic being formed from cellulose microfibrils which are then stabilised within a hemicelluloses and pectin matrix. The spaces in between the matrix can be filled with lignin. These four components form the basis of every cell wall type. In the next four sections of this chapter, the structure and biosynthesis of each of these cell wall components is explored in more detail.

Finally from this information any modification in terms of cell wall structure would have to be tissue specific and thus gene expression patterns in one tissue may not impact the pathway in another. As stated previously, alteration to the cell wall is one of many potential solutions to the challenge of cell wall digestibility. However, before targets for alteration can be determined, the structure and biosynthesis must be considered. Without this knowledge, the

specific task of alteration without compromising structural integrity could not occur.

1.2.2 Cellulose

As stated above the cell wall is formed from four basic components. The main component of these is cellulose, which is also the most abundant biopolymer in nature. Cellulose is common in both the primary and secondary cell wall and is considered vital for load bearing and determining the orientation of cell expansion (Taylor 2008). The structure of cellulose is simple, consisting of β1-4 linked unbranched glucan chains. Each glucose residue is added 180° to the last, forming a unit known as cellobiose. Through addition of multiple cellobiose units they form a flat ribbon structure, this ribbon structure then links together through hydrogen bonds to make insoluble microfibril structures (Brett 2000).

Most of our current knowledge of cellulose biosynthesis comes from research undertaken on cellulose synthase. In 1999 Kimura *et al.*, discovered a hexameric rosette structure by freeze fracture of the plasma membrane. The rosette is 25-30nm in diameter and contains cellulose synthase activity. Currently the only identified proteins known to be part of the cellulose synthase complex are CesA proteins. In *Arabidopsis* CesA proteins have a conserved structure, containing eight trans-membrane domains. The amino-

terminal region contains a RING-type Zinc motif and four CxxC motifs. The central cytosolic domain contains progressive glycosytransferases. The cytosolic domain is highly conserved between all CesA proteins (Saxena *et al* 2001). Genomic analysis of these genes, show they fall into gene pairs, with seven pairs and a single gene. Both members of a gene pair are expressed concurrently. Although there is no evidence for the reason behind this, there are two theories. Firstly, that the genes are redundant and this protects against a loss of function mutation and secondly that concurrent expression is required to produce the required amount of protein product (Djerbi *et al* 2005). Studies undertaken using co-immunoprecipitation show that three CesA proteins form a CesA complex. The primary cell wall requires CesA1, 3 and 6, whereas the secondary cell wall requires CesA4, 7 and 8 (Desprez *et al* 2007). These data correlate well with visual electron micrograph data, which have shown whole complexes being transported via vesicles (Haiger and Brown 1986). The reasons for the CesA gene products forming a complex in this manner are unknown. However, it has been postulated that they could form hexameric complexes which would be highly efficient for synthesis. However, this is not supported by experimental data, only the observation that 36 chains are produced per complex (Arioli *et al* 1998). Although work into cellulose biosynthesis has made considerable progress two crucial questions remain unanswered, how does having only one site per complex allow for the 180° rotation between residues and what are the roles of each *CesA* protein in the process?

24

1.2.3 Hemicelluloses

Around the cellulose backbone of the cell wall, forms a matrix of cross linked hemicelluloses and pectin. Hemicelluloses is structurally more complex than cellulose, with several different backbone and sugar side chains forming many different epitopes. The majority of hemicelluloses backbones are formed from three sugars, glucose, xylose and mannose, withβ-(1$\rightarrow$4) linkages normally predominating. These backbone chains are then converted to, for example xyloglucan, glucuronoarabinoxylan and galactomannan through side chain addition (Scheller and Ulvskov 2010).

Work on hemicelluloses biosynthesis has proved difficult, because proteins involved in hemicelluloses synthesis often do not solubilise in detergent in an active form, which makes them difficult to characterise. The class of enzymes responsible for hemicelluloses synthesis was discovered through identification of candidate proteins that show resemblance to CesA. The first candidate genes were identified by transcriptomics and proteomics. Using sequence tag data, Dhugga *et al.*, (2004) identified a cellulose synthase-like (Csl) member with the ability to synthesis mannose backbones. This gene was named *ManS* from which the CesA-like (Csl) family was described (Pear *et al.*, 1996). A few members of the Csl family were found to have glucomannan synthase activity (Liepman *et al.*, 2005). The candidate synthase for the xyloglucan backbone is

currently unknown. More significant advances have been made with the identification of the enzymes responsible for the side chain decorations, because these solubilise in detergents, allowing for fractionation and characterisation. This has led to the identification of the galactosyltransferase (GalT), frucosyltransferase (FucT) enzymatic activities and a GalT like mutant *mur3* that transfers a galactosyl residue onto a xylose in xyloglucan (Edwards *et al.*, 1999; Perrin *et a.*, 1999; Vanzin 2002). The genome sequence data for *Arabidopsis* shows an over representation of *GalT* sequences compared with amount of expression of galactomannan. Thus the hypothesis has been made that some GalT proteins may have xylosyltransferase activity (Faik *et al* 2002). For the reasons stated above obtaining experimental data on hemicelluloses synthesis has proven difficult and thus there is a lack of information in the literature.

1.2.4 Pectin

Pectin is the most structurally complex of all the cell wall polysaccharides. Pectin is crucial in the formation of the primary secondary wall and the middle lamella. Pectin polymers are formed from a α1-4 linked galacturonic acid backbone, (Mohren 2008). The main domains of pectin are homogalacturonan (HG), rhamnogalacturonan I and II and xylose substituted galacturonan. The most abundant domain is HG, making up about 65% of the total pectin. It is also the most simple, being composed almost entirely of galacturonan

residues (O'Neill et al., 1990). In transit to the cell wall HG is in a highly methyl-esterified state (Zhang and Stathelin 1992). The second most abundant domain is rhamnogalacturonan I, comprising of between 20-35% of the total content. This domain has a repeated backbone of α-D-GalA-1,2-α-L-Rha-1-4-. There is also a wide variety of branched side chains which can be added to this backbone. These are primarily galactans or arabinogalactan chains. For this reason pectin is thought to carry out specific functions dependent on its domain structures (Ridley et al., 2001). Rhamogalacturonan II. Is the most structurally complex of all the pectin domains. It can constitute up to 10% of the pectin and is highly conserved across the plant kingdom. The backbone consists of eight α1,4 linked galacturonic acid residues. The backbone then has many additional side branches with 12 types of sugar in 20 different linkages (O'Neill et al., 2004). There are two other types of substituted galacturonan, xylogalacturonan (XGA) and apiogalacturonan (AP). The structure of XGA is HG with a β-linked xylose substituted at O-3 and the structure of AP is a HG with a D-apiofuranose residue substituted at O-2 and O-3 positions. They are both highly restricted in their expression and so are considered to be functionally specific (O'Neill et al., 2004).

A crucial question in understanding pectin deposition is how pectin may be linked into the wall. However, there is no current consensus about how this occurs. The only data available by Nakamura in 2002 used enzymatic degradation to show evidence of cross linkage with hemicellulosess. Pectin

biosynthesis is also still an evolving research area. There have been a variety of experiments carried out which show pectin is synthesised in the Golgi with co-synthesis occurring in the Golgi stacks. Transport then occurs by membrane bounds vesicles, along actin filaments (Nehbenfuhr and Staehelin 2001). Evidence so far shows that pectin is synthesised in the Golgi lumen. This is thought to occur by glycosyltransferase (GTs) activity which transfers glycosyl residues from nucleotide sugars to their polysaccharide acceptors (Abdel-Massih *et al.*, 2003). It is widely accepted that upon arrival at the cell wall HG is completely methylesterified. It is then de-esterified this conversion is thought be linked with the halting of cell elongation (Goldberg *et al.*, 1996). There are predicted to be 67 GTs and methyltransferases, however because proof of enzyme activity is required, only four have been defined (Mohnen 2008). From the literature currently available it is reasonable to say that there are two main areas which should be focused on in pectin research, first the identification of structure and linkage of pectin with other cell wall components and second, on-going confirmation of biosynthetic enzymes involved in pectin synthesis.

1.2.5 Lignin

The synthesis of lignin was crucial in the evolution from an aquatic to a land environment, particularly through strengthening the stem. Lignin plays a role in protecting against pathogens and transport through the vascular system.

The definition of lignin as a biochemical compound is difficult due to the huge variety of structures which can be produced. However, lignin polymers are racemic aromatic heteropolymers usually derived from hydroxycinnamyl alcohol monomers with a varying degree of methoxylaton (Campbell and Sederoff 1996). Polymers of lignin are formed through a process called lignification. In this process the monolignol units are linked together via radical coupling. This forms a linkage between the β-O-4 position of the two monomers and thus an "end-wise" reaction couples the next monomer (Sarkanen and Ludwig 1971).

Biosynthesis of lignin is extremely complex, with branches in the pathway at all steps, which give rise to the diversity lignin shows in nature. The pathway starts with the deaminiation of phenylalanine, then from successive rounds of hydroxylation, gives rise to cinnamic acid, p-coumaric acid, p-coumaroyl-CoA, p-coumaraldehyde and finally p-coumaryl alcohol. At any point after the formation of p-coumaric acid branching of the pathway can occur, creating hydroxylation or methylation of a lignin precursor monomer which can then follow the standard pathway or itself be polymerised. With the advent of genetic databases the enzymes which catalyse these reactions are becoming ever more defined. However, co-factors and gaps still remain in the pathways, for an excellent review of lignin biosynthesis see Vanholme et al., 2010. After synthesis lignin precursors are transported to the cell membrane where enzymes are present to undertake the process of oxidation and

polymerisation. The method by which precursors are transported to the cell membrane however is currently unknown.

Deposition of lignin occurs at one of the final stages of xylem cell differentiation, during the secondary cell wall thickening. In this process there are three distinct layers, outer (S1), middle (S2) and inner (S3). At each stage lignin is deposited after the deposition of carbohydrates. Lignin is deposited in the middle lamella during S1 formation. During S2 formation lignin is deposited to fill in the gaps around the hemicelluloses, pectin matrix. Highest levels of lignin are deposited in S3 phase after the cellulose backbone and hemicelluloses matrix has been laid down (Roussel and Lim 1995). The orientation of lignin is dependent on the nature of the wall. In the primary cell wall lignin is formed into a spherical structure, while in the secondary wall, lignin aligns with the orientation of the microfibrils (Donaldson 2001).

1.3 Rab GTPase family

Whilst research has delivered a significant amount of detail on the biochemical pathways involved in cell wall metabolism the question of how the cell wall material is actually deposited within the cell wall is far less clear. Compartmentalisation requires tight control and organisation. To do this spatial localisation of many proteins is controlled by small GTP binding proteins. Through knowledge of studies conducted in yeast (*Saccharomyces cerevisae*) it is known that exocytic trafficking is controlled through the Ras-related binding proteins (Rab) and ADP ribosylation factor (Arf) GTPase families (Nielsen *et al.*, 2008). The Rab family in plants was first characterised using data mining techniques. This focused on identifying Rab specific residues, which occurred around the switch mechanism (Pereira-Leal and Seabra 2000). These proteins have the function of; regulating tethering factors and SNARE complexes, through the binding of GTP and cycling of GTP to GDP by hydrolysis (Pereira-Leal and Seabra 2002; Rutherford and Moore 2002), thus acting as a molecular switch for the docking of vesicles in the post Golgi network. The localisation of Rab proteins has been carried out through transport by Rep proteins, which work by GDP to GTP exchange. The localisation occurs through specific modification of cytosolic tails, each of which has a specific cysteine motif (Stenmark and Olkkonen 2001). Through hybrid data it was shown that a single Rab can have many effectors. As expected in such a crucial network some Rabs have been shown to be non-

essential and some are essential (Stenmark and Olkkonen 2001; Pereira-Leal
and Seabra 2002; Rutherford and Moore 2002).

1.3.1 Rab GTPase family

As stated earlier identification of Rabs was conducted using data mining
techniques. This was helped due to the high degree of conservation of these
genes across kingdoms. The initial focus was around five β-sheet structures,
the third of these structures stabilises the switch and makes the second
switch more accessible. This structure though is not Rab GTPase specific. Also
used was a C terminal double cysteine prenylation (Pereira-Leal and Seabra
2000; 2001). In 2002 Rutherford and Moore identified 57 Rab GTPase proteins
in *Arabidopsis*, 48 of these through expressed sequence tags and 9 through
data mining of loci which had Rab structural and functional motifs. Following
phylogenetic analysis these 57 Rabs have been split into 8 Rab clades, which
in turn have their own sub-clades. The compartmental target of these 8 clades
has now been elucidated however; prospective cargoes for subsequent sub-
clades have not been clearly defined with this process and trafficking is
thought to occur through bulk flow. The functions of the sub-clades are also
still poorly defined and the literature on specific genes is sporadic. The 8
clades of Rab run from A-H. The RabA clade is the most numerous clades. It
contains 6 sub-clade, they have currently been identified as aiding trafficking
between the Golgi and the endosomes. There is also evidence of interaction

with actin and the plasma membrane. The localisation of RabB and RabD were identified using GFP fusions, RabB is exclusive to the Golgi and RabD proteins aid cycling between the Golgi and endoplastic reticulum (ER). RabC and RabE are thought to be involved in trafficking from the endosome and the Golgi respectively however, their target is undefined. RabF and RabG both aid cycling from the endosomes, RabG targets the vacuole and the target of RabF proteins is currently unknown. Also of interest is the fact that in the RabF clade the C-terminal is not substituted with geranyl-geranyl phosphorylation in this case the C-terminus has undergone *N*-myristylation instead (Rutheford and Moore 2002).

1.3.2 Function of individual Rab GTPase genes

As discussed in the previous section many targets for the RAB-GTPases have still to be defined. However, there are some data on individual Rab proteins. These are focused mainly around three areas, tip growth, in the root hair and pollen tube, the interaction of Rab proteins with phosphate kinase proteins and Rab proteins in fruit ripening. There are also some studies which directly try to elucidate roles of Rab proteins. These isolated studies, will be discussed briefly here. The first of these studies found that RabD1 and 2 have differing roles in ER and Golgi transport (Pinhiero *et al.*, 2009). However, most importantly this highlighted one crucial feature of Rab proteins, redundancy. Although, it has long been thought that Rab proteins were redundant

(Rutherford and Moore 2002, Stenmark and Olkkonen 2001), it was particularly well highlighted here. The RabD2 clade contains 3 Rab genes. Loss of function in either of these proteins causes no phenotypic effect to the plant. However, loss of function of the entire clade is nonviable (Pinhiero *et al.*, 2009). This feature of Rab proteins has been one of the major problems which groups have had to overcome in the study of this area.

It has long been known that Rab proteins interact with various kinase proteins (Jordens *et al.*, 2005). This was particularly through the study done by Preuss *et al.*, 2006, in which RabA4b was found to bind phosphatidylinositol 4-OH kinase (PI-4Kβ1). Since then a number of other Rab proteins have been found to bind these kinases. This is due to the work conducted by Moore lab at Oxford. The work undertaken was attempting to elucidate interactions between RabE GTPases and phosphatidylinositol-4-phosphate 5-kinase 2 (PIP5K2). Work undertaken using GFP fusions had already shown localisation of RabE proteins and PIP5K2 in the Golgi, leading to the hypothesis that a possible interaction could occur. Using yeast 2 hybrid it was found that all the RabE clade would bind PIP5K2. In particular PIP5K2 would bind the active site of RabE1d. RabA2 and RabD2 proteins could also bind PIP5K2. It was further found that RabE1d increases phosphatidylinositol 4,5-bisphosphate (PtdIns(4,5)). This is to occur by the Rab activating PIP5K2 (Camacho *et al.*, 2009).

The most research which has identified particular functions for particular Rab proteins has been in the polar growth, of the root tip and pollen tube. These studies have shown RabA4 proteins to be of particular importance. This form of growth is known as "tip growth". In this process the cell becomes polarised and grows through elongation using the actin cytoskeleton (Szumlanski and Nielsen 2009). This was discovered using the long known guanine effector inhibitor brefeldin A. Use of brefeldin A halted growth in the root hair and pollen tube. Adding to this, during an active growth phase Rab4b has been shown to localise in the clear area of the root tip, using immunogold electron microscopy. In a quiescent phase this localisation no longer occurs. This is evidence for its activity in the growth of the root tip in *Arabidopsis* (Samaj *et al* 2006, Cole and Fowler 2006). This work led to another study in which, the pollen tube was analysed. Using RT-PCR RabA4d was found to be highly expressed in the pollen tube. *RabA4d* knockouts were found to disrupt the pollen tube, however no sterility was observed. To identify differences in the cell staining was used, which showed the position of pectin within the cell to have been affected (Szumlanski and Nielsen 2009). A recent study showed RabA2a to be present in the extracellular fluids of sunflower, which may indicate cell to cell communication through vesicle transport, similar to in yeast (Regente *et al.*, 2009) and RabA2's are believed to have a role in the symbiosis with *Rhizobium*. Legumes form symbiotic relationships with the nitrogen fixing bacteria *Rhizobium*. Once infected the plant cell wall begins to show invagination, trapping the bacteria. This invagination is caused by

polarisation of the cell wall and seemed to implicate the action of Rab genes. Expression of RabA2c and d in particular seemed to correlate with root hair initiation and expansion A study conducted by Bianco *et al.*, 2009 found that using RNAi to target the RabA2 genes in common bean, it was possible to halt the invagination. These data all point towards RabA2 and RabA4 genes having specific roles in cell wall formation and maintenance. The method by which Rabs affect orientation growth is through both interaction with the exocyst and Ca^{2+} signalling. The main evidence of this comes from treatment of root hairs with the ionophore A23187, which disrupts the Ca^{2+} signals. This is also linked to a dispersal of RabA4b away from the root hairs (Szumlanski and Nielsen 2009).

Studies of cell wall maintenance and plasticity highlight interesting targets for cell wall adaptations. Also studies in fruit ripening, particularly in tomato, have highlighted several target proteins. This work came through the desire to use polygalacturonase (PG) to reduce fruit softening. However, this proved to show the complexity involved in the cell wall, particularly when use of antisense transgenes designed to inhibit the synthesis of PG, showed little effects on fruit firmness (Sheehy *et al.*, 1988; Smith *et al.*, 1988). It was later found that tomato Rab1 proteins are strongly expressed in fruit. Later Rab8 and 11 were also found to be expressed in tomato fruit (Lorraine *et al.*, 1996; Zegzouti *et al.*, 1999). Using antisense transgenes for Rab11a in tomato, it was shown that PG and PE activities were both reduced in ripe fruit, and this was

accompanied by retention of fruit firmness (Lu *et al.*, 2001). Interestingly in *Arabidopsis* SlRab11a is homologous with the RabA1a, which adds further weight for a role in trafficking to the cell wall for this sub-clade. Further work in *Arabidopsis* showed that fluorescently labelled RabA2 and RabA3 were localised to the *trans*-Golgi network (TGN) (Chow *et al.*, 2008). Also preferentially expressed in fruit were the tomato Rab8 genes, these correspond to the *Arabidopsis* RabE clade (Lorraine *et al.*, 1996).

Currently the roles of most individual Rab proteins are yet to be identified. However, the trafficking routes of each clade, particularly in *Arabidopsis* are well established. From knowledge of the literature, it would appear that potential exists in the RabA and RabE clade for effecting trafficking of components to the wall.

1.3.3 Aims and objectives

The project will have the following aims:

- To produce an agronomically viable organism with increased recalcitrance without the need of pre-treatment.
- To tailor cell wall composition for bioenergy using single or multiple Rab GTPase mutants.

The objectives of this project are:

- To identify and isolate single gene knockouts of Rab GTPase proteins using tDNA insertion lines.

- To analyse the cell wall composition of these mutants using biochemical methods.

- To analyse the saccharification of these mutants as indication of recalcitrance.

- To do an in depth growth analysis of the mutants, as a test for agronomic viability.

2 Materials and Methods

2.1 Plant Material

2.1.1 Arabidopsis

Candidate Rab genes were identified using a screen of publically available microarray data through Genevestigator using the data of Zeef *et al* 2006 analysed by heat mapping. *Arabidopsis* stock lines with T-DNA inserts in the target genes were then ordered using the European *Arabidopsis* Stock Centre (NASC) services. The seed stocks obtained were sown on both plate and in pot were stratified to synchronise germination. This was done by incubation at 5°C for 3 days simulating a "winter" period. *Arabidopsis* Col-1 wild-type plants along with the T-DNA insert lines were grown over a 3 month summer period under glass in triplicate, each individual replicate was sown with a month interval. The glasshouse conditions were 22°C with 16 hour light, 8 hour dark period and light intensity of 150μmol $m^{-2}s^{-1}$. Plants were placed in a randomised block structure, with each replicate consisting of 50 plants pooled for cell wall analysis. For phenotypic analysis each replicate comprised of 10 plants

2.1.2 Tomato

Tomato plants, either wild type *Solanum lycopersicum* cv Ailsa Craig or the *SlRab11a* antisense line G4 (Lu *et al* 2001), were grown side by side under glass. Plants were grown on a mixture of M3, JI No3, perlite and vermiculite in a ratio of 6:6:1:1. Glasshouse conditions were maintained to give around 20°C and a 12hr minimum day period. Tomato fruit were tagged at anthesis and harvested at predetermined days post anthesis (DPA) or breaker, as determined by the first sign of colouration, was recorded and fruit harvested at predetermined days post breaker. Photographic visualisation of the phenotype was taken 40 days post breaker

2.2 Phenotype Analysis in *Arabidopsis*

2.2.1 Arabidopsis plate growth conditions

Analysis of early growth stages was conducted on seedlings germinated and grown on plates containing half MS media with sucrose at a concentration of 10mg ml^{-1}. Plants were grown in conditions of 16 hour light period, 8 hour dark period at 22°C.

2.2.2 Growth analysis on plate

Measurements of radicle emergence, cotyledon emergence, cotyledon opening, root length and numbers of lateral roots were taken for principal growth stage 0, 1 and R6 adapted from Boyes *et al.* (2001). Dates recorded were of radicle emergence and hypocotyl emergence for growth stage 0, cotyledons fully opened, 2 and 4 rosette leaves or growth stage 1 and 50% of seed having roots greater than 6cm in length for stage R6.

2.2.3 Stem growth analysis at senescence

Measurements of main bolt length, main bolt dry weight and number of side bolts were taken on *Arabidopsis* plant material grown in pot. Measurements were taken for second stage analysis adapted from Boyes *et al.* (2001). Measurements taken were recorded as main bolt length in cm, number of side bolts and main bolt dry weight in milligrams.

2.2.4 Leaf growth phenotype analysis

Measurements of early leaf emergence (on plate) and late leaf emergence (in pot) were taken on *Arabidopsis* plant material grown in pot. Leaf emergence was recorded as the point at which the second leaf had reached a length of

41

1mm from the time of sowing including stratification. Recordings were taken for every second true leaf (leaves not including the cotyledons) which had reached 1mm of length until the end of leaf emergence.

2.2.5 Seed and flowering development analysis

Measurements of first flower bud emergence and seed weight at harvest were conducted on *Arabidopsis* plant material grown in pot from stage R6 Boyes *et al*. (2001). The data for flower bud emergence was taken in number of days from sowing, with seed weight measured in milligrams at senescence.

2.2.6 *Arabidopsis* water content

Milled *Arabidopsis* senesced stem (particle size 700 microns) was weighed out and oven dried ($90^{o}C$) overnight to remove residual water content. Samples were then weighed and the difference between senesced and dry weight calculated.

2.3 Texture analysis

Texture was assessed using a TAXT-II texture analyser (Micro Systems), probe 6mm, speed 10mm/s, depression 4mm, data was recorded in Newtons. Texture analysis was performed four times, equally spaced around the equator of each fruit. These values were then averaged to give an overall firmness for each replicate. This process was conducted on triplicate fruit for all lines.

2.4 High throughput DNA extraction

This high throughput extraction method was adapted from Edwards *et al* (1991). Fresh leaf sample (1 leaf) was taken from a young plant and ground up in liquid nitrogen. Extraction buffer (400µl) consisting of 200mM Tris HCl pH 7.5, 250mM NaCl, 25mM EDTA, 0.5% SDS was added and mixed by vortex. The samples were incubated at 65°C for 15 minutes and then centrifuged at 16,300g for 10 minutes, before transferring the supernatant to a fresh microcentrifuge tube. The samples was mixed with isopropanol (300µl) and incubated at -20°C for 3 hours, before being centrifuged at 16,300g and the supernatant removed. The pellet was washed twice with 200µl 70% ethanol, and then allowed to air dry. The pellet was then suspended in 50µl dH$_2$O and stored at -20°C.

2.5 High purity DNA extraction

For high purity DNA fresh leaf sample was taken from a young plant and ground up in liquid nitrogen. Samples were then subjected to extraction using GenElute plant genomic DNA miniprep kit (Sigma Aldrich) following the manufacturer's instructions. During this protocol all centrifugation steps were carried out at 16,300g. Samples were subjected to lysis solution part A and part B and incubated at 65°C for 10 minutes. Precipitation solution was added and centrifuged for 5 minutes. Supernatant was placed in GenElute filtration column and centrifuged for 1 minute. Binding solution was added and mixed before being centrifuged for 30 seconds. The supernatant from the filtration column was added to the binding column and centrifuged for 1 minute. Wash solution with ethanol was added to the column and the column washed twice by centrifugation. Elution solution was then added and centrifuged for 2 minutes to precipitate DNA from the column.

2.6 High purity RNA extraction

Fresh stem was taken from a young growing plant and ground up in liquid nitrogen. In this protocol all centrifuge steps are conducted at 16,300g. The protocol used follows the manufactures instructions for the RNeasy Mini Kit

(Qiagen). Buffer RLT was added to samples and vortex mixed before being added to the QIAshredder spin column and centrifuged for 2 minutes. The supernatant was subjected to 0.5 volume of 96% ethanol and mixed through inversion. The sample was added to the RNeasy spin column and centrifuged, with the flow through discarded. Samples were subjected to buffer RW1 and centrifuged for 15 seconds and the flow through discarded. Samples were subjected twice to buffer RPE and centrifuged for 15 seconds and 2 minutes respectively and the flow through discarded. The spin column was then transferred to a collection tube and RNase free water added before being centrifuged for 1 minute to elute the RNA.

2.7 DNase treatment

RNA was subjected to DNase treatment with RNase free DNase (Promega). RNA was added to RNase free DNase, in a concentration of 1 unit/µg of RNA sample with RNase free DNase reaction buffer (400mM Tris-HCl pH 8.0, 100mM $MgSO_4$, 10mM $CaCl_2$) in a concentration of 10 volumes to the RNase free DNase and made up to 10µl with nuclease free water. Samples were incubated at 37°C for 30 minutes and then subjected to 1µl of DNase stop solution (20mM EGTA pH 8.0) and incubated again at 65°C for 10 minutes to inactivate DNase.

2.8 Complimentary DNA generation

RNA (1µg) obtained by the extraction method described (section 2.6) was taken and incubated at 70°C for 5 minutes. Samples were placed quickly on ice and 5 units of M-MLV reaction buffer (Tris-HCl 250mM pH 8.3, 375mM KCl, 15mM $MgCl_2$, 50mM DTT) and 200 units of M-MLV RT, with dNTP mix (10mM, 5µl) added with a final fill volume of 25µl with nuclease free water. Sample was then incubated at 37°C for 60 minutes.

2.9 Polymerase chain reaction

DNA or cDNA (0.5µg) was added to GoTaq Flexi Buffer (10µl), $MgCl_2$ (25mM 5µl), dNTP mix (10mM 1µl), GoTaq DNA polymerase (5units/µl) and upstream and downstream primers (1µM) and made up to 50µl with nuclease-free water. Samples were then incubated in a Mastercylcer PCR machine (Eppendorf) with the following cycling conditions.

- Initial denaturation, 95°C, 2 minutes, 1 cycle.
- Denaturation, 95°C, 1 minute.
- Annealing, temperature dependant on upstream and downstream primer, 1 minute.
- Extension, 72°C, 1 minute/1kb.
- Denaturation, annealing and extension were conducted for 30 cycles.

- Final extension, 72°C, 5 minutes 1 cycle.

- Soak, 4°C, indefinite, 1 cycle.

2.10 Gel electrophoresis

Gels were made using 1% agarose in 1X TBE (Tris, Boric acid, 0.5M EDTA pH 8.0) with ethidium bromide (0.5µg/ml). Gels were run with a buffer of 1X TBE at speed and length dependant on gel size and were imaged through Gel Doc system.

2.11 Fourier transform infrared spectroscopy

FT-IR was conducted using a Bruker, Tensor 2700 spectrophotometer, with 80cN-m torque applied to the sampler. Data was collected through the OPUS software, with zeroing of 128 scans of background before reading of sample. Samples were ball milled (particle size 700 microns) and read in triplicate with 128 scans per replicate. The data was then normalised using vector normalisation and base line corrected using the rubber band method.

2.12 Principal component analysis

Principal component analysis (PCA) was conducted using raw data for FT-IR in the region of 1200nm-800nm which is defined as the fingerprint region for sugar composition. Statistical analysis was conducted using Minitab, multivariate analysis programme.

2.13 Cell Wall Analysis

2.14 *Arabidopsis* acetone insoluble solid preparation

Milled senesced *Arabidopsis* stem (particle size 700 microns), was weighed out. The sample (5g) was homogenised using a pestle and mortar in 80% acetone (500ml). The homogenate was then filtered through nylon cloth using 80% acetone (500ml) followed by 100% acetone (500ml). The solid residue was then dried in a vacuum desiccator with phosphorus pentoxide. Acetone insoluble solid (AIS) material was stored at room temperature (RT) for future analysis.

2.15 Tomato acetone insoluble solid preparation

Fresh tomato pericarp (40g) was skinned, cubed and boiled at 80°C in 95% EtOH (100ml) for 30 minutes. The sample was cooled to room temperature, homogenised using a coffee grinder then then filtered through miracloth and washed successively with hot 85% EtOH (200ml), chloroform:methanol (1:1 v/v) (200ml) and 100% acetone until the run through became clear. Samples were then air dried overnight.

2.16 Determination of starch content of tomato

Starch content was assayed using Starch Assay Kit (Sigma SA-20). Starch was solubilised from AIS using the DMSO/HCl method. Sample (500mg) was incubated with 20ml DMSO and 5ml 0.8M HCl for 30 minutes at 60°C in a shaking water bath. The solubilised sample was then pH adjusted to pH 4.5 and made up to 100ml with dH_2O. Solubilised sample (1ml) was then added to starch assay reagent (1ml) and incubated at 60°C for 30 minutes. Tubes were cooled to room temperature and 200μl of sample was added to 1ml of glucose assay reagent and incubated for 15 minutes at room temperature. Absorbance was then measured at 340nm. Blanks were prepared as above for starch assay reagent, glucose assay reagent and all samples. Starch content was calculated by the follow equation:

A Total Blank = (A Sample Blank – A Glucose Assay Reagent Blank) + A Starch Assay Reagent Blank

ΔA = A Test – A Total Blank

Starch (mg) = (ΔA) (TVSA/SVSA) (TVGA/SVGA) (Starch MW) (F)/(ϵ) (d) (Conversion Factor for μg to mg)

= (ΔA) (2) (TVGA/SVGA) (162.1) (F)/(6.22) (1) (1000)

= (ΔA) (TVGA/SVGA) (F) (0.052)

TVSA = Total Assay Volume from Starch Assay

SVSA = Sample Volume from Starch Assay

TVGA = Total Assay Volume from Glucose Assay

SVGA = Sample Volume from Glucose Assay

Starch MW = 162.1 d = Light path (cm)

F = Dilution Factor from Sample Preparation

ϵ = Millimolar Extinction Coefficient for NADH at 340 nm

2.17 Cell wall extraction and fractionation of *Arabidopsis* and tomato

Ionically bound pectin was extracted from the AIS (500mg) by incubating in 50mM 1,2-cyclohexylenedi nitrilo-tetraacetic acid (CDTA) at a ratio of 5mg/ml for 6 hours at room temperature. The mixture was separated by centrifugation at 10,000g. The liquid fraction was removed by filtration and

the residue treated with 50mM Na_2CO_3 using the same volume as the CDTA overnight at 2°C. After which the second liquid fraction was removed by the same process as with the CDTA fraction. Both liquid fractions, containing the ionic and covalently bound pectin, respectively were then subjected to an uronic acid assay modified from Fillisetti-Cozzi and Carpita (1991) (section 2.13.5) and the results pooled. The remaining residue was fractionated into "hemicelluloses" and "cellulose" rich fractions using 1:20 residue to 4M KOH ratio, for 2h at 25°C. The KOH extracted material was adjusted to pH5.5 using acetic acid and precipitated with 80% acetone by centrifugation 10,000g and dried to give the hemicelluloses rich fraction. The residue was washed to neutral pH and dried to give the cellulose rich fraction. Recovery of each of these fractions was assessed gravimetrically.

2.18 Uronic acid assay for *Arabidopsis* and tomato

Uronic acid as a indicator of total pectin was assayed directly using a modified version of the Fillisetti-Cozzi and Carpita method 1991. Samples were centrifuged at 16,300g and debris free supernatant (300μl) taken and added to a test tube. Then 1 volume of Borax (2% NaCl, 3% boric acid) was added, followed by 5ml concentrated H_2SO_4. Samples were incubated at 70°C for 30 minutes. Samples were cooled at room temperature before adding 0.2ml 3-5 dimethyl phenol and then read at 400 and 450nm with the difference measurement recorded.

51

2.19 Total monomeric sugar analysis for *Arabidopsis* and tomato

2.20 Seaman Hydrolysis

Samples: (30mg) of either milled *Arabidopsis* stem (particle size 700 microns); pre-treated *Arabidopsis* stem residue: "hemicelluloses rich" fraction" or "cellulose rich fraction" were subjected to a two stage acid hydrolysis: initially with 1ml 12M sulphuric acid for 1 hour at 37°C. Samples were then diluted to 1M sulphuric acid and further incubated for 2 hours at 100°C. Samples were then subject to analysis by HPAEC.

2.21 High performance Anion Exchange liquid chromatography (HPAEC)

Samples from the acid hydrolysis (section xxx) were centrifuged at 16200g and the supernatant transferred to a fresh microcentrifuge tube giving a sample clear of debris. The sugar monomer content of the supernatant was determined by high-performance anion exchange chromatography with pulsed amperometric detection (HPAEC-PAD) (Dionex, UK) using a CarboPac

PA20 column with a 50mM NaOH isocratic system and flow rate of 0.5 ml/min at 30°C. Glucose, xylose, arabinose and galactose were used as standards with mannitol as internal standard.

2.22 Measurement Degree of esterification in tomato

Degree of esterification was measured by the reductive method (Klein *et al.*, 1995). AIS samples (200mg) were incubated overnight in 20ml 10mg ml^{-1} NaBH$_4$ in 50% ethanol and 50% NaOH (0.5%). Samples were then dried and washed 5 times with acetic acid and methanol at a ratio of 1:9 respectively and then 2 washes of methanol. Samples were dried and then dissolved in 67% H_2SO_4 and the unesterified pectin determined by the Fillisetti-Cozzi and Carpita (1991) in which a measurement is made of esterified and de-esterified pectin, to measure esterification the analogous reading was taken.

2.23 Lignin quantification in *Arabidopsis*

Lignin was quantified directly using a modified version of the acetyl bromide method of Fukushima and Hatfield (2004). Standards were made using 10mg of lignin (Sigma Batch #: 04414PE) dissolved in 80% dioxane. Aliquots were made ranging from 0.2-0.6ml in increments of 0.1ml. Acetyl bromide (0.5ml, 25%) was added and incubated at 50°C for 30 minutes. Samples were allowed

to cool and then 2.5ml acetic acid (25%), 1.5ml NaOH (0.3M), 0.5ml hydroxylamine HCl (0.5M) were added and the volume was made up to 10ml with acetic acid (100%). Milled *Arabidopsis* stem (particle size 700 microns), was weighed out to 100mg and 4ml acetyl bromide (25%) added. Samples were incubated for 3 hours at 50°C. Cooled samples were made up to 16ml *with* acetic acid (100%). An aliquot of 0.5ml of sample was taken and 2.5ml acetic acid, 1.5ml NaOH (0.3M) and 0.5ml hydroxylamine HCl (0.5M) added and 5ml of acetic acid (100%) added to give a final volume of 10ml.. Blank, standard and samples were read using a scanning UV spectrophotometer through the wavelengths of 250-400nm with lignin reading taken at 280nm.

2.24 Saccharification in *Arabidopsis* Stem

2.25 Pre-treatment of *Arabidopsis* stem biomass

Milled *Arabidopsis* stem (particle size 700 microns), was weighed to 250mg and placed in a glass reaction vial. Samples were incubated in a Monowave 3000 reactor (Anton Paar GmbH, Graz, Austria) set at 121°C and standard pressure for 10, 20 and 30 minutes with each of three treatment regimes, "dry"(no added solution), dH_2O and 1% H_2SO_4 at a ratio of 1:10. The liquor produced from the reaction was then removed by filtration and discarded. Residues from the dH_2O and 1% H_2SO_4 treatments were then separated from

the produced liquor by filtration and wash with two volumes of 100ml dH$_2$O. These residues were suspended in 2.5ml dH$_2$O and brought to pH5.4 by suspending using 2M NaOH. The residue was then placed in aluminium foil and dried overnight in an oven at 60°C and stored in an air tight plastic bag until used in the digestion assay.

2.26 Enzyme preparation for saccharification

A cellulase, from *Trichoderma Reesi* (Sigma Alderich), stock solution was made at a concentration of 10mg/ml in 50mM Na Citratre. The enzyme was dialysed against 2l of 50mM Na Citrate overnight at 4°C.

2.27 *Aradbidopsis* cell wall saccharification assay

Pre-treated or untreated *Arabidopsis* milled stem (100mg) was weighed out and 1ml of the cellulase enzyme stock (section 2.14.3) added to each sample. The sample mix was then made up to 10ml with 50mM Na citrate, giving a 10mg/ml sample to enzyme mix. Samples were then incubated at 55°C in a shaking incubator with mixing at 150rpm. Aliquots of 200μl were taken of the sample at time points 0, 2, 4, 6 and 24 hours.

2.28 *Arabidopsis* metal ion analysis

Milled *Arabidopsis* stem (particle size 700 microns), was weighed out to 100mg and added to reaction tubes. Samples were treated with 2ml HNO_3 (30%), 1ml H_2O_2 (1.45G) and 1ml ultra-pure H_2O independently. Samples were microwaved in a Multiwave 3000 platform with a 48-vessel 48MF50 rotor (Anton Paar GmbH, Graz, Austria). Samples were digested in perfluoroalkoxy (PFA) liners inserted into polyethylethylketone (PEEK) pressure jackets (Anton Paar, Hertford, UK) and digested at 1400W for 15 minutes, at ~140C and 20 bar for 3 hours. Reaction vials were opened and remaining liquid added to universal tubes and made up to 15ml with ultra-pure H_2O. An aliquot of 1ml was taken for analysis by ICP-MS (X-SeriesII; Thermo-Fisher Scientific; Germany).

2.29 *Arabidopsis* and tomato statistical analysis

Statistical analysis for the *Arabidopsis* studies was conducted using GenStat 14th Edition. Data for all analyses were subject to transformation to fit normality using the Log base 10 method. Raw data were subjected to analysis of variance (ANOVA) test to confirm differences between means and then with *post hoc* Tukey test, to test for difference between the wild-type and knockout lines, with significance being taken at $p < 0.05$.

All statistics used for work on tomato were conducted by means of t-test, using Microsoft Excel package, with significance being taken at p <0.05.

3 Rab GTPase target identification and knockout lines

The first challenge was to identify possible candidate genes, from the large Rab gene family. This process can be achieved partly through the known literature for Rab GTPase proteins. Although localisation experiments have shown Rab destinations through fluorescent tagging experiments, this still can leave researchers with a sub-clade of gene targets often numbering greater than 10 individual genes. Fortunately advances in genomic technologies have aided researchers greatly with a wealth of sequence, protein and expression data and in the case of *Arabidopsis* an expansive library of single and multiple gene knockouts, commonly available through public access databases. Access to these resources can allow researchers to identify target genes, which are expressed in a specific cell type at a specific time in a particular point in the life cycle of the organism. From these data it is possible to reduce large numbers of gene candidates to a more manageable number of targets for analysis. In the following chapter target genes will be identified from the RabA clade of the Rab family.

3.1 Microarray analysis of RabA clade

Using publically available data on Genevestigator, from work conducted by Zeef *et al* In 2005 and using accession numbers from *Arabidopsis* gene data

banks, expression data was compiled for each gene of the RabA clade in stem over a variety of stages of development. This large RabA clade is further spilt into six sub-clades, each of these sub-clades was analysed using their unique identifier code. Expression data acquired through the microarray analysis for this unique code was then presented in the form of a heat map. For ease of analysis each RabA sub-clade is displayed as its own heat map, these data are shown in figures 3-1 to 3-6. In all the following heat maps data are shown with one figure for each sub-clade, with the gene designation being displayed above the expression column. Expression values are shown by a blue colour, going from pale blue to dark blue as expression levels increase. At the time data mining was conducted Genevestigator had 6 levels of expression, levels 1 and 2 represent low level expression, levels 3 and 4 medium level expression and levels 5 and 6 high level expression.

These data shown in figure 3-1 are from the RabA1 sub-clade. The genes are displayed from RabA1a through RabA1i. In this clade RabA1d shows a high level of expression throughout all the tissue types analysed. Also highly expressed in inflorescence stem is RabA1b, whose expression decreases in rosette stem. Intriguingly RabA1e and RabA1g were shown to have no expression in the analysed tissue types.

RabA1 gene

Arabidopsis thaliana
├─ inflorescence
│   └─ stem
└─ rosette
    ├─ adult leaf
    ├─ hypocotyl
    └─ stem

Organ

a b c d e f g h i

0%   100%

Percent of Expression Potential
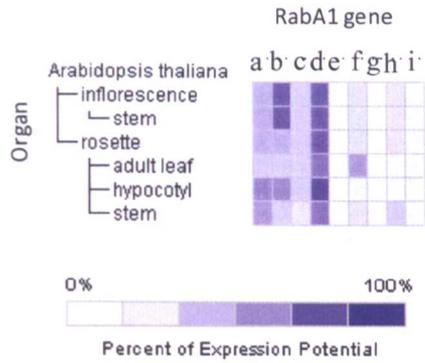
Figure 3-1 Microarray expression pattern of RabA1 mRNA in inflorescence and

rosette tissues

RabA1 gene expression levels shown as a percentage in the inflorescence and

rosette expressed as a percentage from 0-100% as shown by the expression

potential. Data show was obtained using Genevestigator.

Data in figure 3-2 show the expression of the RabA2 sub clade. This sub-clade

contains four genes designated A2a through A2d. Unfortunately in this data

set the database is incomplete only showing three (A2a, A2b, A2d) of the

genes in the sub-clade. Rab genes A2a and A2b show greatest level of

expression rosette stem. Expression data for A2d shows it having a low level

of expression throughout the tissue types assayed.

60
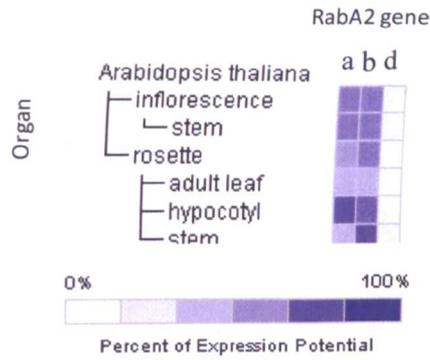
Figure 3-2 Microarray expression pattern of RabA2 mRNA in inflorescence and

rosette tissues

RabA2 gene expression levels shown as a percentage in the inflorescence and

rosette expressed as a percentage from 0-100% as shown by the expression

potential. Data show was obtained using Genevestigator.
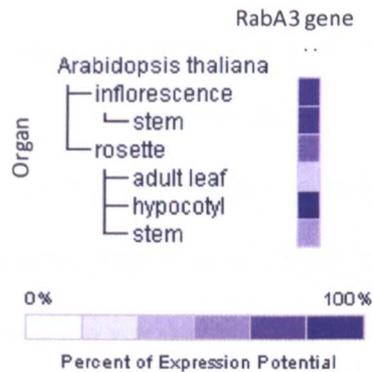
Figure 3-3 Microarray expression pattern of RabA3 mRNA in inflorescence and

rosette tissues

RabA3 gene expression levels shown as a percentage in the inflorescence and

rosette expressed as a percentage from 0-100% as shown by the expression

potential. Data show was obtained using Genevestigator.

61

Figure 3-3 shows the expression data of RabA3. This sub-clade contains one stand-alone gene, which has a high expression level in the inflorescence stem and a medium level of expression in the rosette stem, with the gene being most highly expressed in the hypocotyl.
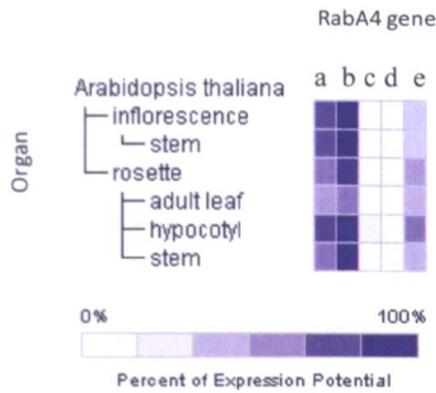
Figure 3-4 Microarray expression pattern of RabA4 mRNA in inflorescence and rosette tissues

RabA4 gene expression levels shown as a percentage in the inflorescence and rosette expressed as a percentage from 0-100% as shown by the expression potential. Data show was obtained using Genevestigator.

Data displayed in figure 3-4 shows the expression pattern of the RabA4 sub-clade. Noteworthy is that one gene RabA4d is not expressed in any of the tissue types assessed in the microarray, this is consistent with the literature, in which studies have shown this gene to be expressed only in pollen tube (Szumlanski and Nielsen 2009). Added to this, RabA4c has no expression in

62

the stem tissues, but does show slight expression in the hypocotyl. Of the genes in this sub-clade A4a and A4b are strongly expressed in every tissue type assayed apart from adult leaf where expression levels were of medium range. Gene RabA4e has a medium level of expression through the tissues analysed apart from in the hypocotyl.
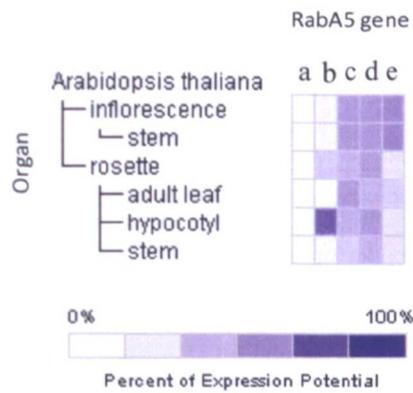

Figure 3-5 Microarray expression pattern of RabA5 mRNA in inflorescence and rosette tissues

RabA5 gene expression levels shown as a percentage in the inflorescence and rosette expressed as a percentage from 0-100% as shown by the expression potential.

Figure 3-5 shows expression data for the RabA5 sub-clade. Expression levels in this sub-clade were medium overall, with one gene, A5b having high expression in the hypocotyl. In the stem tissue types A5e had the highest expression of all the sub-clades.

RabA6 gene

Arabidopsis thaliana   a b
Organ
├─inflorescence
│   └─stem
└─rosette
    ├─adult leaf
    ├─hypocotyl
    └─stem

0%   100%

Percent of Expression Potential
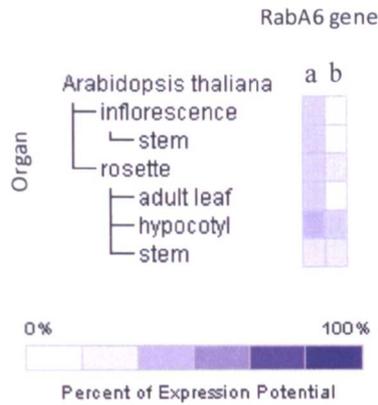
Figure 3-6 Microarray expression pattern of RabA6 mRNA in inflorescence and

rosette tissues

RabA6 gene expression levels shown as a percentage in the inflorescence and

rosette expressed as a percentage from 0-100% as shown by the expression

potential. Data show was obtained using Genevestigator.

Expression data for the RabA6 sub-clade is shown in figure 3-6. The data here

show a continuation of the trend from RabA5 with low expression pattern in

the tissues analysed. The highest expression in stem tissues for both of these

genes was a level 2 using the scale from Genevestigator.

From the data mined using Genevestigator a preliminary set of targets were

identified to be obtained from the Nottingham *Arabidopsis* Stock Centre

(NASC). These genes were as follows; for the RabA1 sub-clade, all genes apart

from A1e and A1g were selected; genes selected for RabA2 were all the genes

investigated through microarray analysis; RabA3 was chosen; RabA4 genes

A4a, A4b and A4e were selected and all genes in the RabA5 and RabA6 sub-

clades were selected. Unfortunately due to restrictions with the stock lines, it was not possible to obtain knockouts for A1f, A1h and any stock lines for the A5 and A6 sub-clade at the time of analysis.

3.2 Genotyping for homozygous T-DNA knockout lines

With target genes identified the next step was to obtain knockout lines for each gene. With the wealth of genomic resources in *Arabidopsis* knockout lines were already available and were obtained through NASC, details of each knockout can be found in appendix table 10-1. . However, these stock lines are not all homozygous for the gene insert and thus the first task was to identify a homozygous line for the relevant T-DNA insert using genomic PCR. The same strategy was used for each knockout line identified. Three PCR primers were designed for each of the T-DNA insert knockout lines. This is illustrated in figure 3.7. The forward (FP) and reverse (RP) primers were designed such that they would produce an amplicon of defined size from a wild type gene. The presence of the T-DNA insert however, would render PCR using these primers inoperative due to the increased size of amplicon. A third primer was designed that was complimentary to a sequence located within the T-DNA insert. This primer, used in conjunction with the RP primer would generate an amplicon of defined size only if a T-DNA insert were present in the target gene. These primers were used to identify homozygous plants, from a population grown from the NASC seed stock, by the application of 4

PCR experiments. In the first PCR the two primers -FP and RP- are used with wild-type *Arabidopsis* Col-1 DNA and would be expected to generate an amplicon of defined size from the target gene. The second PCR again uses wild type DNA but this time the primers are InP and RP. This serves as a control since no amplicon would be expected as there are no T-DNA inserts. The third PCR uses the FP and RP primers but this time with a DNA template from the specific knockout line. In this case the presence of a wild-type gene would still produce a band but no band will be produced if a T-DNA insert is present. In the final PCR the primers InP and RP are used with DNA from the specific knockout and would be expected to generate an amplicon from target genes containing a T-DNA insert. If however the insert direction is opposite to that shown in the example then InP would require the FP to produce a band. Thus for a homozygous T-DNA line the results would be that there were amplicons generated in the first and last PCR reactions showing the presence of wild type and T-DNA insert alleles respectively in wild type and knockout lines. There should be no amplicons generated in either the second or third PCR reactions showing the absence of T-DNA inserts in the wild type plant and the absence of a wild type allele in the knockout, respectively. Primer details for the genotyping are shown in appendix table 10-2.

Data shown in figure 3-8 presents the genotype of the selected parent plant for the *rabA1a* knockout line. In the first lane an amplicon is present between the 1 and 1.2kb size markers showing the presence of the gene product in

wild-type. In lane 4 there is an amplicon between 700 and 800bp showing the presence of the reverse primer and insert primer product and hence the T-DNA insert. The absence of this band in lane 2 proves this is not caused by another, random, binding site in the genome. Finally the absence of an amplicon in lane 3 shows the knockout to be homozygous. The results for the remaining knockout lines are presented in figures 3.9 to 3.17. In each case a homozygous knock out line was successfully generated.
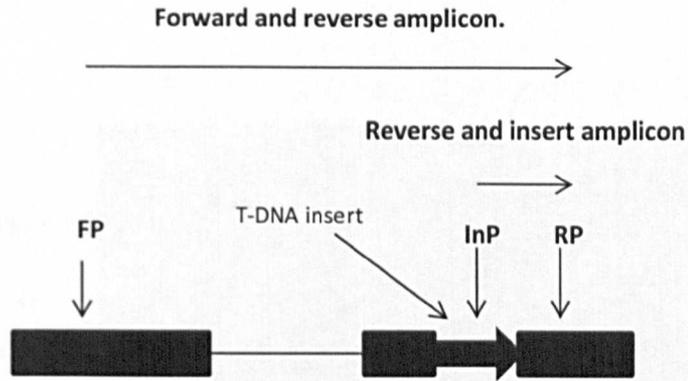
Figure 37 Genotyping experimental design;

Showing details of each amplicon produced by the two genomic and knockout PCRs conducted. The thick and thin lines show the gene structure with the thick bars representing exons, the thin lines representing introns and the blue triangle representing the T-DNA insert. Key: FP = Forward primer; InP = Insert primer; RP = Reverse primer.
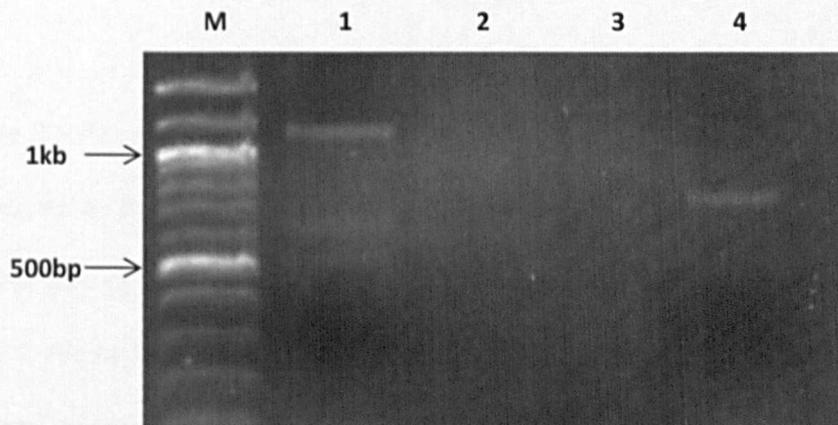
Figure 3-8 Genotyping PCR RabA1a

Lane key as follows: M = Marker; 1 = Wild-type line with forward and reverse primers; 2 = Wild-type line with insert and reverse primers; 3 = Knockout line with forward and reverse primers; 4 = Knockout line with insert and reverse primer.
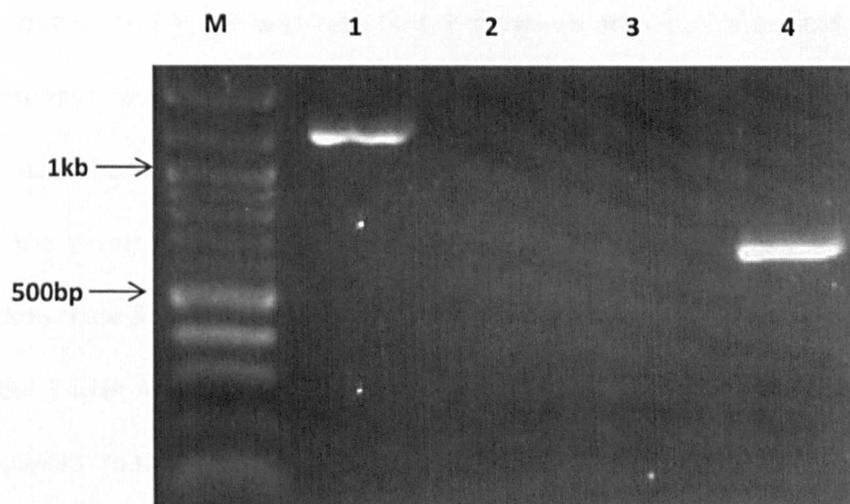
Figure 3-9 Genotyping PCR RabA1c

Lane key as follows: M = Marker; 1 = Wild-type line with forward and reverse

primers; 2 = Wild-type line with insert and reverse primers; 3 = Knockout line with

forward and reverse primers; 4 = Knockout line with insert and reverse primer.

Figure 3-9 displays the genotyping of the parent of the *RabA1c* line. Lane 1

shows an amplicon of around 1.2kb, complimentary to the forward and

reverse size of 1199bp confirming the gene presence in the genomic DNA.

Lane 2 shows through absence of an amplicon that the wild-type cannot

produce a band through random primer binding. The absence of an amplicon

in lane 3 confirms that the parent plant was homozygous, with lane 4

producing a band of around 700bp corresponds to the size of 728bp expected

from the reverse and insert primer.

Figure 3-10 shows the genotyping products for RabA1d and its parent knockout plant. For the wild-type lane 1 shows an amplicon of around 1kb corresponds to the expected band of 1053bp showing amplification of the gene with the forward and reverse primer, with lane 2 being clear showing that the reverse and insert primer cannot produce an amplicon. In the knockout lane 3 was clear showing that the knockout plant was homozygous for the T-DNA insert and lane 4 showed a band of around 800bp which is compliment to the 809bp expected size.
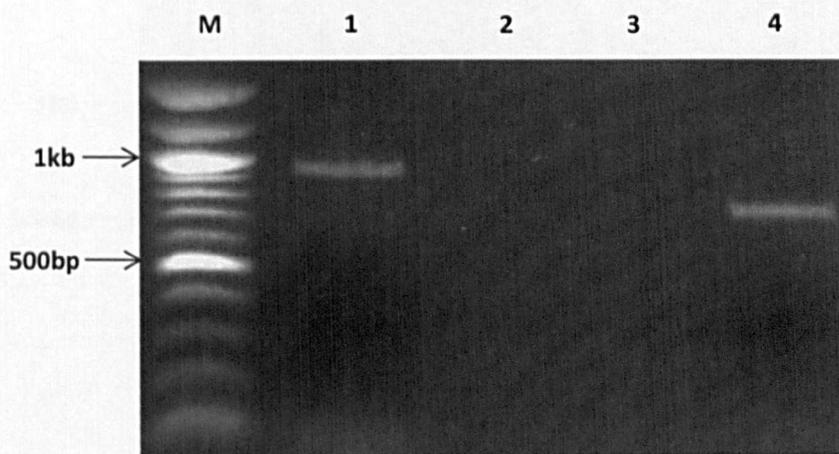
Figure 3-10 Genotyping PCR RabA1d

Lane key as follows: M = Marker; 1 = Wild-type line with forward and reverse primers; 2 = Wild-type line with insert and reverse primers; 3 = Knockout line with forward and reverse primers; 4 = Knockout line with insert and reverse primer.

Figure 3-11 displays the genotyping product bands for the wild-type and knockout plants of gene RabA1i. For the wild-type plant lane 1 an amplicon is shown in between 1 and 1.2kb showing the forward and reverse gene product, while lane 2 is empty showing that the reverse and insert primer cannot produce a band in the wild-type. In the knockout lane 3 is clear showing that the plant in homozygous with respect to the insert and lane 4 shows an amplicon of around 800bp which is corresponds to the expected amplicon of 803bp.
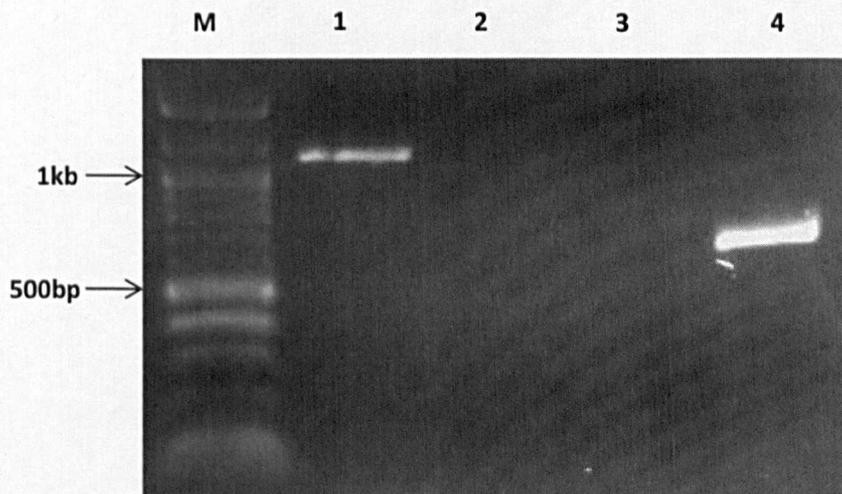

Figure 3-11 Genotyping PCR RabA1i

Lane key as follows: M = Marker; 1 = Wild-type line with forward and reverse primers; 2 = Wild-type line with insert and reverse primers; 3 = Knockout line with forward and reverse primers; 4 = Knockout line with insert and reverse primer.

Figure 3-12 shows the genotyping results of the wild-type RabA2b and the parent of the *RabA2b* knockout line. The genotyping for the wild-type shows a

71

band of around 1.2kb representing the forward and reverse primer of 1191bp, with lane 2 being clear showing that the reverse and insert primer cannot produce an amplicon. In respect to the knockout line lane 3 is clear showing homozygousity and lane 4 contains an amplicon of around 800bp, which is identical to the expected band of 823bp.
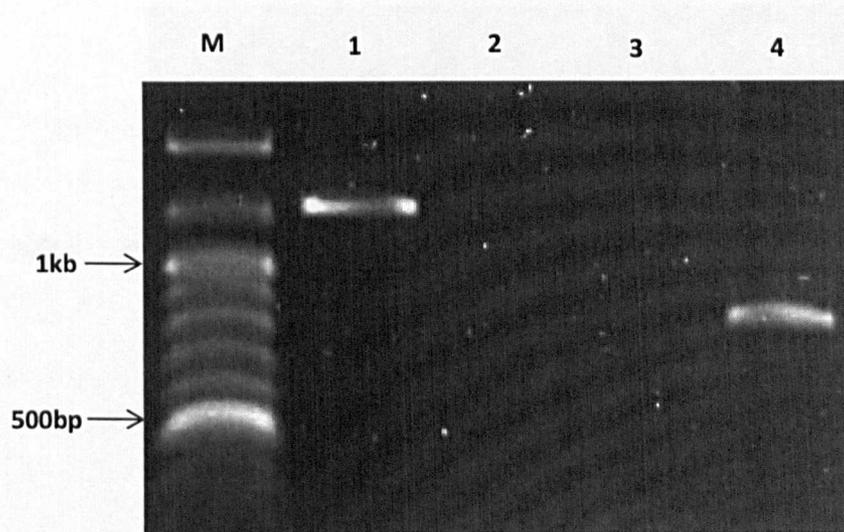
Figure 3-12 Genotyping PCR RabA2b

Lane key as follows: M = Marker; 1 = Wild-type line with forward and reverse primers; 2 = Wild-type line with insert and reverse primers; 3 = Knockout line with forward and reverse primers; 4 = Knockout line with insert and reverse primer.

Figure 3-13 shows the genotyping of the wild-type RabA2d and the parent of the *RabA2d* knockout line. In the wild-type lane 1 contains an amplicon of around 1kb which correlates with the expected amplification of 989bp showing amplification of the gene, while lane 2 is absent of an amplicon showing that the reverse and insert bands cannot be made through

amplification of the genome. In the knockout lane 3 was absent of amplification showing the knockout plant to be homozygous, while lane 4 contained an amplicon in between 500 and 600bp corresponding to the 556bp fragment expected.
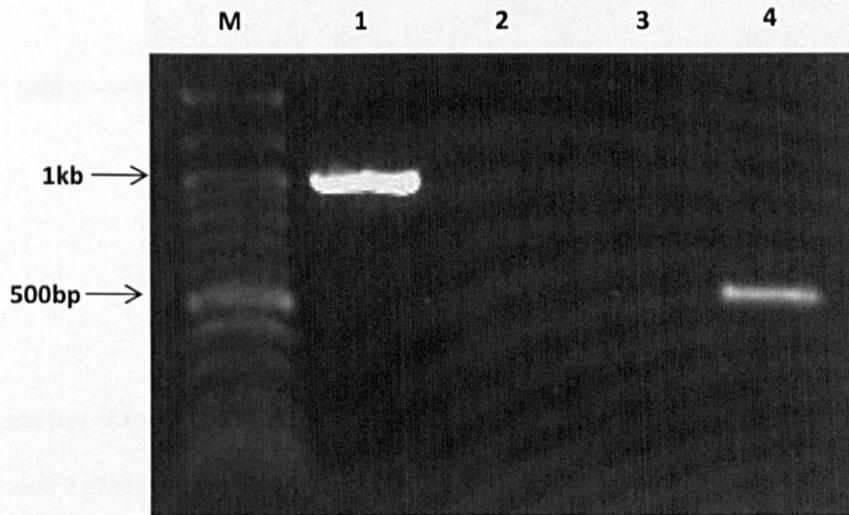

Figure 3-13 Genotyping PCR RabA2d

Lane key as follows: M = Marker; 1 = Wild-type line with forward and reverse primers; 2 = Wild-type line with insert and reverse primers; 3 = Knockout line with forward and reverse primers; 4 = Knockout line with insert and reverse primer.

Figure 3-14 shows the genotyping of the wild-type RabA3 and knockout *RabA3* plant. For the wild-type lane 1 shows an amplicon just above 1kb which corresponds to the expected fragment of 1021bp, while lane 2 remains absent showing that the reverse and insert primers could not produce an amplicon in wild-type. In the knockout plant lane 3 is absent of amplification

showing the plat to be homozygous and lane 4 contains an amplicon of around 500bp complementary to the 524bp expected fragment.
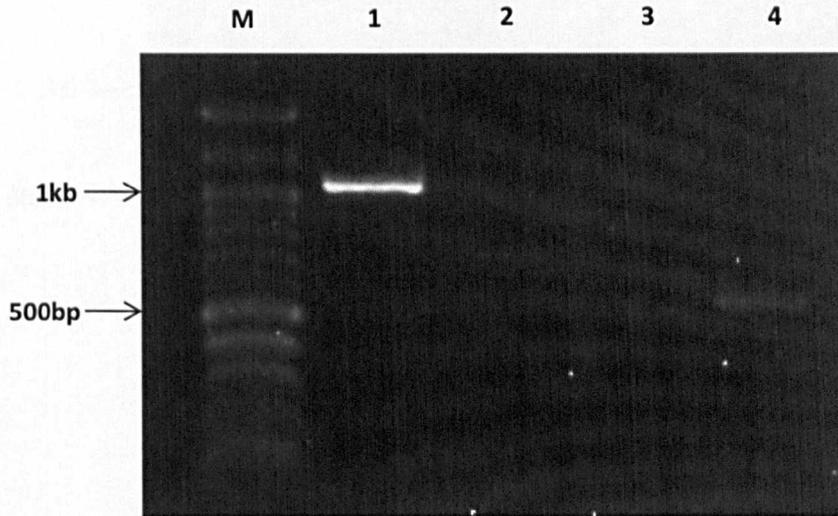
Figure 3-14 Genotyping PCR RabA3

Lane key as follows: M = Marker; 1 = Wild-type line with forward and reverse primers; 2 = Wild-type line with insert and reverse primers; 3 = Knockout line with forward and reverse primers; 4 = Knockout line with insert and reverse primer.

Data displayed in figure 3-15 shows the genotyping results from wild-type and the *rabA4a* knockout line. The genotyping in wild-type show that in lane 1 the forward and reverse primers produce an amplicon of around 1.2kb which is identical to the expected product of 1167bp, while lane 2 remains clear showing that the reverse and insert primers cannot produce an amplified product. In respect to the knockout line, lane 3 was clear of amplification showing that the knockout plant was homozygous for the T-DNA insert and lane 4 produced an amplicon of around 700bp which is identical to the expected product of 694bp.
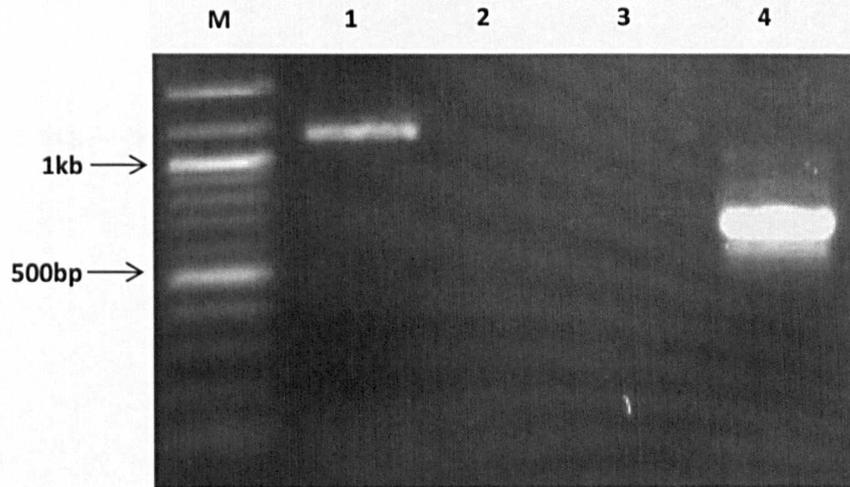
Figure 3-15 Genotyping PCR RabA4a

Lane key as follows: M = Marker; 1 = Wild-type line with forward and reverse

primers; 2 = Wild-type line with insert and reverse primers; 3 = Knockout line with

forward and reverse primers; 4 = Knockout line with insert and reverse primer.

Figure 3-16 shows the product of the genotyping in wild-type and the

knockout line in respect to the RabA4b gene. The results of the wild-type

amplification are shown in lanes 1 and 2. In lane 1 the forward and reverse

primer have given an amplified product of around 1kb which is identical to

the expected band of 1013bp, while lane 2 remains clear showing the absence

of amplification of the reverse and insert primer. The knockout line plant

tested shows lane 3 absent in amplification showing the plant to be

homozygous in nature, with lane 4 containing an amplicon in between 500

and 600bp showing presence of the T-DNA insert.
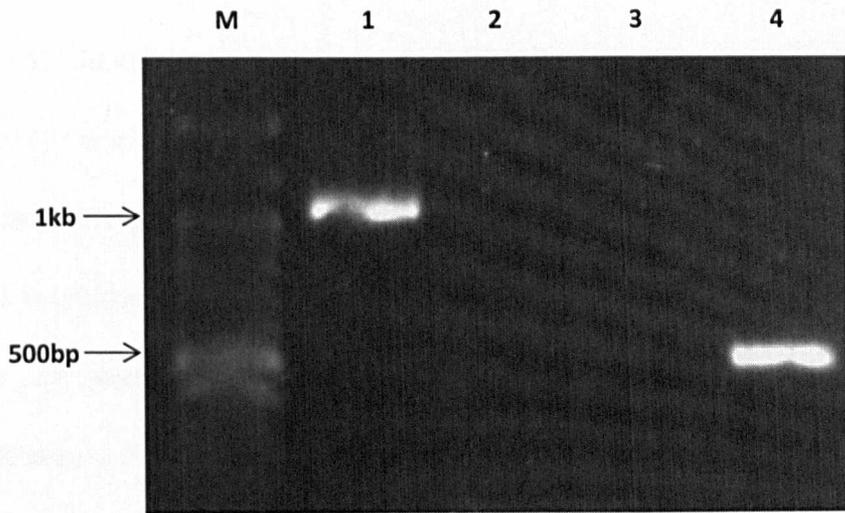
Figure 3-16 Genotyping PCR RabA4b

Lane key as follows: M = Marker; 1 = Wild-type line with forward and reverse

primers; 2 = Wild-type line with insert and reverse primers; 3 = Knockout line with

forward and reverse primers; 4 = Knockout line with insert and reverse primer.
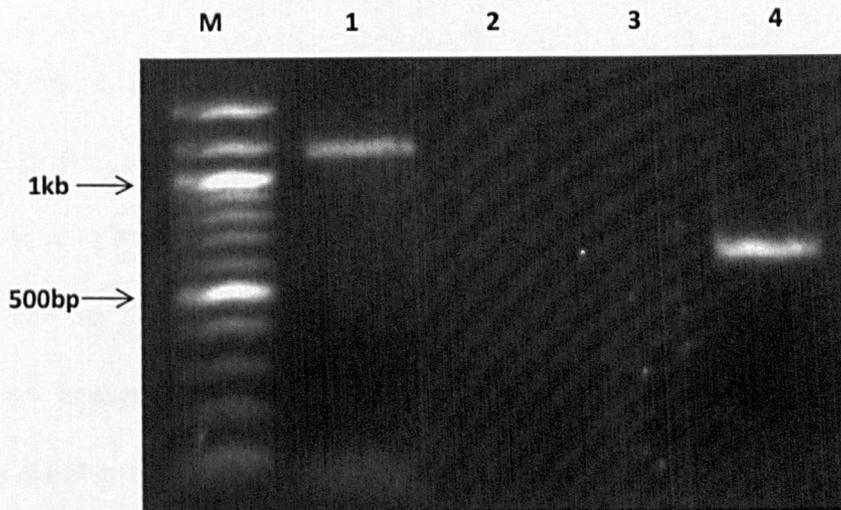

Figure 3-17 Genotyping PCR RabA4e

Lane key as follows: M = Marker; 1 = Wild-type line with forward and reverse

primers; 2 = Wild-type line with insert and reverse primers; 3 = Knockout line with

forward and reverse primers; 4 = Knockout line with insert and reverse primer.

Figure 3-17 shows the genotyping results for wild-type RabA4e and knockout

RabA4e. For wild-type lane 1 contains an amplicon of around 1.2kb showing

presence of the gene using both forward and reverse primer, while lane 2 is

clear of amplification showing no artefact product can be produced from the

reverse and insert primer in the wild-type plant. In the knockout line plant

lane 3 is absent of an amplified product showing that the plant is homozygous

for the T-DNA insertion, while lane 4 produces amplicon in between 600 and

700bp which is identical to the expected 653bp expected product.

3.3 Knockout confirmation by RT-PCR

In the previous section genotyping analysis of knockout lines purchased from

NASC was used to generate homozygous knockout lines, from a homozygous

parent plant. However to further prove that a gene product is not produced,

particularly for T-DNA inserts outside the exon region it is required to

undertake analysis by RT-PCR. To do this, primers were designed to amplify

exon regions in a produced transcript. Extraction of RNA was conducted on

growing stem taken from the main bolt of the progeny of the parent

homozygous plants described above. Through conversion of the RNA to a

cDNA using reverse transcriptase it is possible to show whether a viable

transcript had been produced. A standard analysis was carried out for each

knockout line. In the first instance RT-PCR was carried out using wild-type

RNA showing expression of the transcript in wild-type. A second PCR was conducted directly on the RNA extracted, prior to the RT STEP, to show the product could not be amplified by artifacts in the RNA extraction. The remaining two RT-PCRs would be conducted on RNA from the knockout line. The first of which would analyse whether the T-DNA insert had caused a knockout in the gene product and the second would be conducted on actin to show the RNA was not degraded in the extraction process. Primers and expected products for the RT-PCR reactions for each of the knockout lines are displayed in table 10-3.
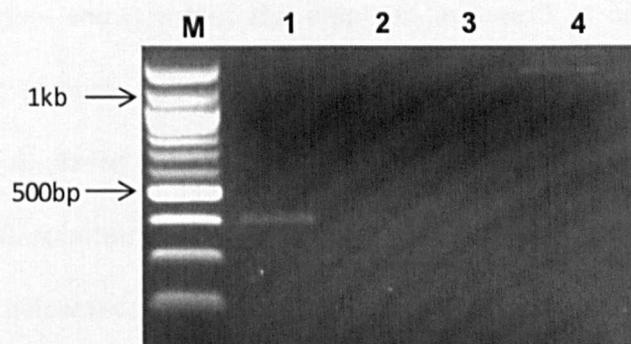
Figure 3-18 Confirmation of RabA1a T-DNA lines using RT-PCR

Lane key as follows: M = Marker; 1 = RabA1a expression in wild-type; 2 = No RT; 3 = RabA1a expression in the insert line; 4 = Actin expression in the insert line.

Figure 3-18 shows RT-PCR results for RabA1a. The RT-PCR products conducted for the wild-type produced an amplicon of around 400bp identical to the expected fragment of 406bp. Lane 2 is clear and shows that the RNA extraction contains no contaminating DNA which could cause the band shown

in lane 1. The RT-PCR using RNA from the knockout line is shown in lanes 3 and 4. In lane 3 the RT-PCR has produced no band showing that the transcript is absent from the knockout plant and in lane 4 there is a band which is identical to the expected ACT2 band of 1454bp for actin. The results for the other knockout lines are shown in figures 3.19 to 3.27.

Displayed in figure 3-19 are the results of the RT-PCR of wild-type and knockout for the RabA1c gene. The results for the wild-type are shown in lanes 1 and 2. In lane 1 there is an amplicon of around 400bp which represents the expected amplified cDNA product of 407bp. Lane 2 contains no amplification showing that the amplicon in lane 1 is not from DNA carryover or through random amplification. The knockout plant RT-PCR products are displayed in lanes 3 and 4. Lane 3 is clear and thus proves that the T-DNA insert in this line does not produce a product, while lane 4 shows an amplicon below the 1.5kb band in the ladder, which is corresponds to the expected size of the identical ACT2 gene, used to show that the RNA used in the RT-PCR is not degraded and capable of producing amplification.
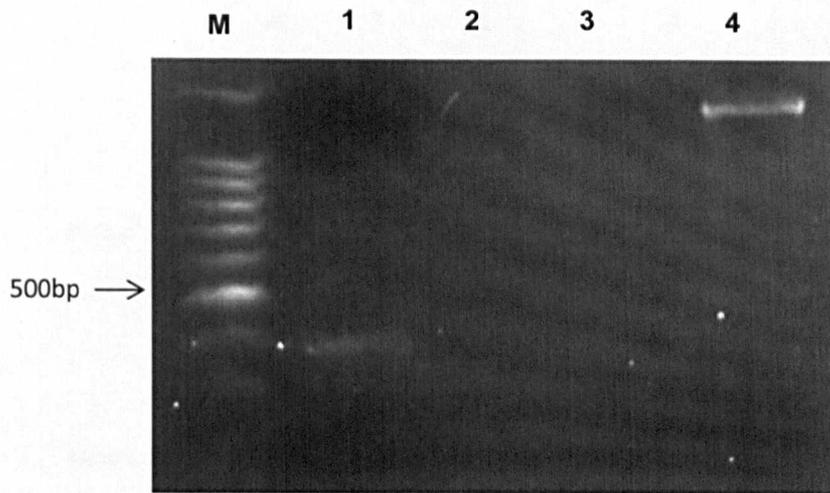
Figure 3-19 Confirmation of RabA1c T-DNA lines using RT-PCR

Lane key as follows: M = Marker; 1 = RabA1c expression in wild-type; 2 = No RT; 3 =

RabA1c expression in the insert line; 4 = Actin expression in the insert line.

Figure 3-20 shows the RT-PCR results for wild-type and knockout line with respect to the RabA1d gene. Analysis of wild-type expression is shown in lanes 1 and 2. Lane 1 contains an amplicon of around 400bp which is corresponds to the 406bp expected fragment, while lane 2 is clear showing that the amplification is not due to artefacts from the RNA extraction. The knockout line results are shown in lanes 3 and 4. Lane 3 shows no amplification which shows that the knockout has not produced a transcript. The presence of a band in between 1.2kb and 1.5kb is match the expected product for the ACT2 gene and shows that the absence of amplification in lane 3 is not due to cDNA sample being used.
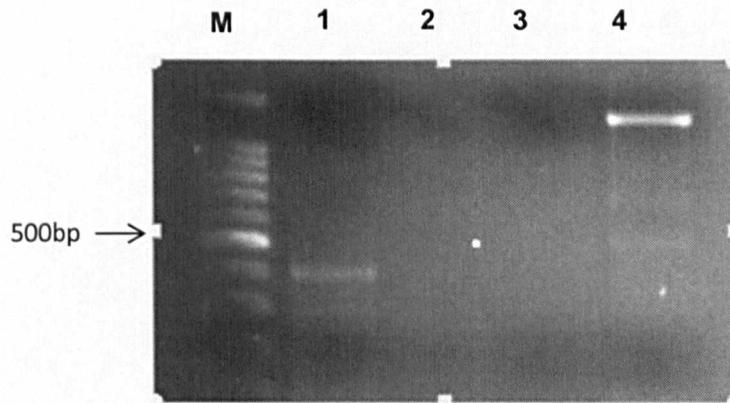
Figure 3-20 Confirmation of RabA1d T-DNA lines using RT-PCR

Lane key as follows: M = Marker; 1 = RabA1d expression in wild-type; 2 = No RT; 3 =

RabA1d expression in the insert line; 4 = Actin expression in the insert line.

Figure 3-21 displays the RT-PCR results for RabA1i. The figure shows the wild-type RT results in lanes 1 and 2. Lane 1 shows an amplicon of around 400bp which represent the expected 406bp fragment, while lane 2 remains clear showing that the product was not produced by artefacts in the reaction. The results of the knockout line are shown in lanes 3 and 4. Lane 3 shows no amplification and proves that no transcript has been produced due to the T-DNA insert, to support that this is not because of errors in the reactants and reaction lane 4 contains an amplicon of around 1.4kb which is around the expected size amplicon of 1454bp.
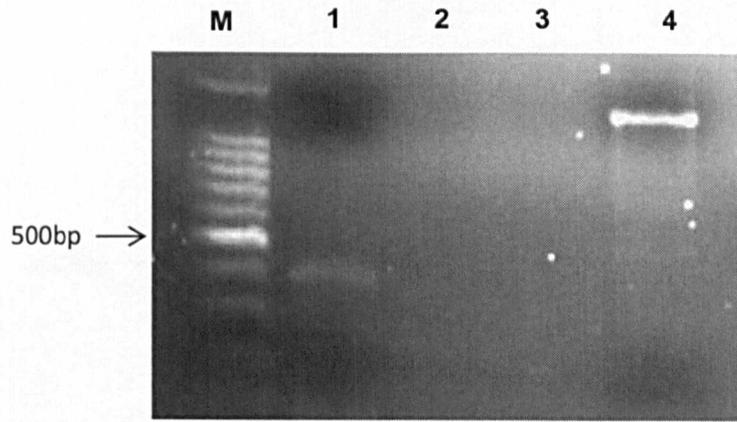
Figure 3-21 Confirmation of RabA1i T-DNA lines using RT-PCR

Lane key as follows: M = Marker; 1 = RabA1i expression in wild-type; 2 = No RT; 3 =

RabA1i expression in the insert line; 4 = Actin expression in the insert line.

Shown in figure 3-22 are the results for the RT-PCR in relation to the RabA2b gene. The wild-type results are displayed in lanes 1 and 2, while the results for the knockout are displayed in lanes 3 and 4. Lane 1 shows amplification around 400bp which is identical to the 407bp amplicon expected. Lane 2 is absent of amplification and shows that the product produced in lane 1 is not from due to artefacts in the reactants. The knockout line results are displayed in lanes 3 and 4. Lane 3 is clear with no amplification showing that there is no transcript produced in the knockout line, while lane 4 is just below 1.5kb representing the 1454bp expected fragment.
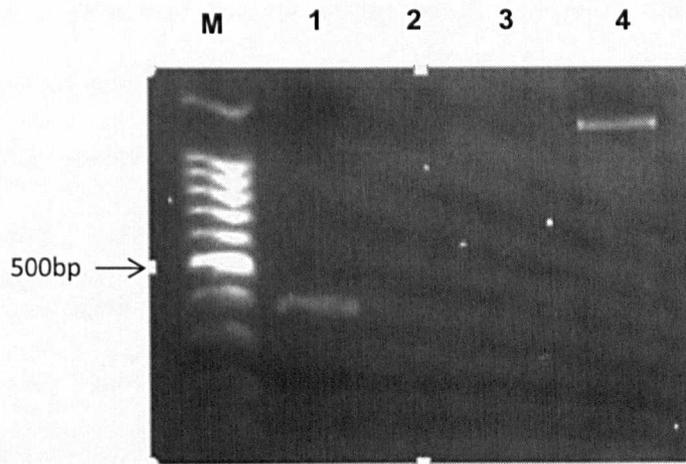
Figure 3-22 Confirmation of RabA2b T-DNA lines using RT-PCR

Lane key as follows: M = Marker; 1 = RabA2b expression in wild-type; 2 = No RT; 3 =

RabA2b expression in the insert line; 4 = Actin expression in the insert line.
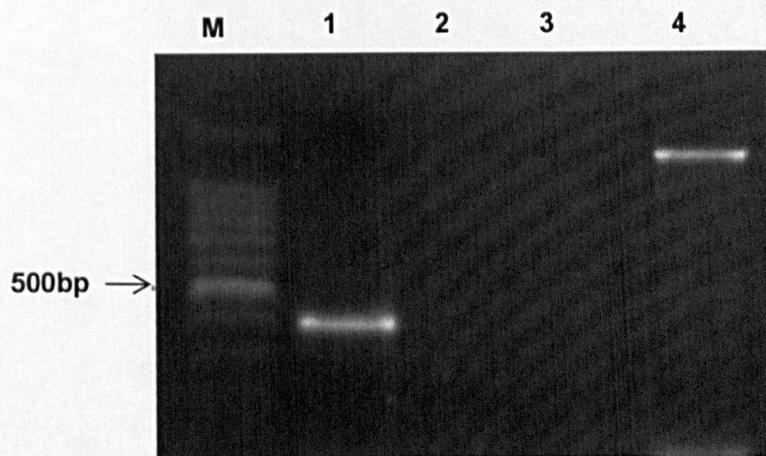
Figure 3-23 Confirmation of RabA2d T-DNA lines using RT-PCR

Lane key as follows: M = Marker; 1 = RabA2d expression in wild-type; 2 = No RT; 3 =

RabA2d expression in the insert line; 4 = Actin expression in the insert line.

Figure 3-23 shows the results of the RT-PCR of RabA2d in wild-type and the

knockout line. The wild-type results are shown in lanes 1 and 2. In lane one

83

there is an amplicon of around 400bp which represents the expected

fragment size of 407bp, while lane 3 is absent of amplification showing that

the product in lane 1 was not created by artefact. The knockout line is shown

in lanes 3 and 4. Lane 3 is clear showing that the T-DNA insert has stopped

production of a transcript and in lane 4 there is an amplicon of just below

1.5kb representing the 1454bp expected ACT2 product showing that the

cDNA created from the RNA was able to produce amplification.
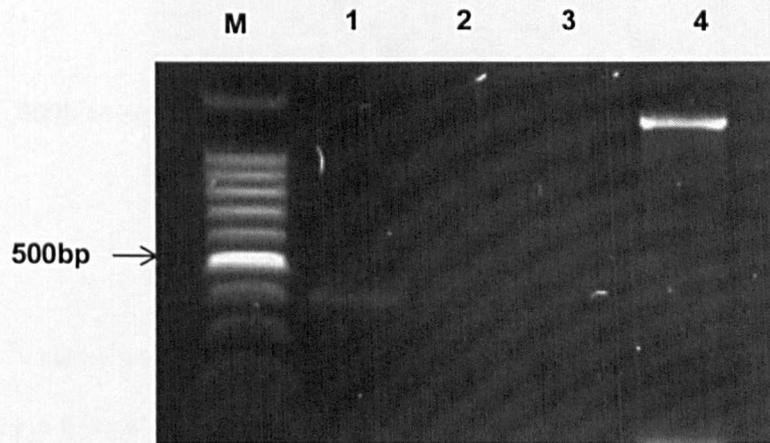
Figure 3-24 Confirmation of RabA3 T-DNA lines using RT-PCR

Lane key as follows: M = Marker; 1 = RabA3 expression in wild-type; 2 = No RT; 3 =

RabA3 expression in the insert line; 4 = Actin expression in the insert line.

Data shown in figure 3-24 shows the RT-PCR results for RabA3. The wild-type

results are in lanes 1 and 2. Lane 1 contains an amplicon of around 400bp

which is identical to the 415bp fragment expected from the primers, while

lane 2 is absent of amplification which shows that the amplification in lane 1

was not caused through artefacts in the reactants. The knockout line data is

84

displayed in lanes 3 and 4. Lane 3 is absent of amplification which shows that the no transcript was present in the cDNA produced, the presence of an amplicon corresponding to around 1454bp in lane 4 adds further weight to this by proving that the absence of amplification was not due to a failure in the reaction, or degradation of the sample.
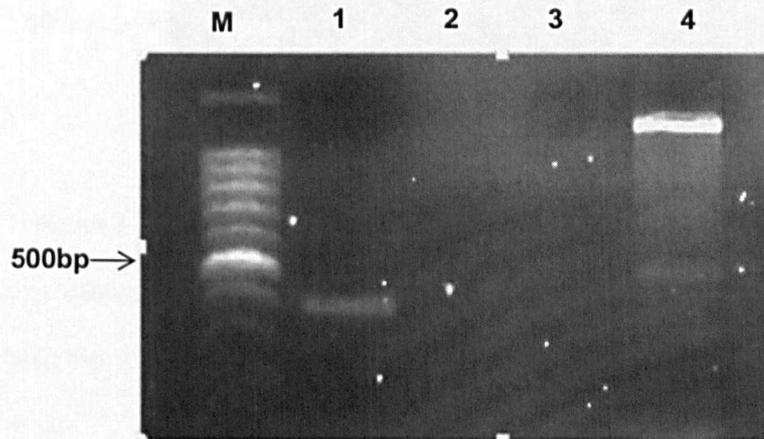
Figure 3-25 Confirmation of RabA4a T-DNA lines using RT-PCR

Lane key as follows: M = Marker; 1 = RabA4a expression in wild-type; 2 = No RT; 3 = *RabA4a* expression in the insert line; 4 = Actin expression in the insert line.

The RT-PCR results for RabA4a are shown in figure 3-25. The results specific to the wild-type are shown in lanes 1 and 2, with the knockout specific results displayed in lanes 3 and 4. Lane 1 displays an amplicon of around 400bp identical to the 407bp expected product, with lane 2 being clear showing that the amplicon in lane 1 was not produced through artefacts in the sample of the reaction process. Lane 3 shows no presence of an amplicon proving that no transcript is produced in the T-DNA line, with lane 4 containing an

amplicon just below the 1.5kb marker showing that the cDNA used in reaction

was capable of producing amplification in lane 3.
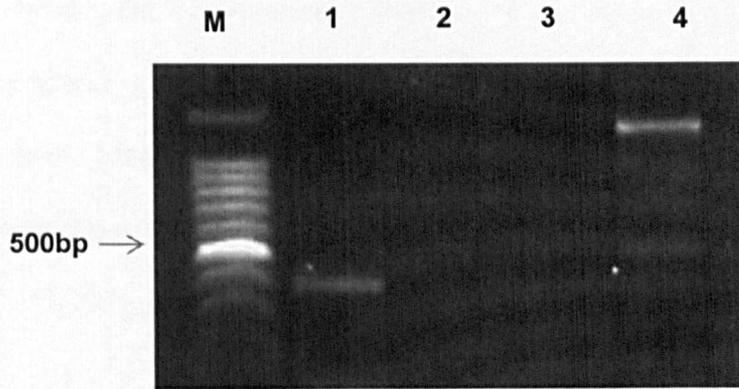
Figure 3-26 Confirmation of RabA4b T-DNA lines using RT-PCR

Lane key as follows: M = Marker; 1 = RabA4b expression in wild-type; 2 = No RT; 3 =

RabA4b expression in the insert line; 4 = Actin expression in the insert line.

Figure 3-26 shows the RT-PCR results for RabA4b. The wild-type results are in

lan1 and 2 and show an amplicon of around 400bp in lane 1, which is identical

to the expected 407bp fragment and a clear lane 2 showing that this product

was not produced through artefacts. For the knockout line there is a clear

lane 3, which show the absence of a transcript due to the T-DNA insertion and

lane 4 shows displays an amplicon just below the 1.5kb marker, identical to

the ACT2 expected fragment showing that the absence of amplification in

lane 3 was not due to failure in the reaction, or sample degradation.

In figure 3-27 are the RT-PCR results for RabA4e. The wild-type results are

displayed in lanes 1 and 2. Lane 1 contains an amplicon around 400bp which

is identical to the 417bp expected fragment, while lane 2 contains no amplified product showing that the lane 1 product is not due to artefacts in the reacts. The knockout is shown in lanes 3 and 4, with lane 3 clear the absence showing the T-DNA insertion stopped the production of a transcript and the presence of an amplicon in lane 4 which is below 1.5kb and thus identical to the 1454bp ACT2 product expected show that the band in lane 3 is not absent due to reactants or degradation of products.
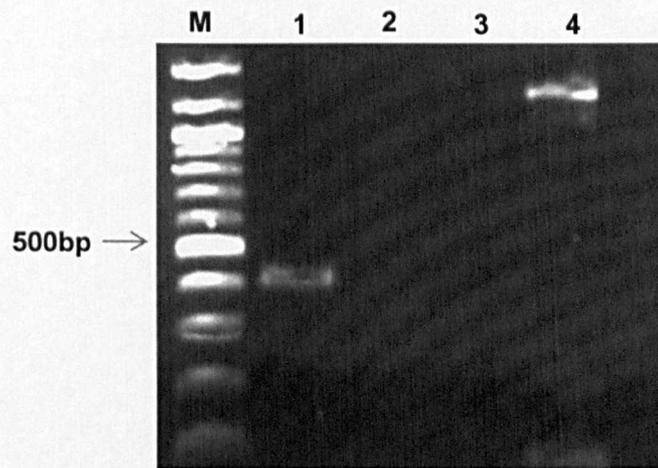

Figure 3-27 Confirmation of RabA1a T-DNA lines using RT-PCR

Lane key as follows: M = Marker; 1 = RabA4e expression in wild-type; 2 = No RT; 3 = *RabA4e* expression in the insert line; 4 = Actin expression in the insert line.

In this chapter I have identified a set of target Rab genes which are expressed in stem tissue. Through the resources available in the post genomic scientific community it has then been possible to isolate knockout lines for many of these genes. Unfortunately despite the wealth of these resources the stock lines are still incomplete with a few compromised stock lines. From those

87

resources I have shown that they the seeds homozygous and breeding true as shown in section 3.2. From these homozygous parent plants I have then shown that the T-DNA inserts have stopped the production of a viable transcript through RT-PCR. In the following chapters these knockout lines will be used to analyse cell wall composition and digestibility.

4 Cell wall composition of Rab GTPase knockout lines

With knockout lines successfully established for the targeted genes the next step was to analyse the composition of the cell wall. This may help provide a biological explanation to any differences which occur in digestion and also answer the key question on the potential role of Rab proteins on cell wall composition. To do this the knockout lines were subjected to a traditional cell wall fractionation process in which the 3 key polymers (pectin, hemicelluloses and cellulose) are extracted sequentially. The knockouts were also subjected to FT-IR analysis as a second independent assessment cell wall composition analysis method.

4.1 Cell wall fractionation

Fully senesced *Arabidopsis* stem material, from wild type and knockout lines, was collected and acetone insoluble solids (AIS) prepared as described in materials and methods. The first two steps in the extraction process are designed to extract pectin from the AIS. First through the use of CDTA which is used to extract the ionically bound pectin from the sample and then using Na_2CO_3 which releases the covalently bound pectin from the sample, the results of this experiment are show in figure 4-1. In the wild-type covalent pectin was around 60mg/g of the total AIS, with the ionic fraction accounting

for around 100mg/g, giving a total of 16% of the total AIS as pectin. In the case of the *RabA1a*, *RabA1c*, *RabA1d* and *RabA1i* knockout lines the amount of total pectin was significantly different from the wild-type (P<0.001). The total average pectin in the knockout lines was around 120mg/g in comparison to 160mg/g in the wild type, representing a 25% reduction in the total pectin. The mean values of the covalently bound pectin were unchanged in all of these knockout lines and it was the ionically bound pectin that was reduced. There were no significant differences in the total levels of total pectin in the other knockout lines and the distribution between ionically and covalently bound pectin remained unchanged from that in the wild type.

After pectin extraction the remaining residue was subjected to treatment with KOH, to give a hemicelluloses rich fraction. The results of this fractionation are presented in figure 4-2. The average gravimetric weight of the hemicelluloses rich fraction from wild type plants was around 250mg/g, representing around 25% of the total AIS. There were significant differences in the recovery of the hemicelluloses rich fraction between wild-type and the *RabA4a*, *RabA4b* and *RabA4e* knockout lines. The knockout lines had an average value for the hemicelluloses fraction of around 200mg/g, representing around a 20% reduction from the level in the wild type. There were no statistically significant differences between the wild type and any of the other knockout lines.
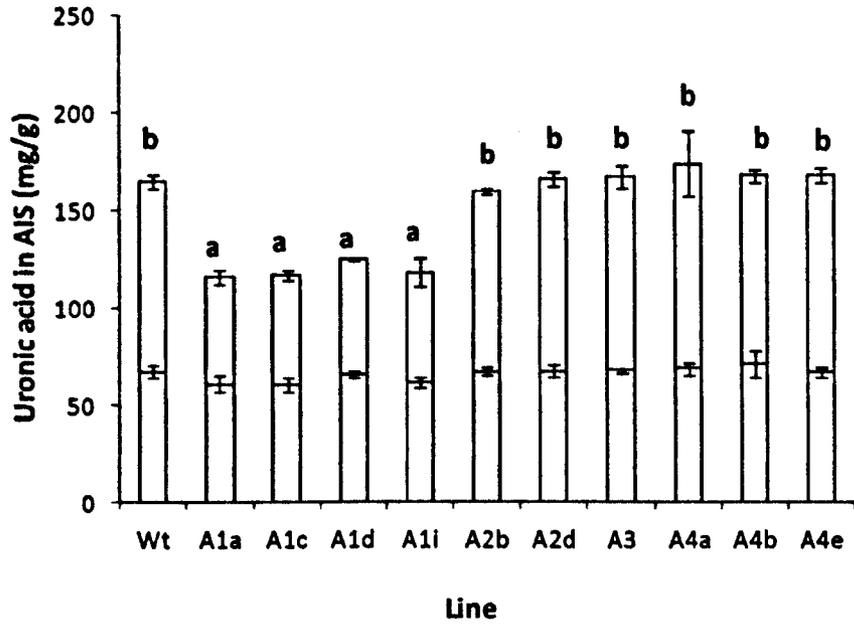
Figure 4-1 Pectin levels (as estimated by uronic acid content) in senescent stem tissue from wild type and *rabA* knockout lines

Ionically bound pectin (clear) and covalently bound pectin (grey) Significance values are as follows; (p < .001) with letters annotating significant difference between means. Error bars show standard deviation from the mean of 3 replicates of 50 plants pooled.
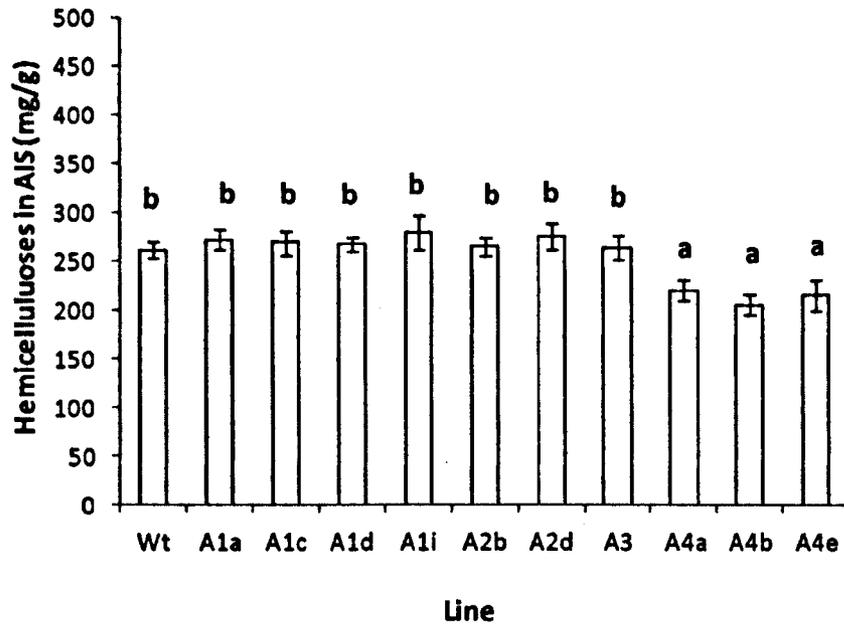
Figure 4-2 Levels of hemicelluloses rich fraction in stem of *Arabidopsis*

The statistical values are as follows; "hemicelluloses rich" fraction $p < .001$ (d.f,32

v.r,6.8); "hemicelluloses rich" fraction $p < .001$ (d.f,32 v.r,15.04) with letters

annotating significant difference between knockout means and wild-type. Error bars

show standard deviation from the mean of 3 replicates of 50 pooled plants.

The residue from this extraction process was then taken as being the cellulose

rich fraction. These data are shown in figure 4-3. The average value for the

cellulose rich fraction in the wild-type plant was around 500mg/g,

representing around 50% of the total AIS. The cellulose rich fraction was

significantly (P<0.001) reduced in both the RabA2b and RabA2d knockout

lines. The value of cellulose in these two knockout lines was around 400mg/g,

representing a 20% reduction in the cellulose rich fraction compared to wild

type plants. There were no statistically significant differences between the

wild type and any of the other knockout lines.
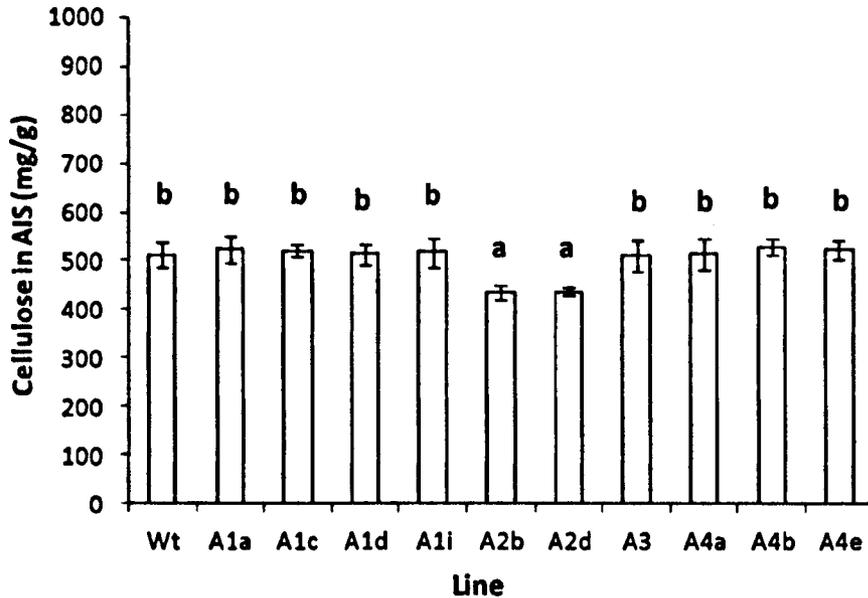
Figure 4-3 Cellulose rich fraction in stem tissue of *Arabidopsis*

Statistical values are as follows; "cellulose rich" fraction $p < .001$ (d.f,32 v.r,6.8) with

letters annotating significant difference between knockout means and wild-type. The

error bars shown indicate standard deviation of 3 replicates of 50 pooled plants per

replicate.

The hemicelluloses and cellulose rich fractions were both further analysed for

their sugar composition. The fractions obtained were subjected to the two

stage acid hydrolysis and monomer sugar composition assessed by HPAEC, as

described in materials and methods. The results for the hemicelluloses and

cellulose rich fractions are displayed in figure 4-4 and 4-5, respectively.

The results for the hemicelluloses rich fraction indicate that the major sugar

detected was xylose, which at 500mg/g in the wild type represents around

50% of the sugar in this fraction. Glucose, at around 200mg/g, and galactose,

at around 50mg/g, represent the other major constituents of this fraction. There were no significant differences in sugar composition detected between the wild type and any of the knockout lines. Thus although a reduction in the level of the hemicelluloses rich fraction was observed in the Rab4 sub-clade (figure 4.2) this is not accompanied by any major changes in the monomer composition of this fraction.

The results for the cellulose rich fraction show that glucose was the major sugar in wild type accounting for 800mg/g in wild type plants. There was a smaller amount, around 50mg/g, of xylose indicating that, as expected, this fraction is contaminated by a small amount of hemicelluloses. Again there were no significant differences in sugar composition detected between the wild type and any of the knockout lines. Thus although a reduction in the level of the cellulose rich fraction was observed in the Rab2 sub-clade (figure 4.3) this again is not accompanied by any major changes in the monomer composition of this fraction.
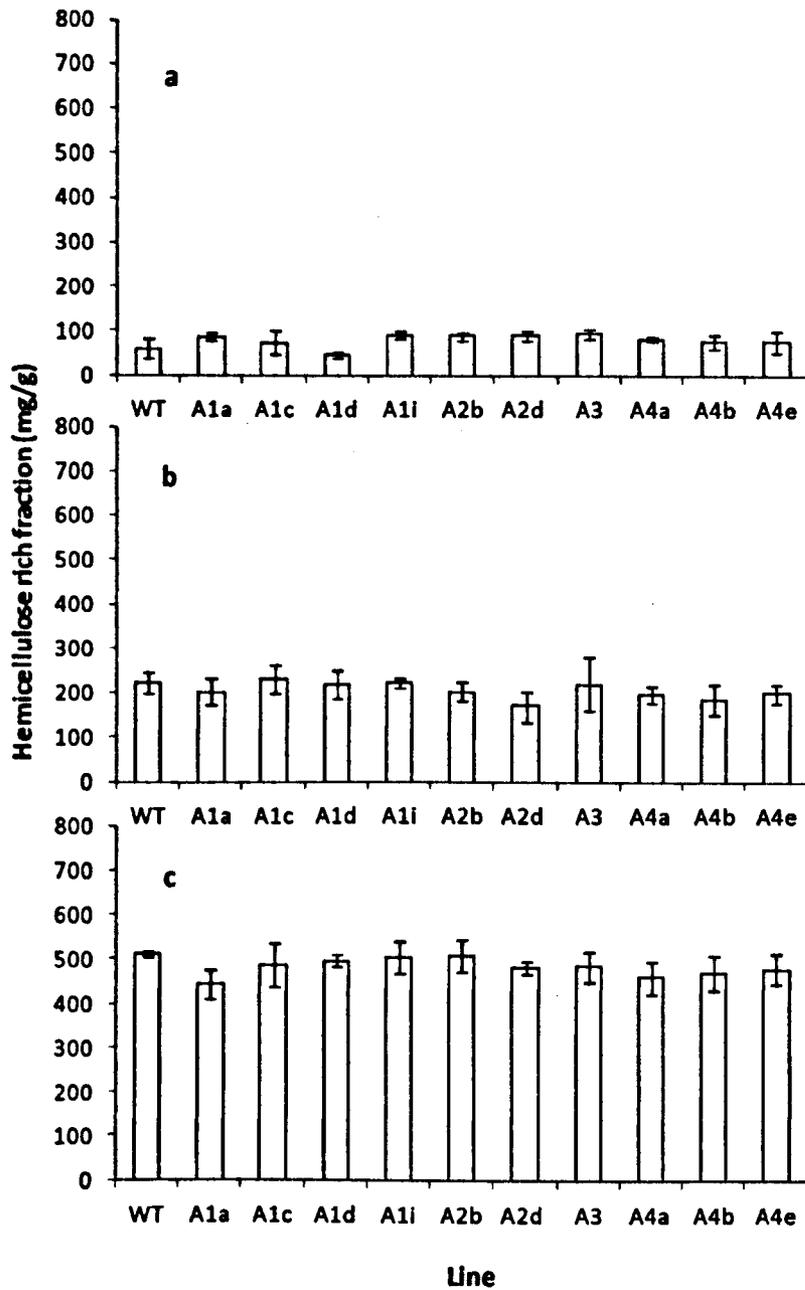
4-4 Sugar composition of the hemicelluloses rich fraction of wild type and rabA knockout lines

The hemicelluloses rich fraction was subjected to hydrolysis and monomer sugar composition in terms of (A) Galactose, (B) Glucose and (c) Xylose assessed by HPAEC. Statistical values are as follows; glucose $p < .0494$ (d.f,32 v.r,0.97); xylose $p < .362$ (d.f,32 v.r,1.17); galactose p 0.022 (d.f,32 v.r,2.7). The error bars shown indicate standard deviation of 3 replicates of 50 pooled plants per replicate.
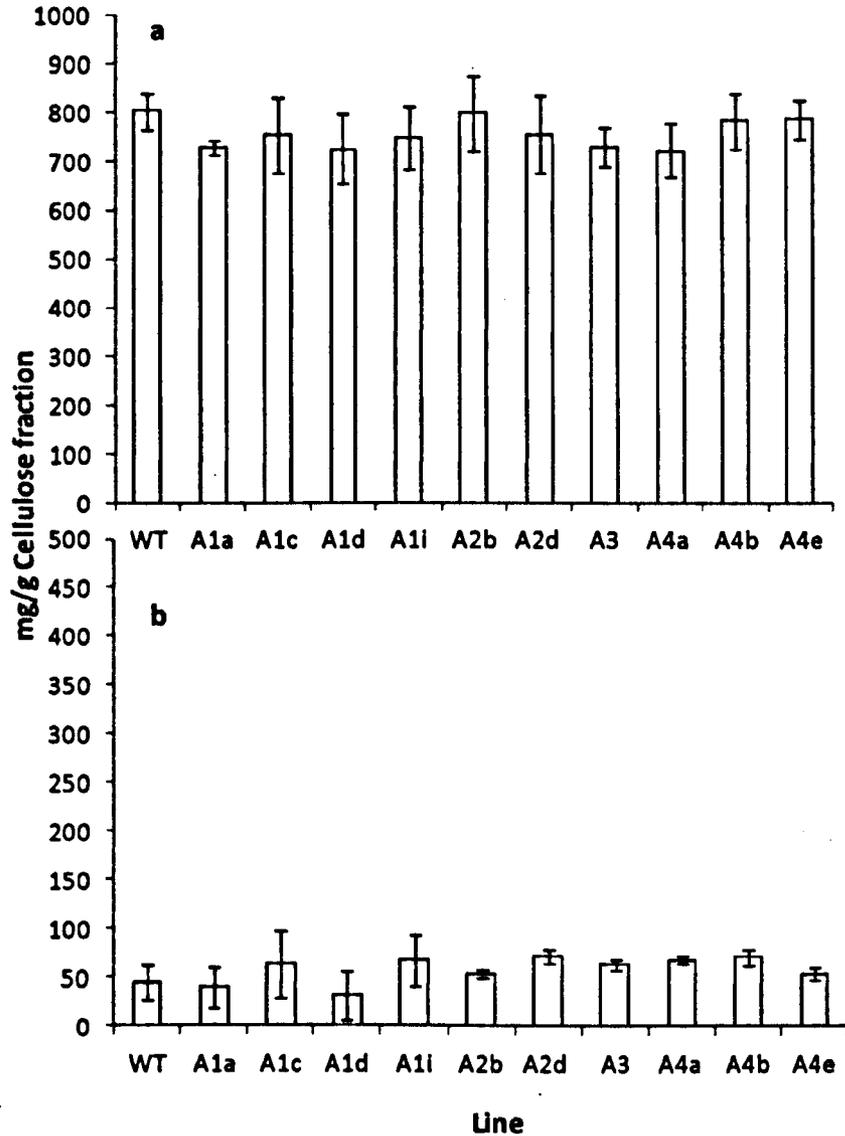
4-5 Sugar composition of the cellulose rich fraction

The hemicelluloses rich fraction was subjected to hydrolysis and monomer sugar composition in terms of, (A) Glucose and (B) Xylose assessed by HPAEC. Statistical values are as follows; glucose p <.0494 (d.f,32 v.r,0.97); xylose p < .362 (d.f,32 v.r,1.17); galactose p 0.022 (d.f,32 v.r,2.7). The error bars shown indicate standard deviation of 3 replicates of 50 pooled plants per replicate.

To get an appreciation of the monomer composition with regard to the initial AIS the percentage monomer in the "hemicelluloses rich" and "cellulose rich"

fractions were calculated back the original AIS. These data are shown in table 4-1.

A final validation of the cell wall fractionation was conducted by a mass balance analysis and is shown in table 4-2. The mass balance table for the three constituents analysed shows a recovery of between 88% and 95% of the total AIS.

Table 4-1 Monomer composition in AIS

Hemicellulose "rich" fraction

	WT	A1a	A1c	A1d	A1i	A2b	A2d	A3	A4a	A4b	A4e
Glucose	57±6.2	60±6.4	59±6.3	58±6.3	61±6.6	58±6.2	60±6.5	58±6.2	48±5.2	45±4.8	47±5.1
Xylose	133±1.5	138±1.6	137±1.6	136±1.6	143±1.6	135±6.2	140±1.6	134±1.5	112±1.3	104±1.2	109±1.3
Galactose	15±5.7	16±5.9	15±5.8	15±5.8	16±6.1	15±5.8	16±6.0	15±5.7	13±4.8	12±4.5	12±4.7

Cellulose "rich" fraction

	WT	A1a	A1c	A1d	A1i	A2b	A2d	A3	A4a	A4b	A4e
Glucose	411±37.2	421±24.6	418±83.5	413±73.1	417±68.6	350±16.4	351±19.1	410±38.8	414±57.4	425±68.9	421±48.4
Xylose	22±17.3	23±21.9	22±22.8	22±22.5	22±22.7	19±0.8	19±4.0	22±4.9	22±4.7	23±8.8	23±6.7
Galactose	0±0	0±0	0±0	0±0	0±0	0±0	0±0	0±0	0±0	0±0	0±0

Table 4-2 Mass balance of AIS (mg/g)

	Cellulose	Hemicellulose	Pectin	Total
WT	583 ± 17	261 ± 7	165 ± 6	938 ± 38
A1a	605 ± 21	271 ± 10	115 ± 0.6	910 ± 36
A1c	605 ± 18	268 ± 12	117 ± 4	905 ± 29
A1d	611 ± 23	266 ± 7	125 ± 1	905 ± 29
A1i	618 ± 29	280 ± 18	118 ± 10	916 ± 57
A2b	513 ± 15	265 ± 10	159 ± 3	859 ± 28
A2d	516 ± 15	275 ± 13	165 ± 3	877 ± 24
A3	603 ± 22	263 ± 12	166 ± 6	940 ± 49
A4a	660 ± 27	220 ± 10	173 ± 13	908 ± 53
A4b	645 ± 15	205 ± 10	167 ± 8	901 ± 36
A4e	656 ± 17	215 ± 15	168 ± 1	906 ± 33

4.2 Cell wall analysis by FT-IR

FT-IR was used as an independent second as a non-destructive method of analysis to determine if cell wall composition had been impacted in the Rab knockout lines. Using 50mg of sample 128 FT-IR readings were taken as a composite for each of 3 replicate samples. The data were then normalised using vector methodology and base line corrected using the rubber band method. Finally an average was taken of the replicate data for graphical analysis.

The resulting spectra for the RabA1, RabA2 and RabA4 sub-clades are shown in figures 4-6 through 4-8, respectively. From the literature (Kačurákova *et al* 2000) the region between 1200 and 800 wavenumber units was identified as the fingerprint for the cell wall polymers.

The data in figure 4-6 shows the spectra of wild-type stem compared with the *rabA1* knockouts. The figure also shows the wavenumbers of the absorption bands associated with pectic polysaccharides, which are highlighted on the graph at 1017 and 1100 cm^{-1}. At 1017 cm^{-1} the wild-type and all the knockouts form their highest peak giving a band intensity of 0.14. At this point both wild-type and knockout lines overlap with their spectral curve indicating that there is no difference in band intensity. However, at 1100 cm^{-1} there is a

clear difference between the spectra. At this point the wild-type band intensity is around 0.09, while all 4 of the knockout lines have a reduced band intensity of around 0.08, showing a reduction of .01. Noteworthy is the overlapping spectra of the *four* rabA1 knockout lines at this wavenumber.

The *rabA2* knockout lines plotted against the wild-type are shown in figure 4-7. The analysis here was conducted around absorption bands at 1033 and 1059 cm^{-1} thought to be related to cellulose. At the wavenumber 1033 cm^{-1} the wild-type spectra shows an intensity of around 0.13, similarly at this point both *rabA2* knockout lines have a band intensity of 0.13 equal to that of wild-type. At the 1059 cm^{-1} wavenumber the wild-type has a band intensity of around 0.08. Both the knockout lines analysed have decreased band intensity in this region with *rabA2b* giving an intensity of around 0.06 and *rabA2d* giving an intensity of around 0.07, this gives a reduction of .01 and .02, respectively.

Figure 4-8 shows the comparison of the *rabA4* knockout spectra compared with the wild-type spectra. The literature defines wavenumbers of 1041 and 1078 cm^{-1} as the key regions corresponding to a xyloglucan epitope of hemicelluloses. At 1041 cm^{-1} the wild-type has an intensity of around 0.13, with one knockout line having a similar intensity and two knockout lines appearing to have increased intensity. Knockout lines *rabA4a* and *rabA4b* have intensity around 0.14, while *rabA4e* has a similar value to the wild-type.

The intensity at 1078 cm^{-1} in respect to the wild-type is around 0.08, differing from the 3 knockout lines analysed. Lines *rabA4b* and *rabA4e* have an intensity of 0.07 which represent a .01 reduction compared to the wild-type. The remaining A4 line *rebA4a* has an intensity of around 0.06 representing a .02 reduction compared to the wild-type.
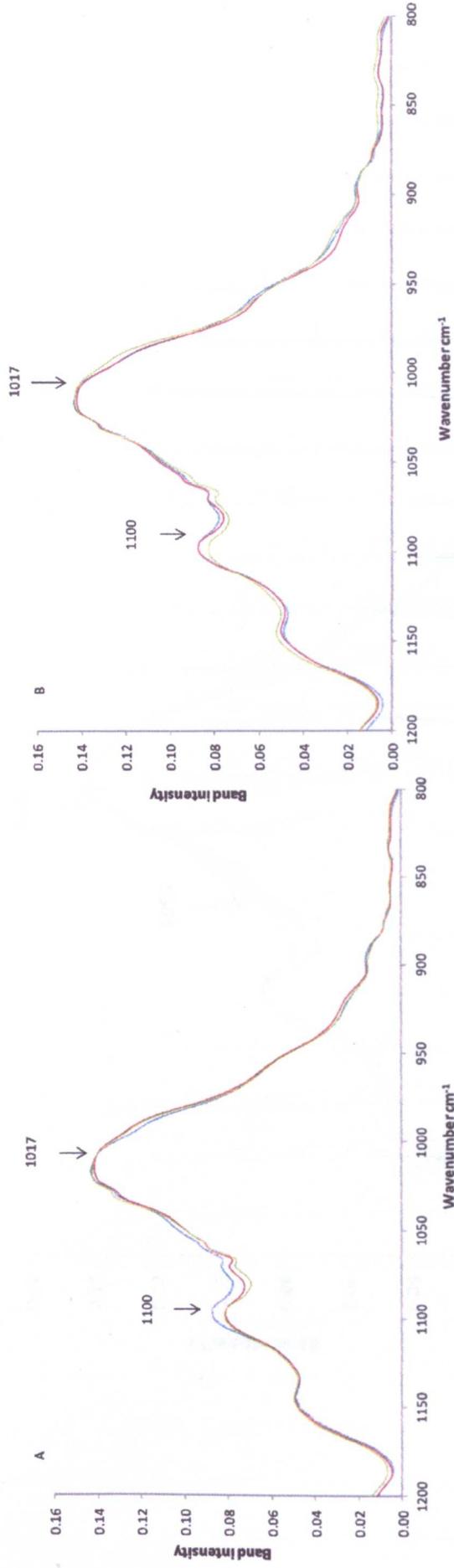
Figure 4-6 FT-IR Spectra of wild type and *rabA1* knockout lines

FT-IR spectra of *rabA1* knockouts, showing fingerprint regions for pectic functional groups. Key: A) Wild type (blue) against knockout lines *rabA1a* (red), *rabA1c* (green): B) Wild type (blue) *rabA1d* (red) and *rabA1i* (green)

103
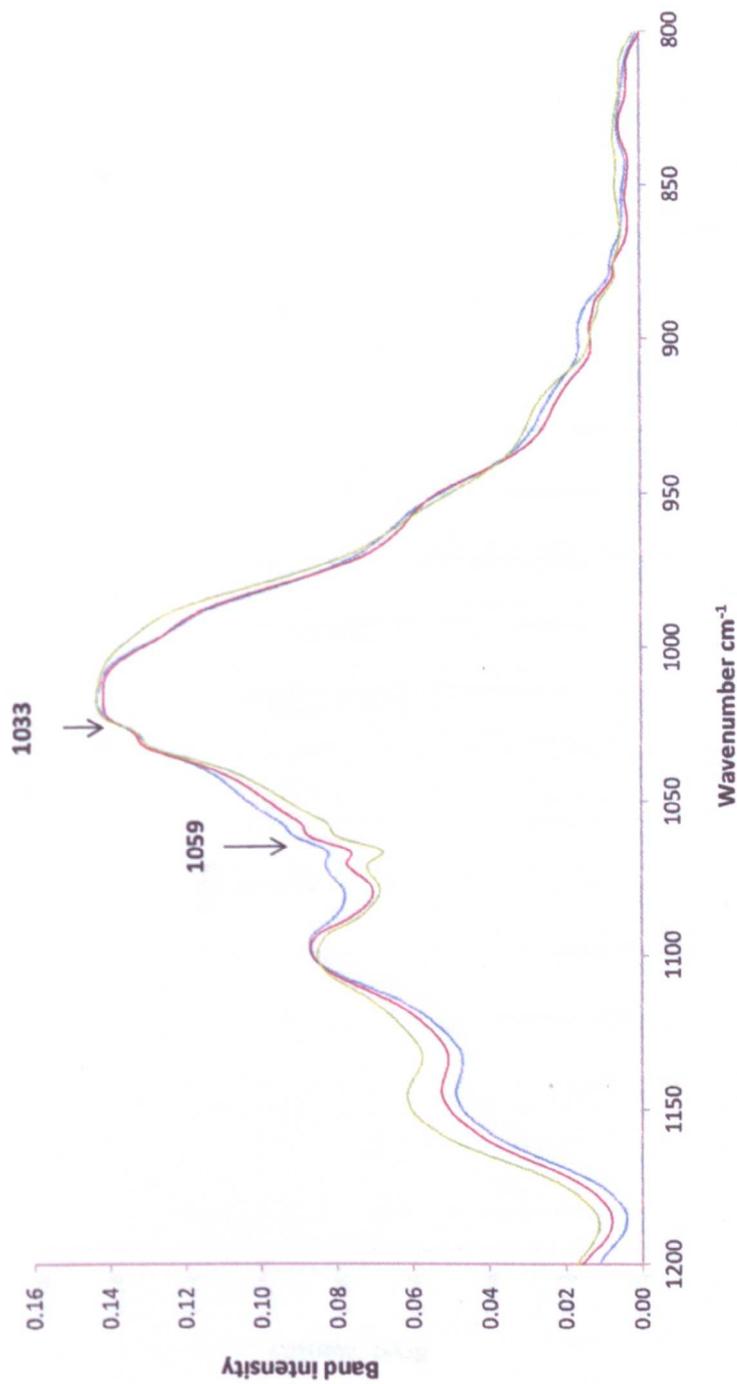
Figure 4-7 FT-IR Spectra of wild type and *rabA2* knockout lines

FT-IR spectra of *rabA2* knockouts, showing fingerprint regions for cellulosic functional groups. Wild type (light blue) against knockout lines *rabA2b* (green)

and *rabA2d* (red)

104
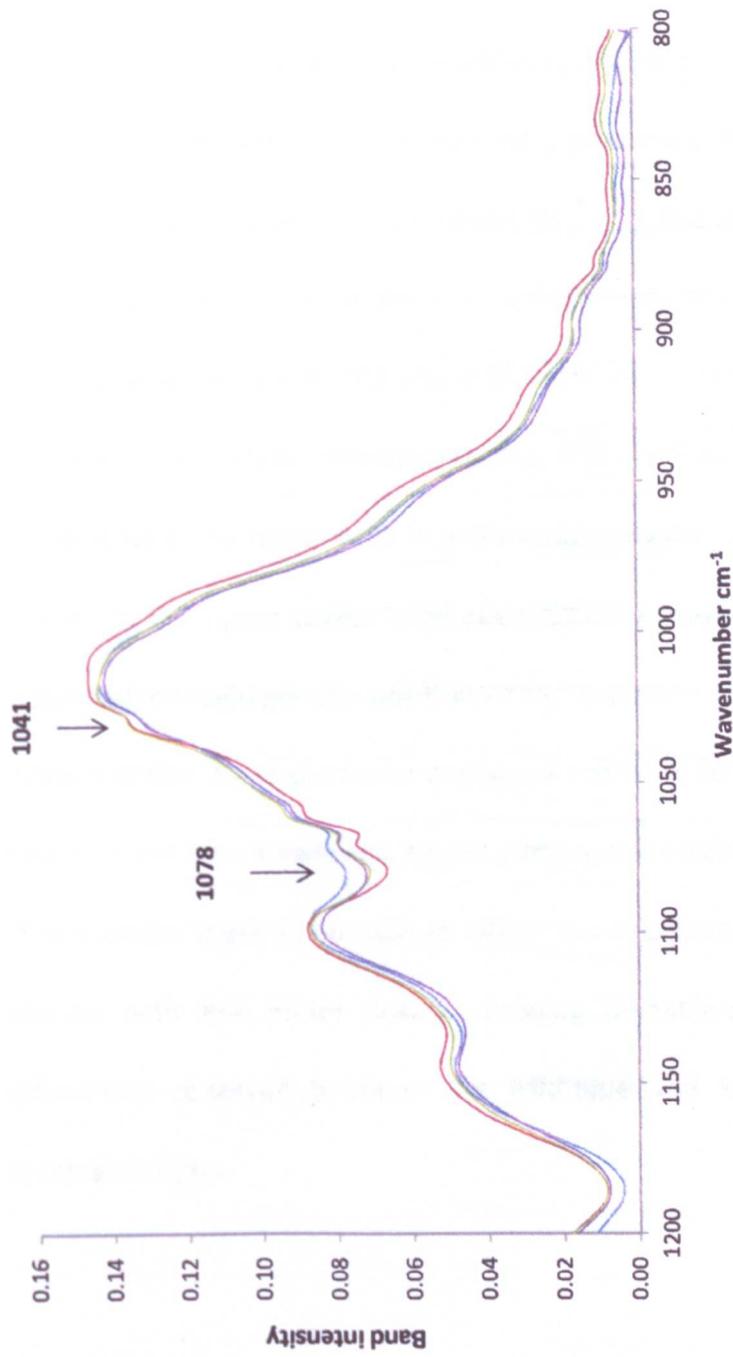
Figure 4-8 FT-IR Spectra of wild type and *rabA4* knockout lines

FT-IR spectra of *rabA4* knockouts, showing fingerprint regions for hemicellulosic functional groups. Wild type (light blue) against knockout lines *rabA4a* (red), *rabA4b* (green) and *rabA4e* (purple)

The FT-IR results were subjected to a principal component (PCA) analysis. To achieve this data for each replicate was taken between wavenumbers 1200-800cm^{-1} and used to formulate the matrix for the analysis (as described in section 2.26). The statistical package then formulated a biplot which is shown in figure 4-9, to which circles were added to define grouping on the PCA. From the statistical data the residuals formed 2 principal components of variation. These principal components represent PC1 and PC2 on the axis and in the figure legend. The total variation accounted for by PC1 was found to be 0.59 and the variation due to PC2 was 0.39, with the remaining variation totalled by several minor <0.01 components. The PCA contained 3 main clusters with the wild-type and *rabA3* each in a standalone cluster either side of the main cluster. In the figure circles have been drawn around the plots in the main cluster which highlight the position of the sub-clades. These circles highlight clusters within the main cluster and show a definite split between all the sub-clades of the *rabA* knockouts. Noteworthy is that despite the arbitrary nature of the circles there is no case in which the knockouts from the sub-clades overlap with the circles drawn, showing a statistical confidence in the differences observed between the wild-type and knockout line in FT-IR spectral analysis.
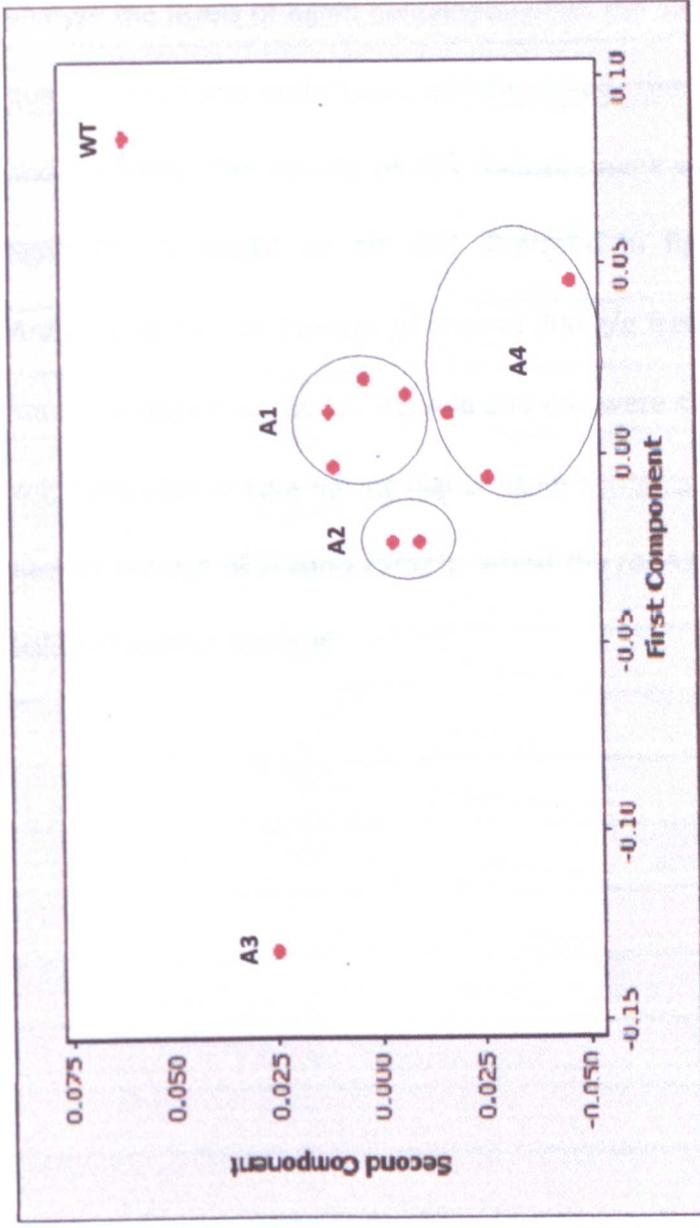
Figure 4-9 Principal component analysis (PCA) of FT-IR spectra of Arabidopsis stem

Principle component analysis produced using the MiniTab statistics program from the data of the polysaccharide fingerprint region

of 1200-800 wavenumbers. The total number of principle components identified was 5, PC1 =0.59 PC2 =0.39, with the remaining

components each totalling less than 0.1 of the variation.

4.3 Lignin analysis

Out of all the cell wall components discussed in the introductory chapter, lignin was only one which was not analysed in the cell wall fractionation. To analyse the levels of lignin contained within the sample material a direct UV quantification was undertaken directly milled stem as described in materials and methods. The results of this measurement were converted into mg/g lignin (fresh weight or AIS and displayed in figure 4-10. The wild-type *Arabidopsis* had an average of around 20mg/g fresh weight of lignin. Of the knockout lines only *rabA1i, A3, A4a and A4e* were significantly different to the wild type with all four having higher lignin contents. The *rabA1i, A4a and A4e* had an average of around 25mg/g, whilst the *rabA3* line had an average lignin value of around 30mg/g.
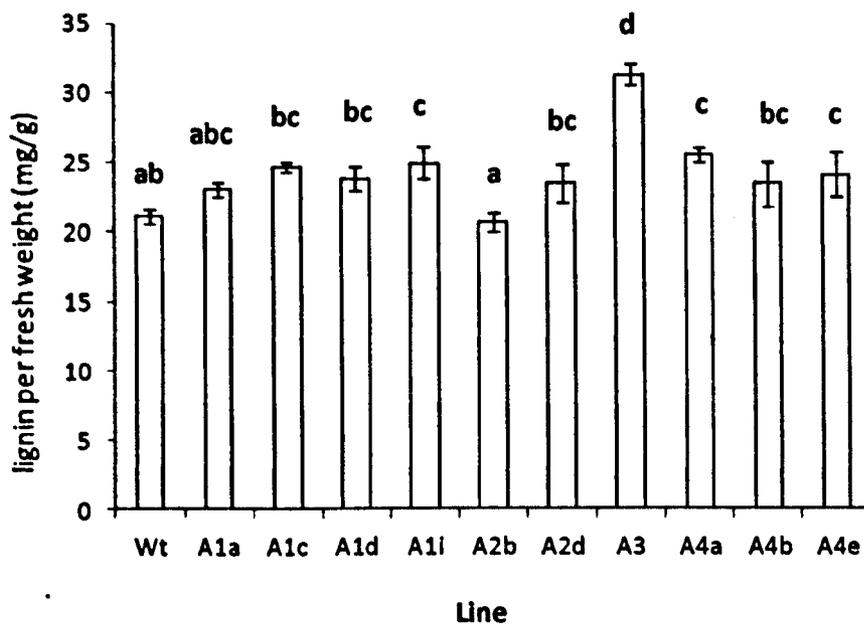
Figure 4-10 Compositional comparison of wild type and knockout lines and lignin

Amount of lignin contained in dry *Arabidopsis* stem biomass. The error bars show standard deviation from the mean of 3 replicates, with each replicate being a pooled composite of 50 plants. The statistical values are as follows; p <0.001 (d.f,32 v.r,20.36) with letters annotating groups of means defined by Tukey test.

4.4 Metal ion analysis

With the major cell wall polymers analysed and differences observed the question was asked as to whether there would be any differences in mineral composition of the *Arabidopsis*. This question was particularly interesting in terms of a reduction in the proportion of pectin, which is known to form calcium bridges, in the egg box structure. To do this wild type and knockout lines of *Arabidopsis* were grown in glasshouse conditions with every effort made to control mineral availability, the plants were allowed to undergo

senescence fully dried.. The samples were then hydrolysed with strong acid

and hydrogen peroxide at high temperature and sent for ICP-MS analysis and

the results are shown in figures 4-11 to 4-14.

Figure 4-11 displays the levels of sodium in wild-type *Arabidopsis* stem in

comparison with the knockout lines. The wild-type samples had a total of

around 7mg/g dry weight of sodium. Only two knockout lines- A1a and A1i -

were found to be significantly different to wild-type. Thus there were no

consistent trend differences seen between the sub clades and the wild type

plants.
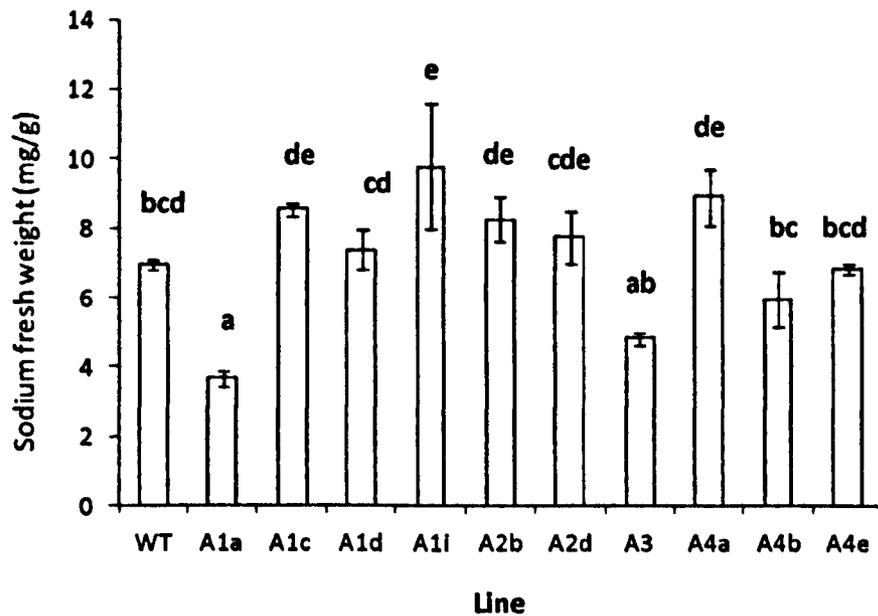
Figure 4-11 Sodium content of wild-type and knockout lines

Amount of sodium contained in dry *Arabidopsis* stem biomass. The error bars show

standard deviation from the mean of 3 replicates, with each replicate being a pooled

composite of 50 plants. The statistical values are as follows; p<.001 (d.f,32 v.r, 17.72)

with letters annotating groups of means defined by Tukey test.

110

Figure 4-12 shows levels of magnesium in the wild-type and knockout lines. The data displayed shows a compositional total of around 14mg/g of magnesium within the wild-type, with the knockout lines ranging from around 8-17mg/g. All lines apart from A1c, A3 and A4b where to be significantly different to wild-type. Thus only sub clade 2 showed a consistent trend but the results in general were highly variable.
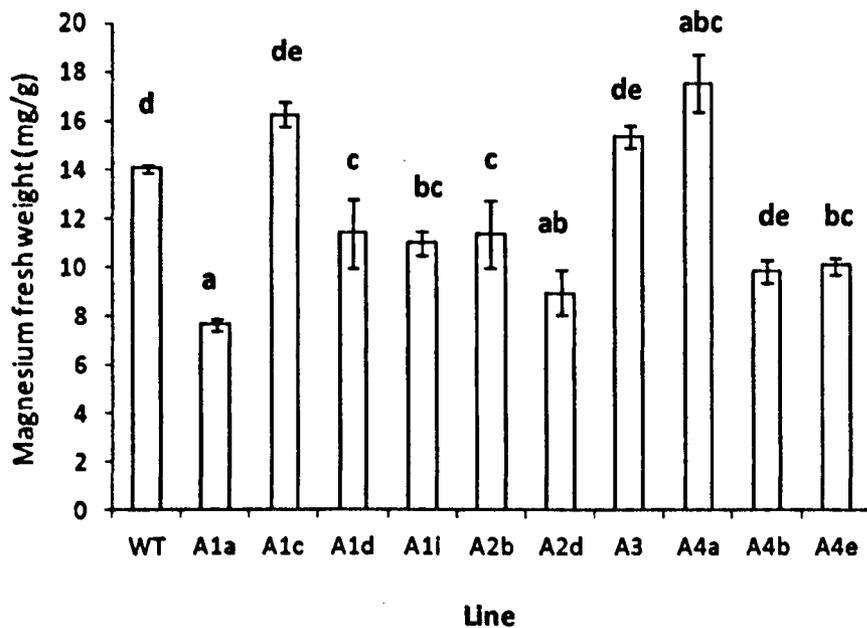
Figure 4-12 Magnesium content of wild-type and knockout lines

Amount of magnesium contained in dry *Arabidopsis* stem biomass. The error bars show standard deviation from the mean of 3 replicates, with each replicate being a pooled composite of 50 plants. The statistical values are as follows; p<.001 (d.f,31 v.r, 47.02) with letters annotating groups of means defined by Tukey test.

Figure 4-13 shows the results for Potassium. Potassium gave the highest level of all the minerals analysed in wild-type, giving a total of around 40mg/g. The data produced was also the least variable and with only one line (A1a) significantly varying from wild-type.
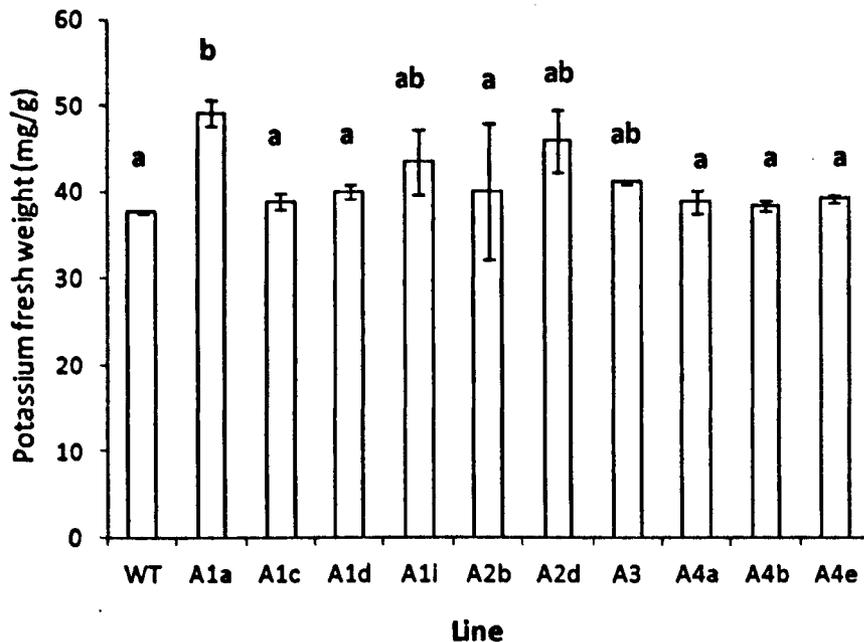
Figure 4-13 Potassium content of wild-type and knockout lines

Amount of potassium contained in dry *Arabidopsis* stem biomass. The error bars show standard deviation from the mean of 3 replicates, with each replicate being a pooled composite of 50 plants. The statistical values are as follows; p=.002 (d.f,32 v.r, 4.48) with letters annotating groups of means defined by Tukey test.

Calcium levels in the wild-type and knockout lines are shown in figure 4-14. From the data shown it was determined that the average calcium level in the wild-type was around 17mg/g. The wild-type was significantly different to all

the lines analysed except for A1c, A3 and A4a. The only consistent sub clade

was A2 with both members showing reduced levels of calcium.
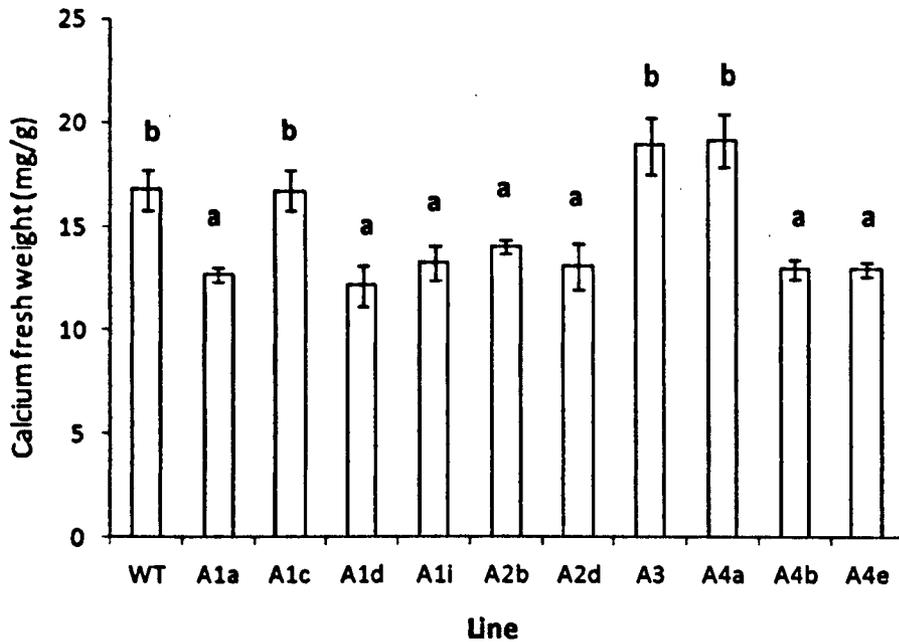
**Figure 4-14 Calcium content of wild-type and knockout lines**

Amount of calcium contained in dry *Arabidopsis* stem biomass. The error bars show

standard deviation from the mean of 3 replicates, with each replicate being a pooled

composite of 50 plants. The statistical values are as follows; $p < .001$ (d.f,32 v.r25.08)

with letters annotating groups of means defined by Tukey test.

5 Effect of Rab GTPase knockouts on stem digestibility

The previous chapter suggested that the Rab knockout lines appear to have had an effect on cell wall composition. This chapter aims to determine whether this has any accompanying effect on cell wall digestion. To answer this question, lines were subjected to a standard pre-treatment and enzymatic hydrolysis (cellulase) and the amount of glucose released determined.

5.1 Selection of *Arabidopsis* pre-treatment conditions

A crucial first step in evaluating the digestion profile of any samples put through a digestion assay is the pre-treatment optimisation. For purposes of Industry the key factors in pre-treatment are percentage glucose released and time taken. However, for the purposes of this thesis the key factor in pre-treatment is the identification of conditions for the release of 50% of the total glucose in the sample. This 50% release allows the identification of both increased and decreased digestion efficiencies, which are both of interest in their own right. Unfortunately as stated in the introduction at the time of writing no pre-treatment had been described within the literature. In this section a variety of different pre-treatment methods were used; these being a mild pre-treatment, which uses a temperature of 121°C and the moisture

content of the sample; a moderate pre-treatment at the same temperature and pressure and dH_2O added; and a severe pre-treatment consisting of the mild treatment conditions and 1% H_2SO_4. Time of exposure was also varied with a 10, 20 and 30 minute exposure time for each treatment. Following the pre-treatment the residue was collected and dried, the glucose content of the residue determined using enzyme hydrolysis and HPAEC as described in materials and methods. The results are expressed as the percentage of the glucose in the residue. Analyses of variances were conducted at the 6 and 24 hours, with 6h representing the end of the log phase, and 24 hours being a final end point. The results of these experiments are shown in figures 5-1 through 5-3.

Figure 5-1 shows the percentage glucose release when wild-type sample are exposed to the mild pre-treatment conditions. Analysis of untreated sample shows a total release of around 15% after 24 hours and with a total of 12% release after 6 hours incubation. The time required for 50% of the total hydrolysed glucose to be released was around 4 hours of incubation. With a mild treatment of heat, pressure and moisture glucose release was increased significantly after 24 hours with all the time exposures tested (p=<.001, p=.01, p=<.001 for 10, 20 and 30 minutes respectively). The total glucose released was around 35%, 40% and 40% respectively, with a total release after 6 hours of around 25%, 35% and 40% and was significantly increased compare with wild-type (p=.007, p=.01, p=<.001 for 10, 20 and 30 minutes respectively).

Half of the total hydrolysed glucose was released after around 3 hours with a

mild treatment for 10 minutes, after 3 hours with a 20 minute and after 2

hours with 30 minutes. Through analysis of the means it was found that after

24 hours of incubation there was no statistical difference between the length

times of exposure to the treatment.
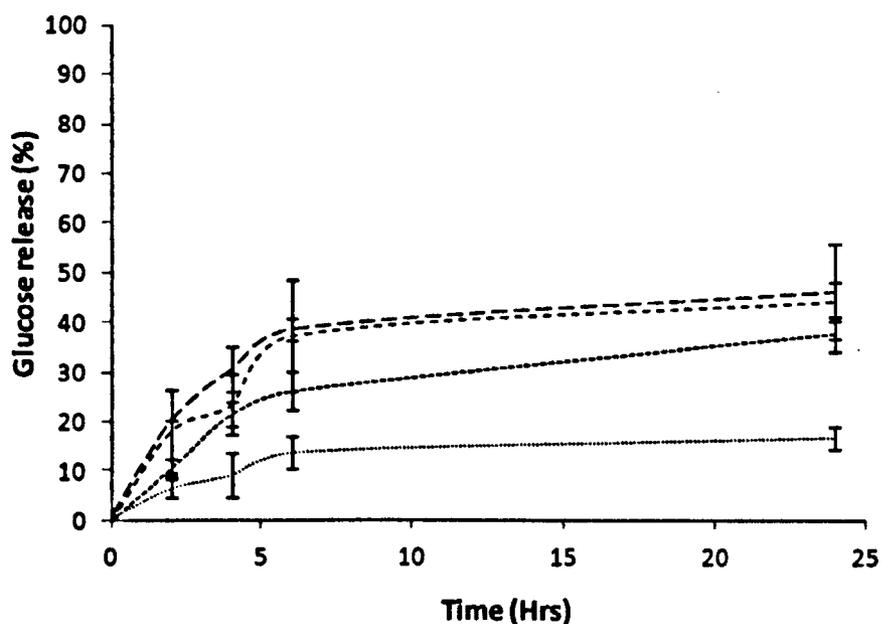
Figure 5-1 Saccharification of *Arabidopsis* stem biomass with mild pre-treatment

Saccharifications of wild-type stem biomass over 10, 20 and 30 minutes. Error bars

show standard deviation from the mean, of 3 replicates, each replicate being a

composite of 50 plants. Key; Untreated (round dot); Mild 10 minute (short dash);

Mild 20 minute (dash); Mild 30 minute (long dash)
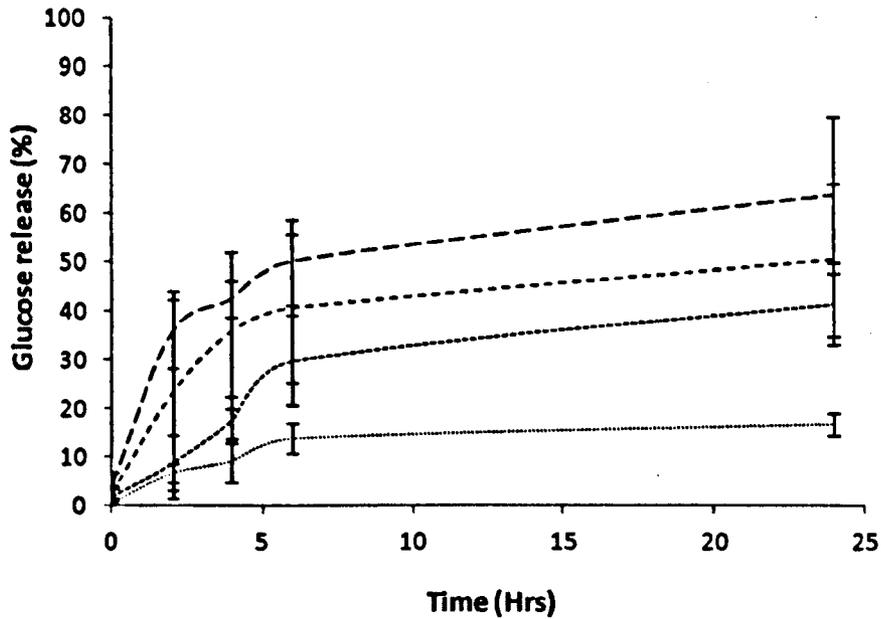
Figure 5-2 Saccharification of *Arabidopsis* stem biomass with moderate pre-treatment

Saccharifications of wild-type stem biomass over 10, 20 and 30 minutes. Error bars show standard deviation from the mean, of 3 replicates, each replicate being a composite of 50 plants. Key; Untreated (round dot); Moderate 10 minute (square dot); Moderate 20 minute (dash); Moderate 30 minute (long dash)

The data in figure 5-2 relate to the percentage total glucose release upon moderate treatment. In this case the treatment was H_2O. The data for the untreated sample is the same throughout all the varying degrees of pre-treatment. With H_2O pre-treatment a total percentage glucose of around 40, 50 and 60 can be solubilised after exposure to the treatment for 10, 20 and 30 minutes respectively after 24 hours. After 6 hours of the percentage total glucose released was around 25, 40 and 50 for 10, 20 and 30 minutes exposure to treatment. The midpoint of glucose released was around 4 hours

for 10 minutes exposure and around 2 hours for 20 and 30 minutes exposure. Statistical analysis was performed by t-test and showed a significant difference between the untreated and treated for 10 minutes after both 6 and 24 hours (p=.02, p=.003). This significant difference from wild-type was also shown for the 20 and 30 minute exposure at 6 and 24 hours (20 minutes; p=.02, p=.01; 30 minutes; p=<.001, p=.002). The difference between the 3 exposure times was tested for statistical significance. The length of exposure was significantly different after 6 and 24 hours between 10 minutes and 30 minutes (p=.02, p=.05).

Figure 5-3 shows the digestion curves with severe pre-treatment. Here 1% H_2SO_4 was used with expectation of a 100% glucose release. Again the untreated data is the same as for the other treatments (discussed above). By the 24 hour time point the total glucose released for 10, 20 and 30 minutes exposure, was around 65%, 80% and 85% respectively. After 6 hours the total release was around 55% for 10 minutes and around 65% for 20 and 30 minutes exposure. The midpoint for glucose release was achieved after 2 hours for all the different exposure times. Statistical analysis of the data showed that after 6 hours the treatment at all exposure times was significantly different from untreated (10 minute; p=<.001; 20 minute; p=.04; 30 minute; p=<.001). This trend was continued through to 24 hours, with the treated samples being significantly different regardless of exposure time (10 minute; p=<.001; 20 minute; p=<.001; 30 minute; p=<.001).
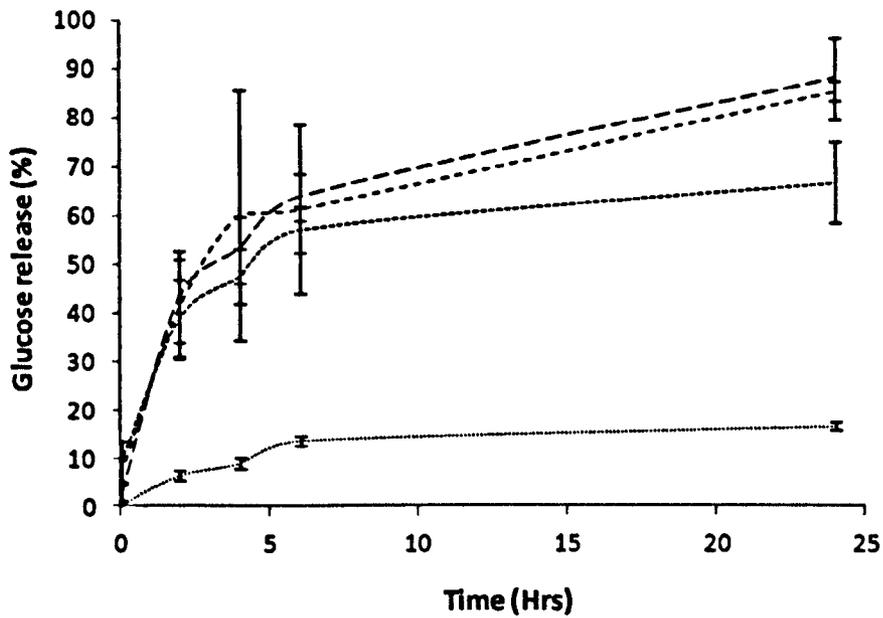
Figure 5-3 Saccharification of *Arabidopsis* stem biomass with moderate pre-treatment

Saccharifications of wild-type stem biomass over 10, 20 and 30 minutes. Error bars show standard deviation from the mean, of 3 replicates, each replicate being a composite of 50 plants. Key; Untreated (round dot); Severe 10 minute (square dot); Severe 20 minute (dash); Severe 30 minute (long dash)

5.2 Saccharification of *rabA* knockouts pre-treated stem biomass

With a pre-treatment condition selected the next question was whether the knockout lines established in chapter 3 would digest at a rate differing from

the wild-type. To achieve this pre-treatment in H_2O at 121°C, for 20 minutes was chosen, as it gave the most reproducible glucose release of around 50%. Stem tissue from wild type and knockout lines was milled and subjected to the "standard" pre-treatment as described above. The dried residues were then assessed for glucose content and the results are shown in figure 5-4 in all cases the pre-treatment produced an average glucose 85%. The residues from this pre-treatment were then subjected to hydrolysis with cellulase enzymes and the percentage glucose released recorded over 24 hours
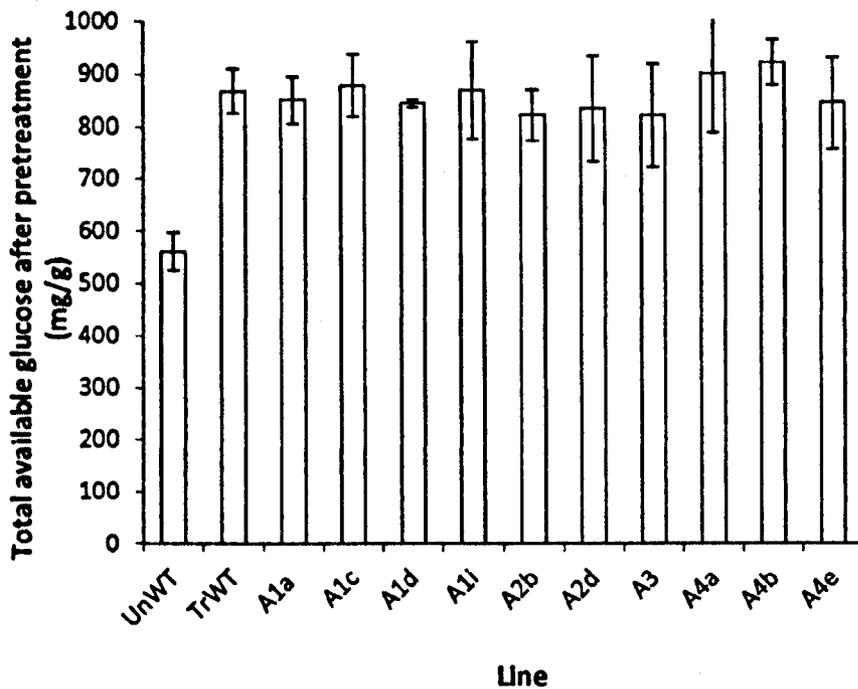
Figure 5-4 Total available glucose for hydrolysis after pre-treatment. Available glucose from acid hydrolysis untreated, pre-treated and Rab knockouts. The error bars show standard deviation from the mean, of 3 replicates, each replicate being a composite of 50 plants. Key: UnWT = Untreated WT; TrWT = pre-treated WT; Remaining correspond to their individual Rab gene.

The results from the digestion assay in respect to the knockout lines for the RabA1 sub-clade are shown in figure 5-5. These data show that the pre-treatment for wild-type resulted in around 50% of the total glucose being released over 24 hours, with around 25% of the total released after 6 hours, with this also representing the midpoint of the total glucose release. With respect to the knockout lines, all the RabA1 mutants analysed released around 50% of the total glucose after 24 hours of incubation. Using t-test analysis showed that there was no statistical difference between the wild-type and knockouts after 24 hours (rabA1a; p=0.4; *rabA1c;* p=0.3; *rabA1d*; p=0.4; *rabA1i* p=0.3). The midpoint of glucose release was achieved by all the knockout lines and the wild-type at around 4 hours, after 6 hours only *rabA1c* mutant did not have around 25% of the total glucose released with a total of around 20% released. Statistical analysis showed the knockout lines to be insignificantly different from the wild-type (*rabA1a*; p=0.3; *rabA1c*; p=0.08; *rabA1d*; p=0.4; rabA1i p=0.4).
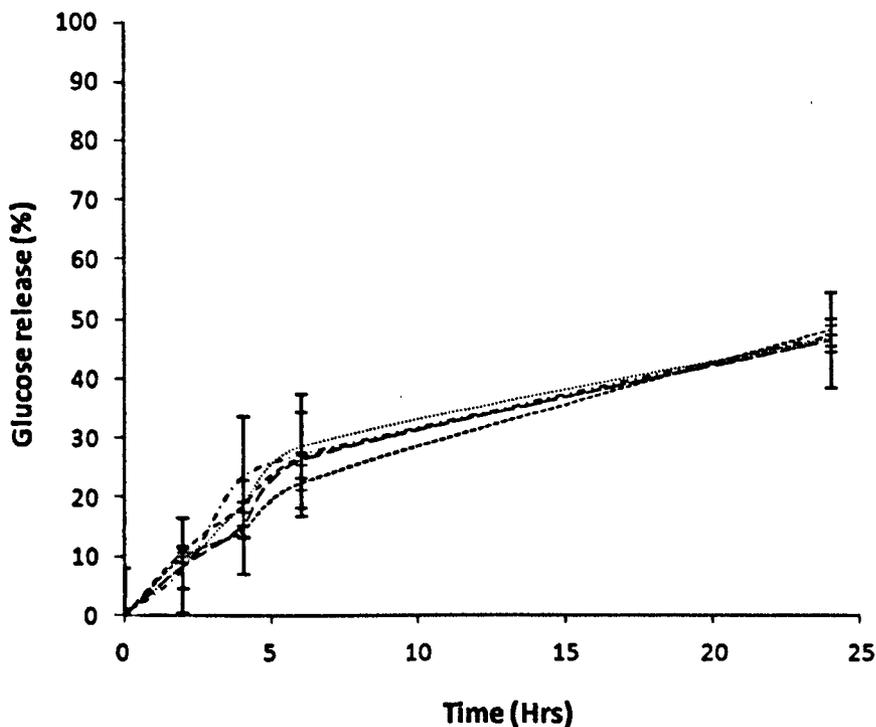
Figure 5-5 Saccharification of pre-treated *rabA1* knockouts

Glucose released upon saccharification of pre-treated *rabA1*knockouts. Error bars

showing standard deviation from the mean, of 3 replicates of 50 plants per replicate.

Key; Wild-type (long dash); *rabA1a* (round dot); *rabA1c* (square dot); *rabA1d* (dash)

rabA1i (dash dot)

Figure 5-6 shows the data produced from the digestion assay with respect to

the wild-type against the *rabA2* knockout lines. Data in relation to wild-type is

as described above. The total glucose released after 24 hours was around 50%

for both the knockout lines in the A2 sub-clade. Statistical analysis showed

that there was no significant differences between the wild-type and

knockouts (*rabA2b*; p=0.2; *rabA2d*; p=0.2). The midpoint of the total glucose

released was around 4 hour for both knockout lines in comparison to 6 hours

for wild-type. After 6 hours the percentage glucose release was around 30%

for *rabA2b* and around 40% for *rabA2d*. Statistical analysis showed that

rabA2d was significantly different to wild-type at this time point (p=0.02)

however, *rabA2b* was not significantly different (p=0.1).
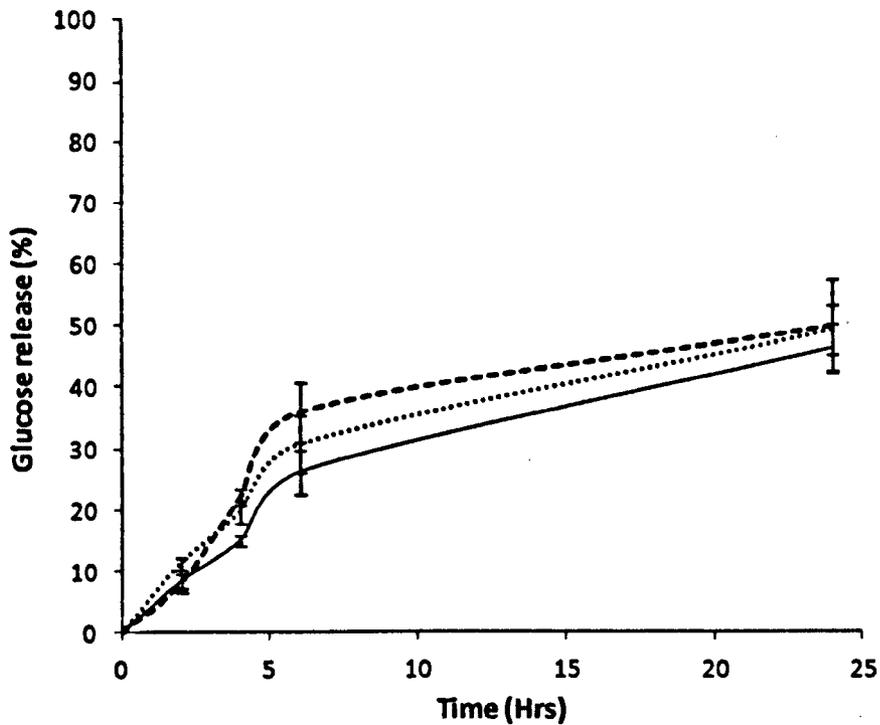
Figure 5-6 Saccharification of pre-treated *rabA2* knockouts

Glucose released upon saccharification of pre-treated *rabA2* knockouts. Error bars

showing standard deviation from the mean, of 3 replicates of 50 plants per replicate.

Key; Wild-type (solid); *rabA2b* (round dot); *rabA2d* (square dot)

Data in figure 5-7 show the digestion assay of wild-type compared to the

rabA3 knockout line. The glucose release data for the pre-treated wild-type

was discussed above. The total glucose released with the *rabA3* mutant after

24 hours was around 35% of the total available glucose. With statistical analysis *rabA3* was found to significantly decrease hydrolysed glucose after 24 hours (p=0.02). The midpoint for glucose release was around 5 hours, which was the same as the wild-type from the data shown. After 6 hours the level of glucose release in *rabA3* knockout was around 25%, with the wild-type being around 30%. Statistical analysis of this time point shown no significant difference between the wild-type and knockout line (p=0.2)
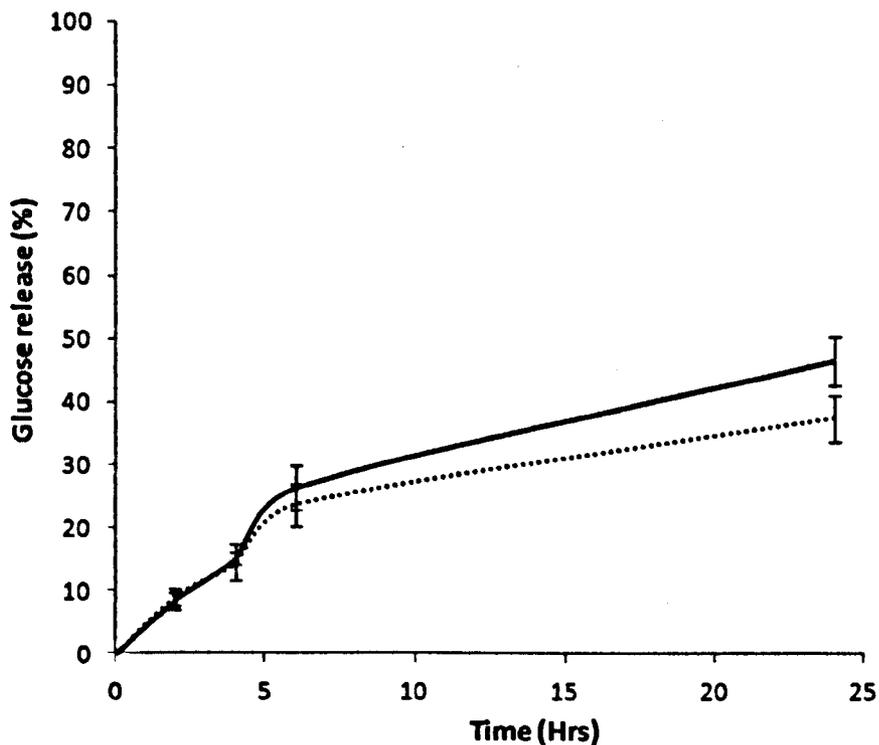
Figure 5-7 Saccharification of pre-treated *rabA3* knockouts

Glucose released upon saccharification of pre-treated *rabA3* knockouts. Error bars showing standard deviation from the mean, of 3 replicates of 50 plants per replicate.

Key; Wild-type (solid); *rabA3* (round dot)

Digestion data for the final sub-clade, RabA4 is shown in figure 5-8. After 24 hours of incubation the knockout lines analysed produced an increased level of glucose release. The average glucose hydrolysed was around 70% for *rabA4a*, around 65% for *rabA4b* and around 75% for *rabA4e*, compared with the 50% glucose released from the wild-type. Statistical analysis showed a significant difference between each line and wild-type (*rabA4a*; $p = <0.001$; *rabA4b*; $p = <0.001$; *rabA4e*; $p = <0.001$). The midpoint of the glucose release with the knockout lines was around 5 hours into incubation, showing 50% of the final glucose released was achieved 1 hour earlier in the knockout lines, when compared with the wild-type. After 6 hours the average glucose release was around 50%, 55%, 40%, for *rabA4a rabA4b* and *rabA4e*, respectively. Statistical analysis showed these differences to be significantly different from wild-type (*rabA4a*; $p = 0.01$; *rabA4b*; $p = <0.001$; *rabA4e*; $p = <0.001$).
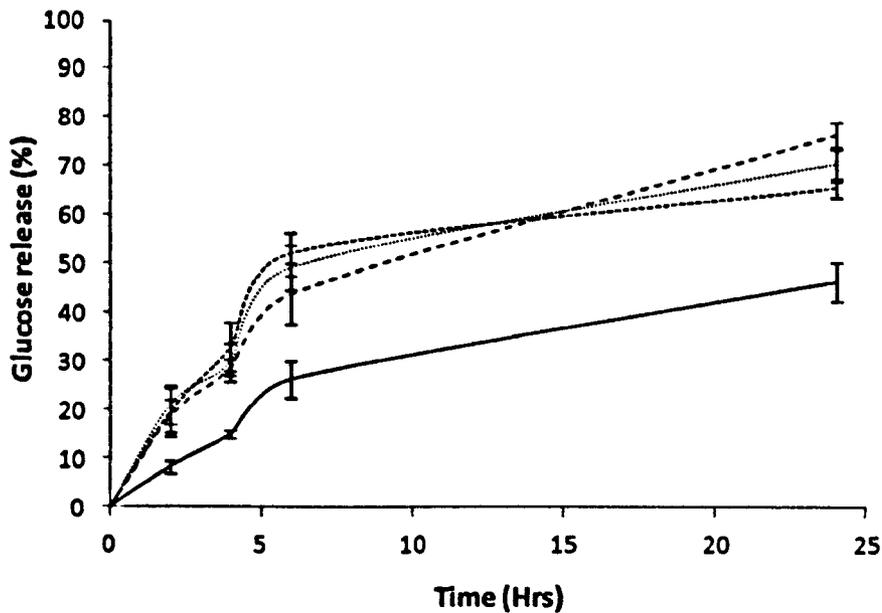
Figure 5-8 Saccharification of pre-treated *rabA4* knockouts

Glucose released upon saccharification of pre-treated *rabA4* knockouts. Error bars showing standard deviation from the mean, of 3 replicates of 50 plants per replicate.

Key; Wild-type (solid); *rabA4a* (round dot); *rabA4b* (square dot); *rabA4e* (dash)

5.3 Saccharification of *rabA* knockouts untreated stem biomass

In the light of the statistically significant different digestion rates shown above for stem tissue following pre-treatment the question was asked whether these lines would also show reduced recalcitrance in untreated feedstock. To do this the experiment was repeated as above but without any pre-treatment. Milled stem tissue was assessed for glucose content and then subjected directly to enzyme digestion. Again results are presented as

126

percentage of total glucose released over time. The glucose content of the wild type and knockout lines is shown in figure 5-9 in most case the average available glucose was around 55%, with around 45% in the *rabA2* knockouts.
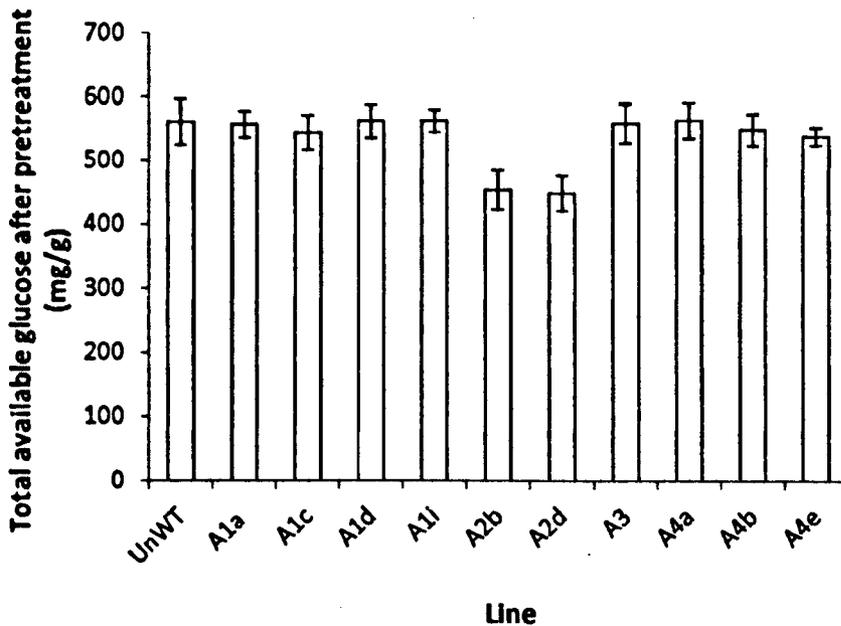
Figure 5-9 Total available glucose for hydrolysis before pre-treatment. Glucose released upon saccharification of pre-treated *rabA4* knockouts. Error bars showing standard deviation from the mean, of 3 replicates of 50 plants per replicate.Key: UnWT = Untreated WT; Remaining correspond to their individual Rab gene.

Results comparing digestion of *rabA1* with wild-type are shown in figure 5-10. All RabA1 knockout lines gave a digestion of between 12 and 20% of the total glucose available, comparable to the wild-type glucose release of around 12% after 24 hours. Statistical analysis found a significant difference between the *rabA1c* mutant and wild-type (p=0.008) however, the biological significance of

127

these results is doubtful. The midpoint of glucose release was achieved for all lines tested around 2 hours of incubation. After 6 hours the knockout lines had achieved around 15% total glucose release, with *rabA1c* being slightly higher around 20%, compared with wild-type digestion of around 10%. Statistical analysis found significant differences between wild type and *rabA1c* and *rabA1d* (p=0.03; p=0.01, respectively).

The digestion data for the RabA2 knockout lines are shown in figure 5-11. Here after 24 hours *rabA2b* and *rabA2d* had a glucose release of 20 and 15% respectively, compared with around 12% digestion in wild-type. Statistical analysis of the data showed no significant differences between knockout lines and wild-type. The midpoint of the total glucose release was achieved after 3 hours for both knockout lines and wild-type. After 6 hours *rabA2b* and *rabA2d* had a glucose release of 15%, compared with around 10% digestion in wild-type. Using statistical analysis both knockout lines were found to be significantly different from wild-type after 6 hours, as with the RabA1 lines though it is unlikely that this is biologically meaningful.
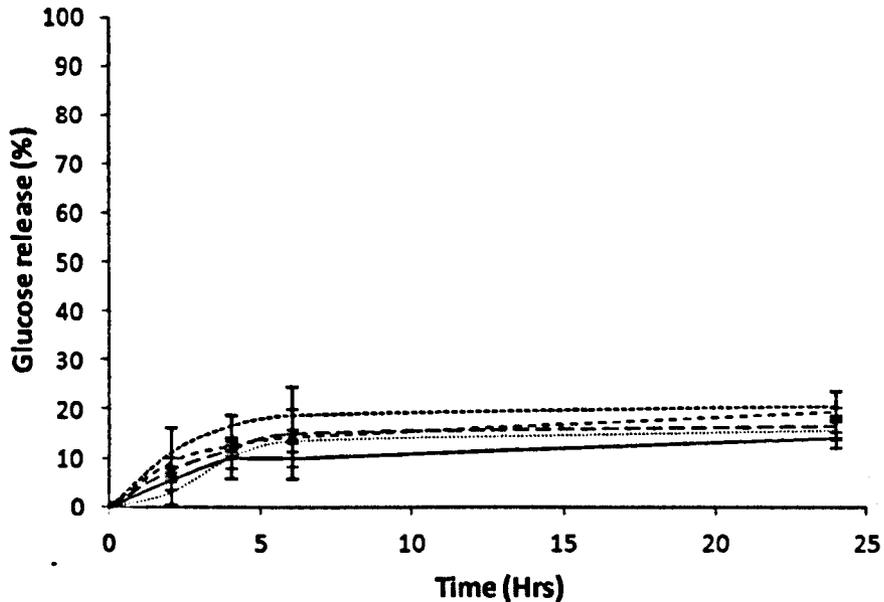
Figure 5-10 Saccharification of untreated *rabA1* knockouts

Glucose released upon saccharification of untreated *rabA1* knockouts. Error bars

showing standard deviation from the mean, of 3 replicates of 50 plants per replicate.

Key; Wild-type (solid); *rabA1a* (round dot); *rabA1c* (square dot); *rabA1d* (dash)

rabA1i (long dash)

Data in figure 5-12 show the digestion pattern of *rabA3* against wild-type. Samples taken at 24 hour show that *rabA3* had total glucose release of around 12%, the same as the wild-type. Similar patterns are also shown at the midpoint and 6 hour time point, with both the knockout line and wild-type having a midpoint of 2 hours and 10% glucose release. Statistical data also support this with no significant differences at either time point (p=0.4; p=0.4 respectively).
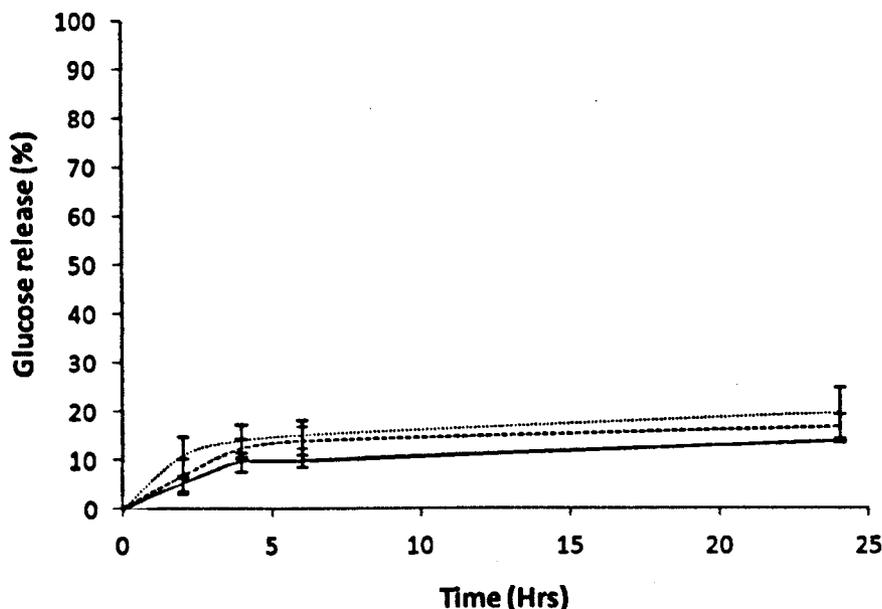
Figure 5-11 Saccharification of untreated *rabA2* knockouts

Glucose released upon saccharification of untreated *rabA2* knockouts. Error bars

showing standard deviation from the mean, of 3 replicates of 50 plants per replicate.

Key; Wild-type (solid); *rabA2b* (round dot); *rabA2d* (square dot)

Data for RabA44 digestion are shown in figure 5-13. The total glucose

hydrolysed after 24 hours was around 30% for all the knockout lines,

compared with 12% from the wild-type feedstock. The midpoint of glucose

release for the lines was achieved around 4 hours into the assay, compared

with 3 hours in the wild-type. The total glucose release by 6 hours varied

between all the lines being 25, 20 and 16%, respectively, compared with 10%

in the wild-type. The data were run through a t-test for purposes of statistical

analysis. All members of the RabA4 sub-clade were found to be significantly

different from wild-type at both 6 and 24 hours incubation, giving a p value in

all cases of less than 0.001.
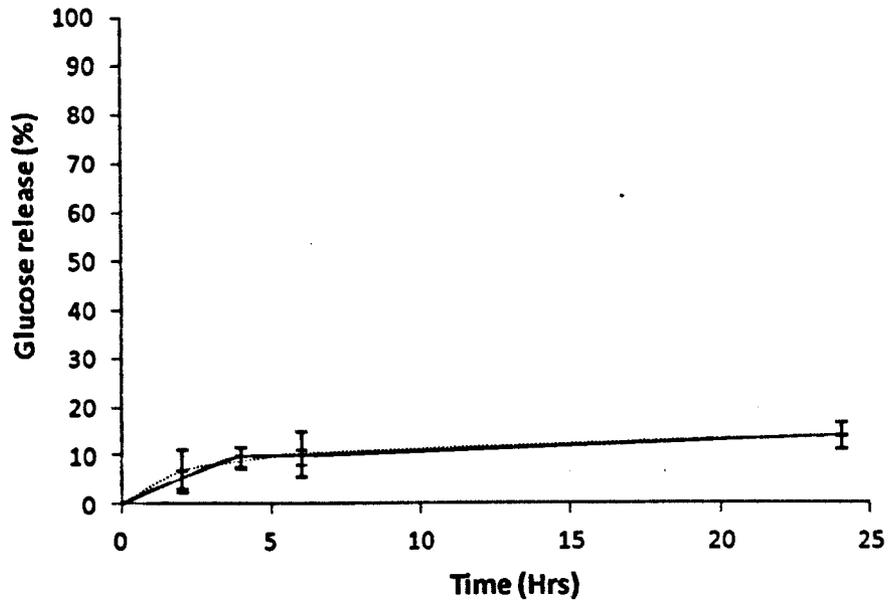
Figure 5-12 Saccharification of untreated *rabA3* knockouts

Glucose released upon saccharification of pre-treated *rabA4* knockouts. Error bars

showing standard deviation from the mean, of 3 replicates of 50 plants per replicate.

Key; Wild-type (solid); *rabA3* (round dot)
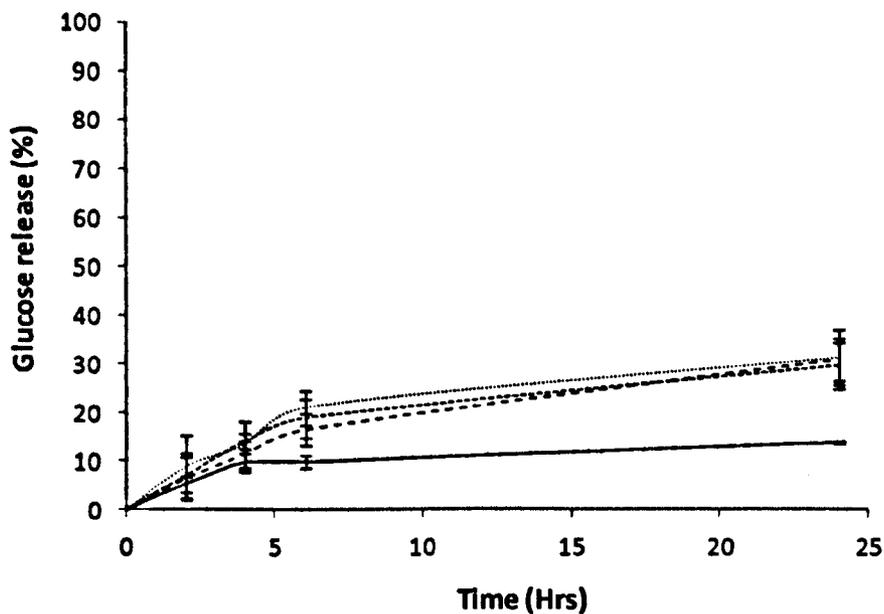
Figure 5-13 Saccharification of untreated *rabA4* knockouts

Glucose released upon saccharification of pre-treated *rabA4* knockouts. Error bars

showing standard deviation from the mean, of 3 replicates of 50 plants per replicate.

Key; Wild-type (solid); *rabA4a* (round dot); *rabA4b* (square dot); *rabA4e* (dash)

5.4 X-ray diffraction analysis

With the changes observed in both the biochemistry and digestion shown in

the previous and current chapters, it was interesting to ask whether any of

these knockouts had caused changes in the cellulose crystal structure.

Particularly of interest were the *rabA4* mutants which showed increased

digestion. To do this, one knockout line from each of the 4 sub clades was

chosen to represent the clade and subjected to X-ray diffraction analysis, the

results of which are shown in table 5-1. The data show the shown the unadjusted crystallinity around 26%. To get the actually crystallinity in the sample the adjusted values need to be corrected using the total cellulose in the sample. After this calculation there was a cellulose crystallinity of 63.2% in wild-type. With analysis by t-test there was found to be a statistical difference only between the wild-type and the *rabA2b* knockout line. All Rab knockout lines had a lateral dimension similar to expected values of between 2 and 3. Upon statistical analysis there was no significant differences found.

Table 5-1 Analysis of cellulose crystallinity by X-ray diffraction

Sample	Crystllinity %	Cellulose adjusted crystallinity	lateral dimension (nm)
WT	26 ± 1.5	63.2 ± 3.6	2.6
A1a	28 ± 1.5	57.8 ± 3.9	2.2
A2b	28 ± 1.5	74.7 ± 4.3	2.6
A3	23 ± 1.5	65.4 ± 3.9	2.5
A4a	26 ± 1.5	67.0 ± 4.0	2.5

6 Phenotypic analysis of RabA clade Knockouts

With both biochemical and digestion differences shown in the chapters above, it was important to test the knockout lines for the presence of any distinguishable phenotype. This was important both in terms of characterisation of any effects of the cell wall compositional changes and for the possibility of producing a viable bioenergy crop utilising knockouts in the genes shown. To achieve this in depth phenotypic analysis was decided upon based around the method described by Boyes *et al.* 2001. Stages were selected incorporating early plant development, leaf emergence, stem development and seed production. All the following growth points were chosen as key to development of a functional agronomic crop. Furthermore initial microarray data did not include a complete expression pattern across all tissues and as such effects could potentially occur in tissues other than the stem. All data shown is a composite of 3 replicates each comprising of 10 individual plants.

6.1 Growth analysis on plate

Early growth stage analysis focuses on the first 10 days of plant development, dealing with radicle and cotyledon emergence. These data were taken using seeds grown on agar plates under growth room conditions.

Data shown in figure 6-1 relates to radicle emergence from the seed. Data collected shows that wild-type radicle emergence was between 4 and 5 days. The knockout lines analysed had similar emergence times to wild-type.
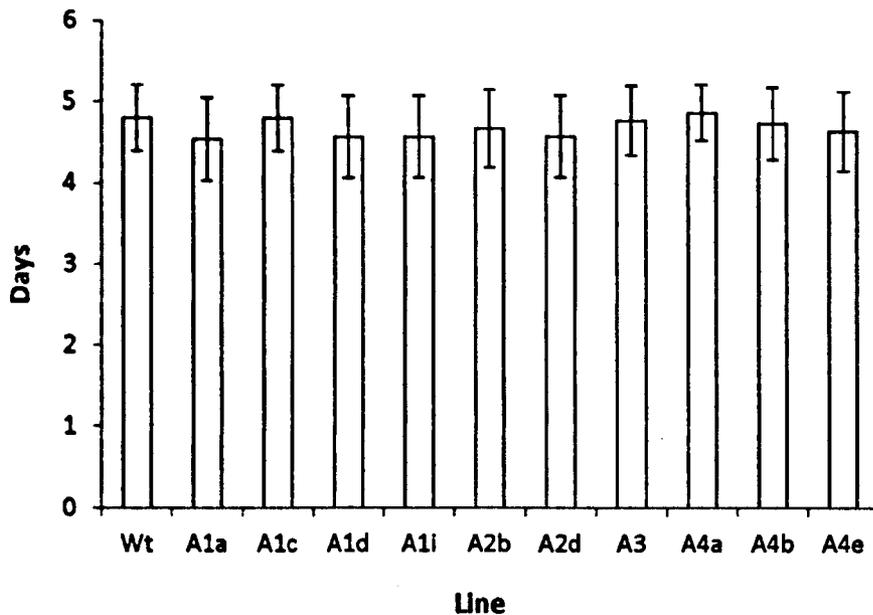
Figure 6-1 Time to radicle emergence of wild-type and knockout lines

Time to radical emergence in days of wild-type col-1 compared with the knockout lines, with error bars representing standard deviation from mean of 3 replicates of 10 plants.

Figures 6-2 and 6-3 show the data for cotyledon emergence, number and time of opening. Wild-type plants had cotyledon emergence around 5-6 days, with the cotyledons opening around 6-7 days, 1 day after the emergence. Cotyledon number for wild-type was the expected 2 for the dicotyledonous *Arabidopsis*. Again with all cotyledon data all knockout lines displayed 2

cotyledons with emergence being around 6-7 days and opening of the cotyledons around 1 day later.
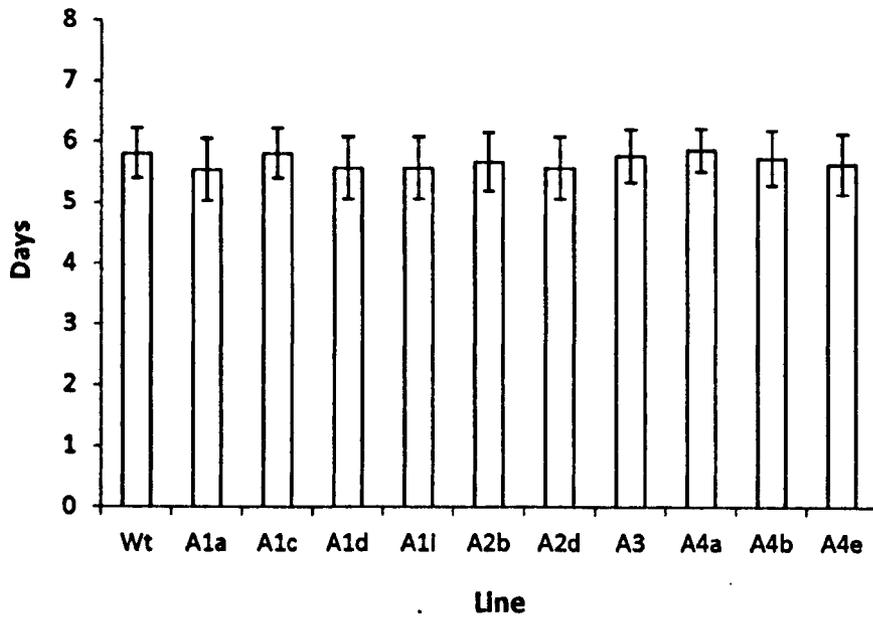
Figure 6-2 Time to cotyledon emergence in wild-type and knockout lines

Time in days until both cotyledons being visible in wild-type col-1 compared to the knockout lines. Error bars shown represent standard deviation of the mean of 3 replicates of 10 plants.
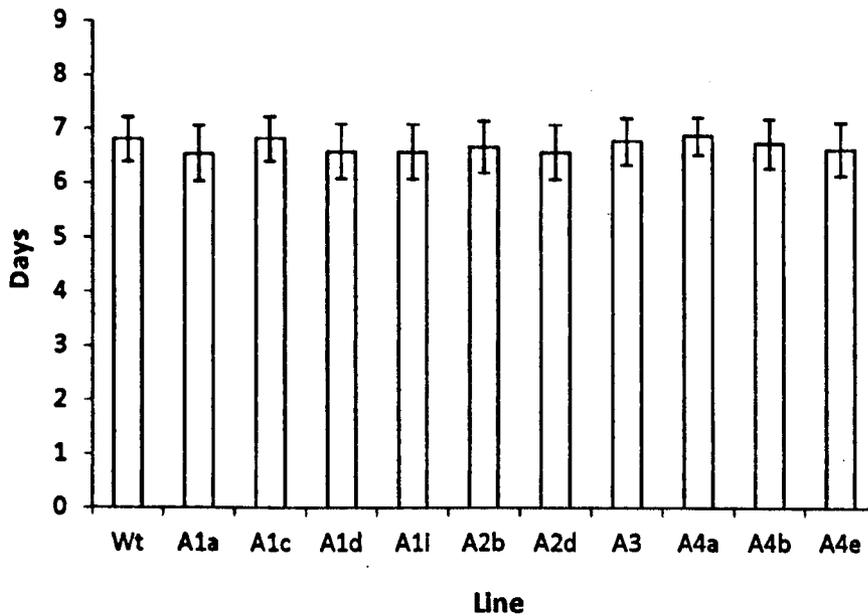
Figure 6-3 Time to opening of cotyledons in wild-type and knockout lines

Time in days until the cotyledons have fully opened in wild-type col-1 compared to the knockout lines. Error bars representing standard deviation from the mean of 3 replicates of 10 plants.

6.2 Root analysis

Data were collected on root architecture through measurement of root length and number of lateral roots. The data was taken at stage R6 which is defined as 12 days after sowing on the plate.

The data in figure 6-4 shows average root length for the 30 plants analysed at stage R6. The wild-type *Arabidopsis* by this time averaged a root length of around 5.5 cm, with a roughly 1 cm deviation from the mean. Root lengths for

all the knockout lines were found to have an average length similar to wild-type.

The number of lateral roots at stage R6 is shown in figure 6-5. Wild-type plants were found to have an average lateral root number of around 15, with around 3 lateral roots deviance around the mean. Again similar values were found for all the knockout lines.
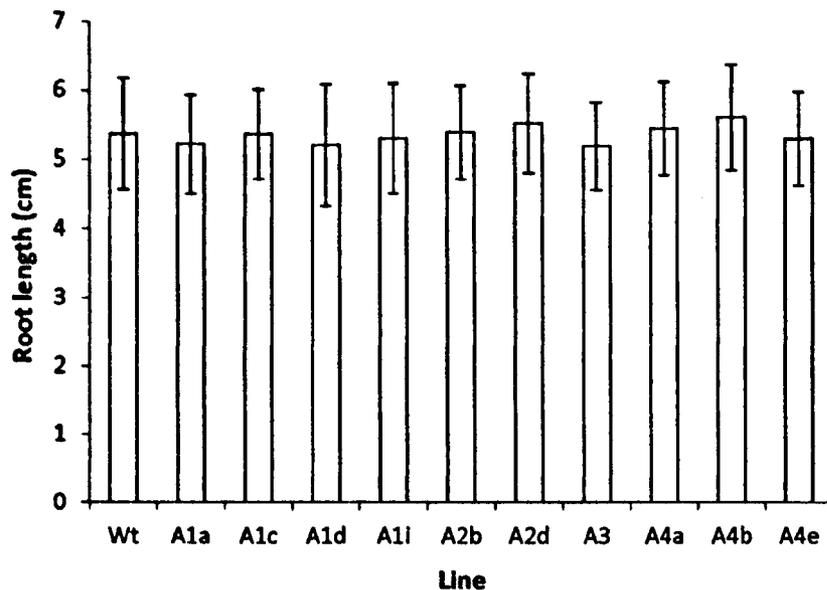
Figure 6-4 Root length of wild-type and knockout lines after 14 days

Total root length in centimetres of wild-type col-1 and the knockout lines after 14 days, which is defined as stage R6 in the methodology. Error bars shown display the standard deviation of the mean of 3 replicates of 10 plants.
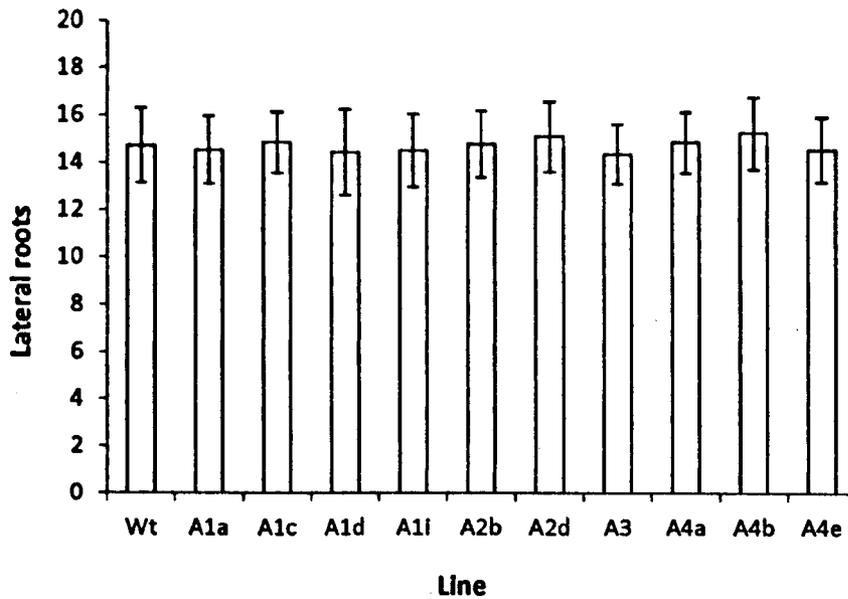
Figure 6-5 Number of lateral roots in wild-type and knockout lines after 14 days

Total number of lateral roots in wild-type col-1 compared with knockout lines after

14 days, which is defined as stage R6 in the protocol. Error bars shown represent

standard deviation from the mean of 3 replicates of 10 plants.

6.3 Leaf emergence

Phenotypic data related to leaves centred on leaf emergence. These data were then split into two specific sections, early and late leaf emergence. The early stage relates to before stage R6 (12 days) analysis, which were sown on agar and late stage refers to in plants sown on soil, with the leaf taken after stage R6 (12 days). Leaf emergence was recorded as number of days post sowing, to the point at which the "true-leaf" was 1 mm in length.

Early leaf development is shown in figure 6-6. Leaf emergence in respect to wild-type occurred around 10 days for the second leaf and around 14 days for the fourth leaf. A majority of the knockout lines analysed followed a similar pattern to wild-type for both the emergence of the second and forth leaves. However *rabA1d* and *rabA1i* had a slightly later leaf emergence of around 11 days, for the second leaf and 15 day for the 4th leaf, this was shown by statistical analysis to significantly different to wild-type with a p value of <.001 for both leaf emergences.

Post R6 leaf emergence data is displayed in figure 6-7 and deals with the emergence of leaves 6, 8 and 10. The time of emergence of these leaves in wild-type was around 16, 18 and 20 days, respectively. The knockout lines followed a similar pattern to the early stage with all lines expected for *rabA1d* and *rabA1i* having similar emergence times to wild-type. As with early leaf emergence *rabA1d* and *rabA1i* had significantly different emergence times to wild-type of around 18, 20 and 22 days (p = <.001 in all cases.)
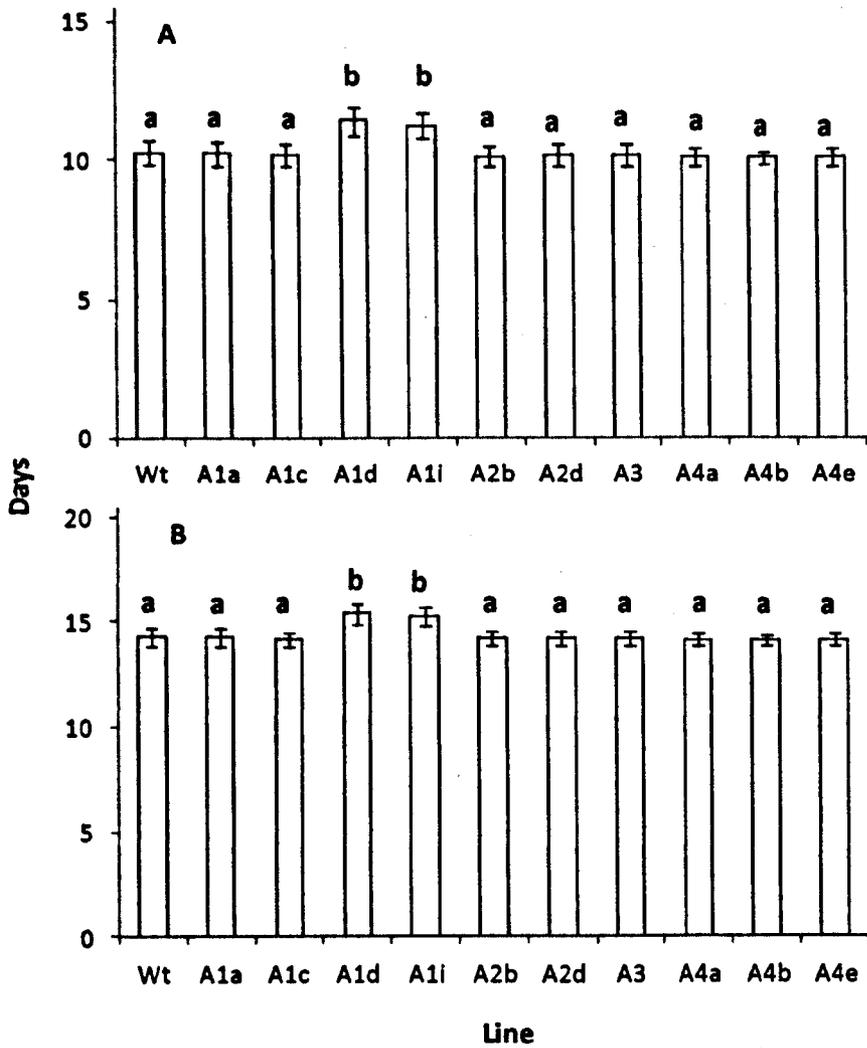
Figure 6-6 Early stage leaf emergence in wild-type and knockout lines

Total time in days to leaves reach 1mm in length for wild-type col-1 and knockouts,

during the first 14 days of development. These measurements were taken from the

on plate data. Errors bars shown represent the standard deviation from the mean of

3 replicates of 10 plants. Key: (A) 2 leaves. (B) 4 leaves.
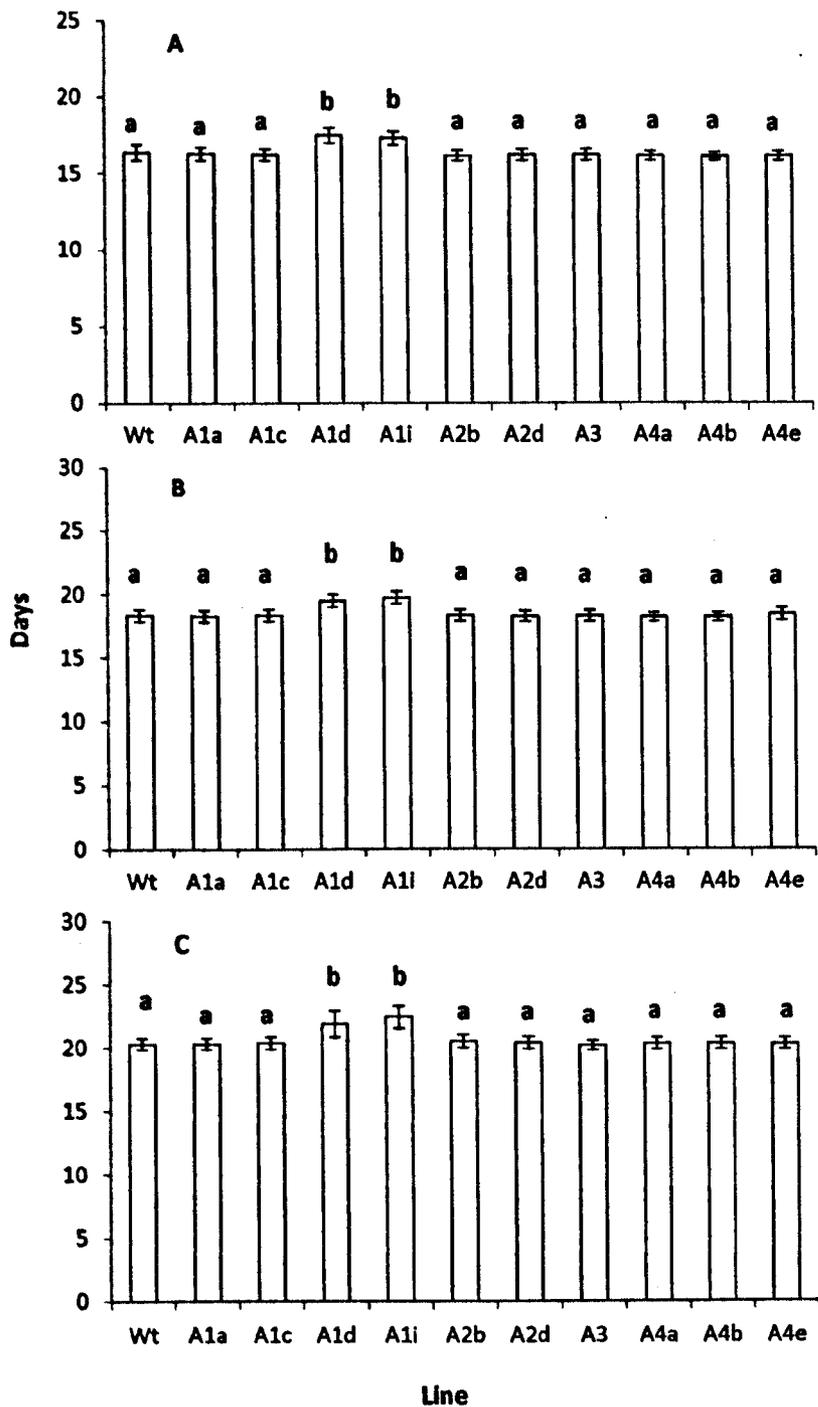
Figure 6-7 Post stage R6 leaf emergence in wild-type and knockout lines

Total time in days to leaves reach 1mm in length for wild-type col-1 and knockout

lines for every second leaf post stage R6 (14 days after sowing) in pot. Error bars

showing standard deviation from mean of 3 replicates of 10 plants.. Key: (A) 6 leaves

(B) 8 leaves (C) 10 leaves.

6.4 Stem at senescence

As a determination of agronomic output, measurements were taken of the main bolt length and weight, with number of side bolts. These measurements were taken after full senescence at which point a total harvest could be ascertained. Data for main bolt length was taken using a ruler, with stems adjusted to run as straight as possible. The data for each stem was measured 3 times and an average taken to try and reduce measurement errors. Dry weight of the main bolt was measured after overnight incubation at 100°C, with the bolt weighed and dried again until a stable weight was measured. The number of side bolts was simply counted as they were stripped from the main bolt.

Data for main bolt measure is displayed in figures 6-8 and 6-9. The wild-type was found to have a main bolt length of around 22.5 cm; with a large variance of around 5 cm. Data relating to the knockout lines produced similar results, apart from *rabA3* which had a slightly higher average of around 26 cm. however this was found to be statistically significant. However, on Tukey analysis this difference was between the *rabA3* and *rabA2d* knockout and thus not significantly different from wild-type. Data displayed in figure 6-9 relates to the total dry weight of the main bolt. Wild-type plants produced main bolts of around 160 mg dry weight with a high variance of around 50

mg; with the knockout plants producing similar weights of around 160 mg and similar variance.
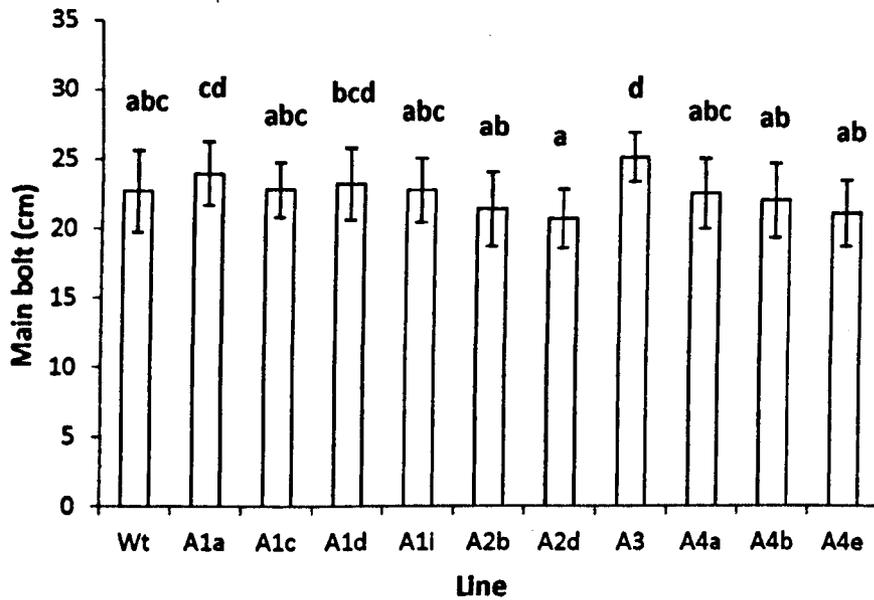
Figure 6-8 Main bolt length at senescence of wild-type and knockout lines

Length of the main bolt at senescence of wild-type and knockout lines, with error bars showing standard deviation of 3 replicates of 10 plants. Statistical analysis was performed by ANOVA with post-hoc Tukey test giving differences between the means displayed by letters.
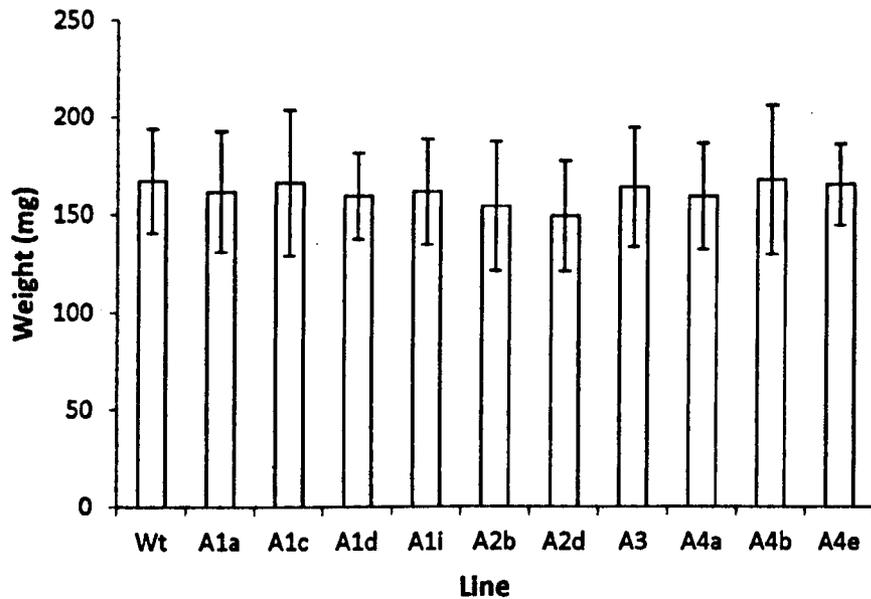
Figure 6-9 Dry weight in milligrams of main bolt of the wild-type and knockout lines

Weight of wild-type and knockout stem biomass at senescence after being subjected to oven drying overnight of wild-type and knockout lines. Error bars shown represent the standard deviation from the mean with 3 replicates of 10 plants.

The number of side bolts is shown in figure 6-10. Data shown for wild-type indicates there were on average between 3 and 4 side bolts per plant, with a variance of around 2 bolts. A similar number of side bolts was found for knockout lines, with a similar variance, with no statistically significant differences identified.
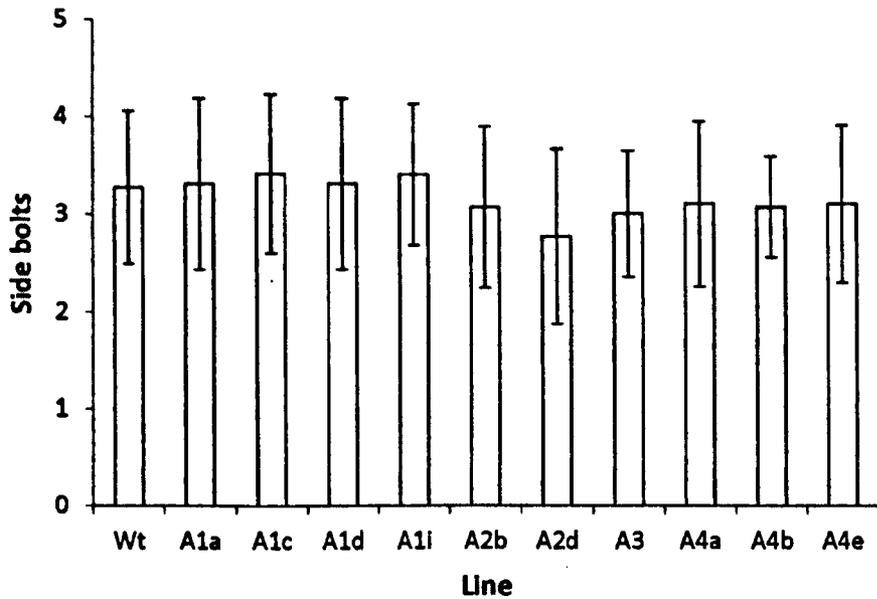
Figure 6-10 Number of side bolts from the main bolt of wild-type and knockout

lines

Total number of side bolts projected from the main bolt of the wild-type col-1 and

knockout lines. Errors bars shown display the standard deviation from the mean of 3

replicates of 10 plants.

6.5 Flowering

Seed production is of critical commercial agronomic property of the plant. For

this reason flowering was considered a crucial point of interest in the

phenotype study. The two main traits analysed were flower bud emergence

and total seed weight. Flower bud emergence was taken as the day of first

flower bud and seed weight was measured post-harvest. Seeds were not

dried before weight being measured.

147
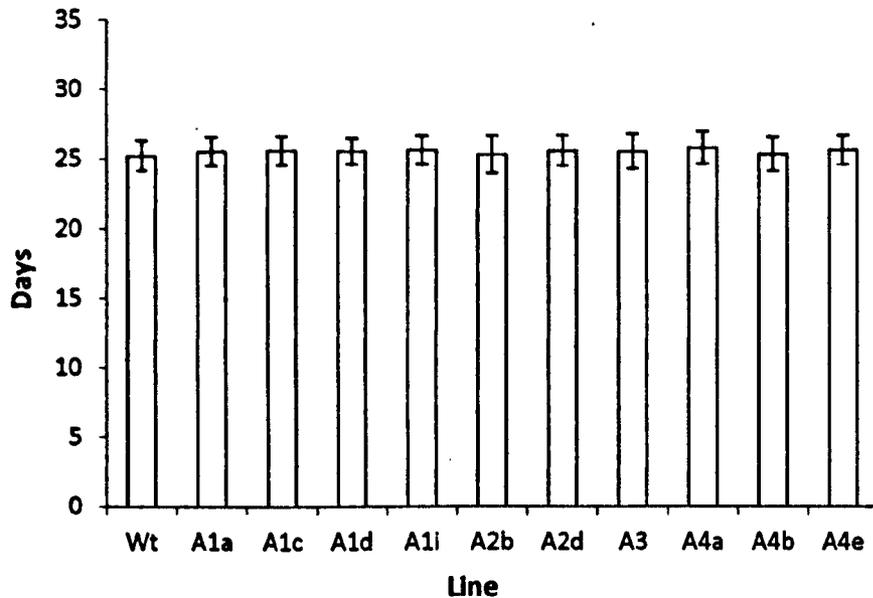
Figure 6-11 Time to first flower bud emergence in wild-type and knockout lines

Time to first flower bud emergence in days for wild-type col-1 and knockout lines, with errors bars showing the standard deviation from the mean of 3 replicates of 10 plants.

The data in relation to flower bud emergence is shown in figure 6-11. For all lines both wild-type and knockout the first flower bud emerged around 25 days after potting. The variance was low with around 3 days plus/minus the average. There were no significant differences found between the lines.

Figure 6-12 shows the data relating to seed weight at harvest. The average seed weight of wild-type was around 350mg, with as much as 120mg of variance. Averages of the knockout lines varied to similar levels, however the data showed a statistical difference by ANOVA (p<0.001 d.f. 329, v.r. 0.65), however Tukey analysis shows no differences between the wild-type and

148

knockout lines with the difference occurring between the *rabA2b* and the

rabA3 knockout. In this occurrence it is possible that some outlaying data

point affected the statistical test.
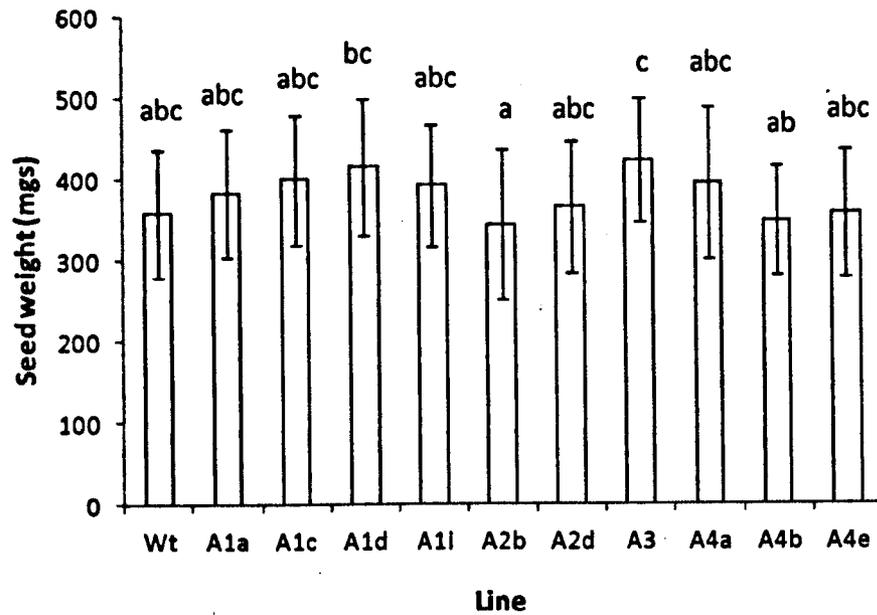
Figure 6-12 Seed weight at harvest of wild-type and knockout lines

Average seed weight at senescence for wild-type col-1 and knockout lines with errors

bars showing standard deviation from the mean of 3 replicates of 10 plants.

Statistical analysis was performed by ANOVA with post-hoc Tukey test giving

differences between the means displayed by letters.

7 Effect of Rab11a antisense on cell wall composition in tomato fruit

An antisense (G4 antisense) knockout of the *Arabidopsis* RabA1a homologue exists in tomato. In tomato this homologue is termed *Rab11a*. This knockout has been implicated in relation to retention of fruit firmness during ripening (Lu *et al* 2001). Further characterisation of *Rab11a* expression patterns however, found that *Rab11a* was mostly expressed pre-breaker in the developing fruit, with expression falling rapidly in the post-breaker period. These observations combined with the pectin compositional data shown in chapter 4.1, of this thesis, might suggest that the changes in firmness, shown in the G4 antisense fruit, could have been due to changes in cell wall structure occurring during fruit development. Thus a study was undertaken to analyse the cell wall composition in the G4 antisense tomato fruit during development and to compare this with wild type fruit.

7.1 Confirmation of G4 antisense phenotype.

Initially it was important to check the antisense plants, to make sure that they contained the transgene and that the reported phenotype was displayed. To achieve this, a number of methods were employed, first of which was the analysis of the genetic makeup for the presence of the transgene. Due to the nature of the antisense knockdown lines an RT-PCR confirmation of transcript

reduction would be technically difficult. The issue being that the antisense transcript is full length, making it impossible to design primers which would amplify the normal and antisense RNA strands separately. However, presence of the insertion can be determined by PCR. From previous work the expected amplicon relating to the insertion in the tomato lines was described as being 1.1kb in length, using primer 3 targeted to the 35S promoter and primer 8 targeted to the antisense cDNA (Lu 2000). Figure 7-1 through 7-3 shows the amplified products from these reactions, in the three plants used in this thesis. In figure 7-1 the G4 lane shows an amplified product between the 1kb and 1.2kb markers which confirms the presence of the antisense insertion in the plant. The remaining lanes check for a presence of this amplicon in AC^{++} (Alisa Craig variety). In both cases these lanes showed the absence of amplified product confirming that the amplicon in lane 3 was not through random primer amplification. Figure 7-2 and 7-3 show the same result for plants 2 and 3.
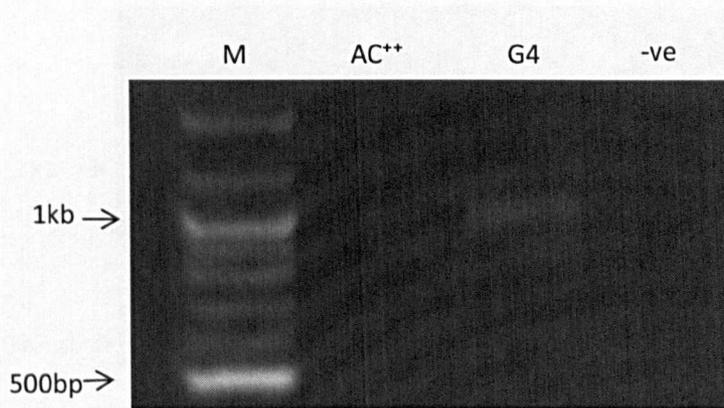
Figure 7-1 PCR to confirm presence of G4 antisense in plant 1

Gel image showing the presence of the G4 antisense construct in plant 1. Key: M=

Marker; AC⁺⁺= Alisa Craig; G4= antisense line; -iv= negative control
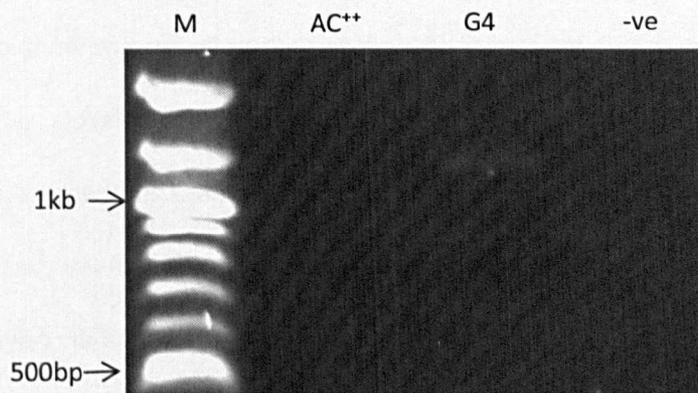
Figure 7-2 PCR to confirm presence of G4 antisense in plant 2

Gel image showing the presence of the G4 antisense construct in plant 1. Key: M=

Marker; AC⁺⁺= Alisa Craig; G4= antisense line; -iv= negative control
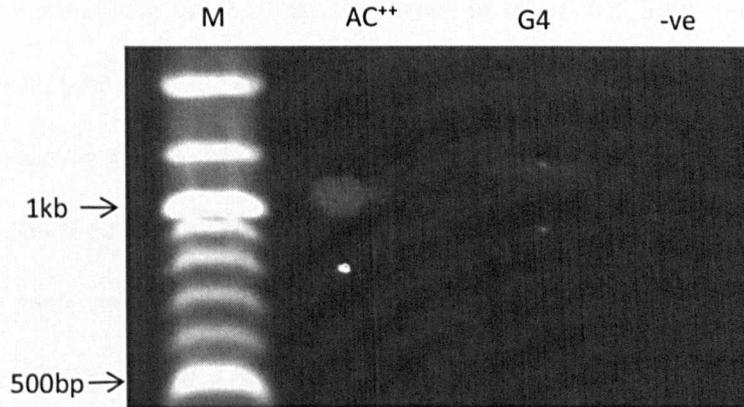
7-3 PCR to confirm presence of G4 antisense in plant 3

Gel image showing the presence of the G4 antisense construct in plant 1. Key: M=

Marker; AC^{++}= Alisa Craig; G4= antisense line; -iv= negative control

In addition to confirmation of the presence of the transgene it was also required to show the reported phenotype was also being displayed by these plants. The visual phenotype is shown in figure 7-4. From the visual phenotype is it obvious that the fruit harvested from wild type AC^{++} fruit 40 days post anthesis had begun to decay showing cracks in the epidermis and pericarp layers. In contrast fruit from the G4 antisense line still maintained a smooth and solid epidermis and pericarp. Despite these obvious visual differences it was still important to place a quantitative value on the changes observed, through texture analysis. Softening was measured by applying pressure to four sides of the fruit and then an overall fruit average was taken, resulting in one replicate, these data were taken over a period from 15dpa to breaker plus 35. To achieve texture analysis was employed. In this method a probe is used to push against the fruit, measuring the total resistance to the

probe. The results for this analysis are shown in figure 7-5. Both plant lines, started with a force of around 1400 Nat 15dpa. The firmness of both lines decreases slowly during the period leading to the breaker stage, dropping to around 1200 N by breaker. It is at this point where the G4 line diverges from AC++, however the general pattern is still maintained. In the period post breaker both lines show a decrease in fruit firmness, reducing more rapidly than at the pre-breaker stages. However the, AC++ lines decreased at a significantly increased rate (p=<.001) compared with the G4 line. This trend and level of significance was maintained for each of the post breaker stages analysed. Crucially these data are similar to those reported by Lu et al., 2001.
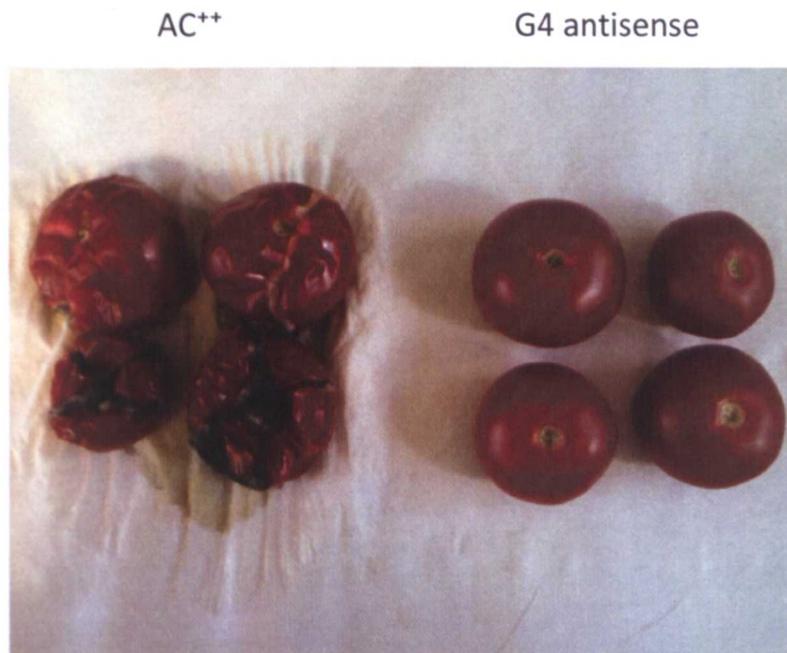
AC++   G4 antisense

Figure 7-4 Visual phenotype of AC++ fruit compared with G4 antisense line fruit after 40 days post anthesis
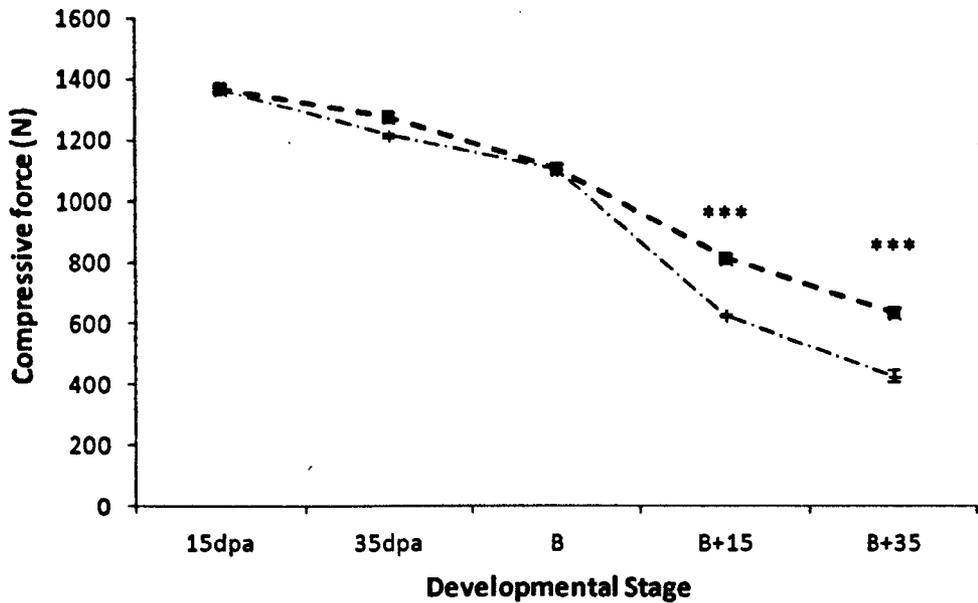
Figure 7-5 Texture analysis of fruit firmness of Alisa Craig and G4 antisense lines

Texture analysis of fruit firmness measured in Newtons. Statistical significance

conducted by T-test is shown by *** at the developmental stage, showing p<0.001.

Key; AC++ = Cross with a long dash dot; G4 = Square with a dash. Developmental

stage key: 15 and 35 days post anthesis, breaker and breaker +15 and 35 days.

7.2 Cell wall fractionation

The data shown above demonstrated both the presence of the insertion and

expression of the antisense. For cell wall analysis 3 time points were chosen,

15 and 35 days post anthesis, as these represented an early and midpoint

stage of development, and breaker stage as a final point of development. Cell

wall fractionation was performed in the same way as the *Arabidopsis*, with

the extraction of the two pectin fractions and then hemicelluloses rich and

cellulose rich fractions. In addition starch was also assayed as this was

155

expected to be transiently deposited in the developing fruit and formed part of the cellulose rich fraction. However, the method of AIS production was different (described in detail in section 2.32). The reason for this difference in AIS production was to disable any enzymes that would be active within the fruit tissues during this period of development. The results of this fractionation are displayed as a mass balance in table 7.1. The total varied from around 830mg/g to 889mg/g with an error range of between 22mg/g and 65mg/g.

Levels of starch in the fruit were, as expected, highest at 15dpa and declined as the fruit developed to breaker. There was no apparent difference between wild type and G4 antisense fruit in the content of starch or in the rate of loss during development. The relative levels of pectin, hemicelluloses and cellulose during fruit development are shown in figure 7.6.

7-1 Mass balance for AIS composition from developing wild type and G4 antisense tomato fruit

All values are expressed as mg/g AIS

	Pectin	Cellulose	Hemicellulose	Starch	Total (mg/g)
AC15	127 ± 6	201 ± 21	271 ± 7	289 ± 36	889 ± 35
AC35	269 ± 31	305 ± 16	166 ± 13	109 ± 22	851 ± 62
ACB	460 ± 9	257 ± 16	113 ± 20	51 ± 20	882 ± 45
G415	115 ± 2	255 ± 20	235 ± 15	253 ± 13	859 ± 38
G435	208 ± 5	381 ± 10	146 ± 6	94 ± 18	830 ± 22
G4B	347 ± 12	353 ± 16	104 ± 10	44 ± 23	850 ± 39

To give a figure of cell wall polysaccharide composition by percentage the cellulose fraction was adjusted for starch and the remainder taken as 100%. The remaining three In AC[++] pectin levels was low at the outset of development, shown from the data to be around 20% of the total AIS composition. This level then increased across development, at the midpoint being the second highest component assessed accounting for around 35% of the total AIS. By the time breaker had been reached, though, pectin levels were then dominant in the fruit accounting for around 55% of the total AIS. Pectin levels throughout development in the G4 antisense followed a similar but not exact pattern. As with the AC[++] the initial pectin levels started out at around 20% of the AIS and increased from 15 days post anthesis (dpa) to a level of around 25% by 35dpa. The difference in pectin level at this time period was significantly different from the pectin level shown in the AC[++]. At breaker stage both the antisense line and AC[++] had a similar pattern of increasing pectin levels over the period of development. However, the antisense line differed from AC[++] having total pectin of around 45% at breaker stage. Showing a significant "lag" in pectin levels compared with the AC[++]. Also interestingly this led to a situation whereby pectin never became the dominant component in the cell wall.

The next component to be fractionated was the "hemicelluloses" rich fraction. This fraction in the AC[++] fruit was around 45% of the AIS initially and then reduced as breaker was approached, accounting for around 20% by

35dpa and 20% of the AIS at breaker. A similar pattern was found with G4 antisense, with the fraction accounting initially for around 40% of AIS. This level decreased towards breaker, being around 20% after 35dpa and then 10% at breaker. Interestingly the "hemicelluloses" rich fraction in G4 antisense was not the dominant cell wall component initially whereas in the AC⁻⁻ this was the case. The final fraction in the extraction method was the "cellulose" rich residue. In the AC⁻⁻ the levels of cellulose followed a bell shape distribution, after 15dpa accounting for around 30% of the AIS and by 35dpa becoming the dominant cell wall component of around 40% of the AIS. At breaker stage the cellulose was no longer dominant and percentage wise had a reduced level of 30%. A similar pattern was observed in the G4 antisense line. However, initially the "cellulose" residue accounted for the highest proportion of the total AIS at around 40%. This level then increased to around 50%, before decreasing at breaker stage accounting for around 45%.
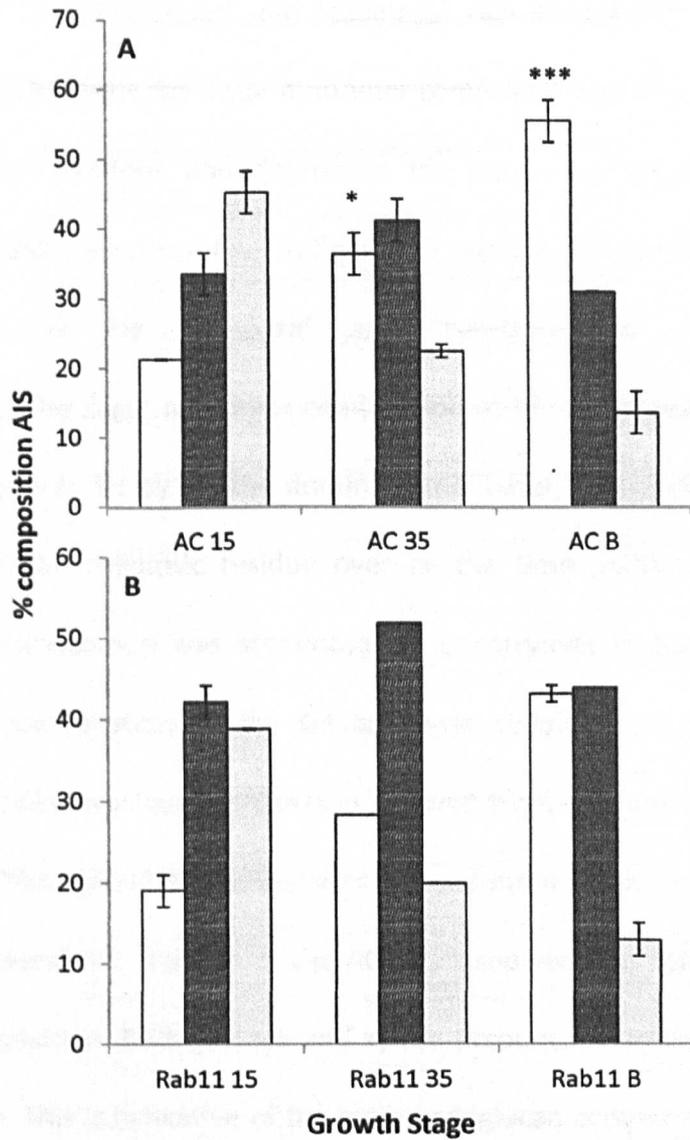
Figure 7-6 Cell wall composition across fruit development

Percentage composition of AIS displayed with error bars showing the standard deviation of 3 replicates of fruit taken from 3 different plants. Statistical significance conducted by T-test is shown by *** at the developmental stage, showing p<0.001. Key: A) AC** B) G4 antisense. Developmental stages 15, 35 days post anthesis and breaker stage.

Key = Pectin; (☐) Cellulose; (◥◣) Hemicelluloses (☐)

As with the "hemicelluloses" and "cellulose" rich fractions in *Arabidopsis* it was required to check the sugar monomer composition by HPLC to assess the purity of the fractions and determine the nature of the hemicelluloses isotopes. These data are shown in figure 7-7 and figure 7-8, representing the composition of the "cellulose" and "hemicelluloses" rich fractions respectively. The sugar monomer composition of the "cellulose" rich fraction shows glucose to be by far the dominant monomer, accounting for around 700mg/g of the cellulosic residue over all the time points analysed. The remaining composition was accounted for in carryover of the other sugars analysed. From analysis of the G4 antisense cellulosic residues a similar pattern was displayed to that shown in the wild-type, with glucose accounting for around 700mg/g of the residue with minor contaminants carried over. The "hemicelluloses" rich fraction of the AC^{++} fruit showed two major monomers in the composition. Both glucose and xylose account for around 425mg/g of the fraction. This is indicative of the major xyloglucan component of the fruit tissue and primary cell wall. The remaining composition can be accounted for by various side chains, or pectin carryover. The G4 antisense shows again a similar pattern to the wild-type, with glucose and xylose each providing around 400mg/g of the total sugar monomers. Crucially neither of the fractions analysed showed a significant difference between wild-type and G4 antisense discounting the idea that differential impurities in the fractionation could account for the differences shown in cell wall fractionation.
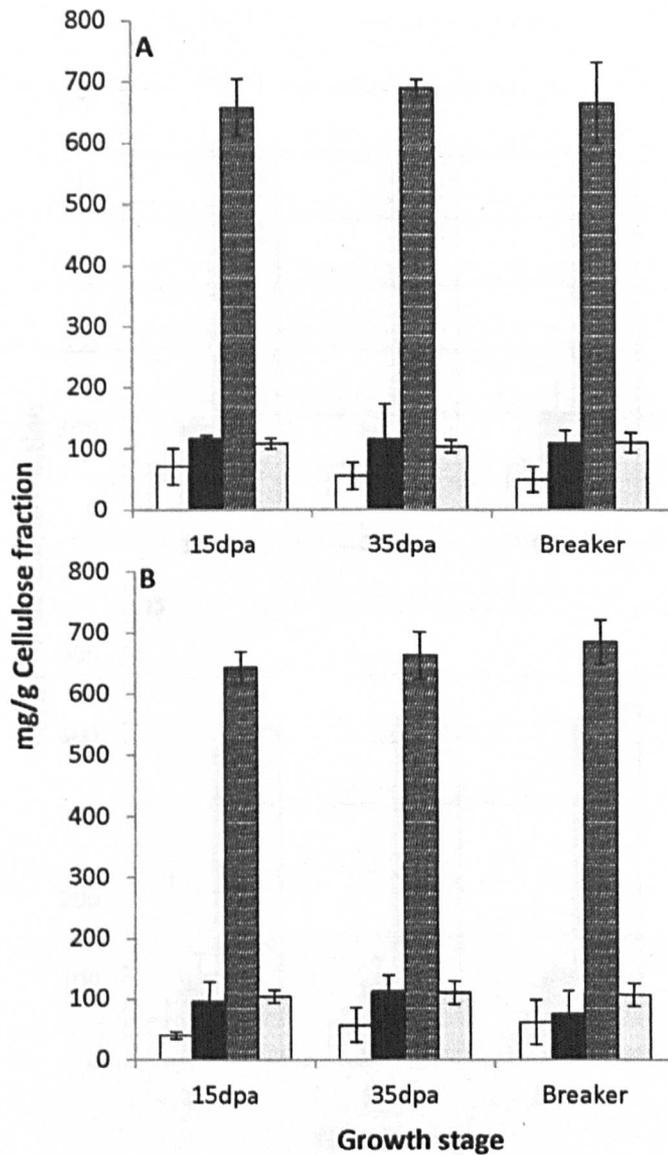
Figure 7-7 Monomer composition of the "cellulose rich" fraction

Monomer composition of the "cellulose rich" fraction displayed with error bars

showing the standard deviation of 3 replicates of fruit taken from 3 different plants.

Key: A) AC** B) G4 antisense. Developmental stages shown are 15 and 35 days post

anthesis and breaker.

Key = arabinose (▢), galactose (■), glucose (◨), xylose (▢).
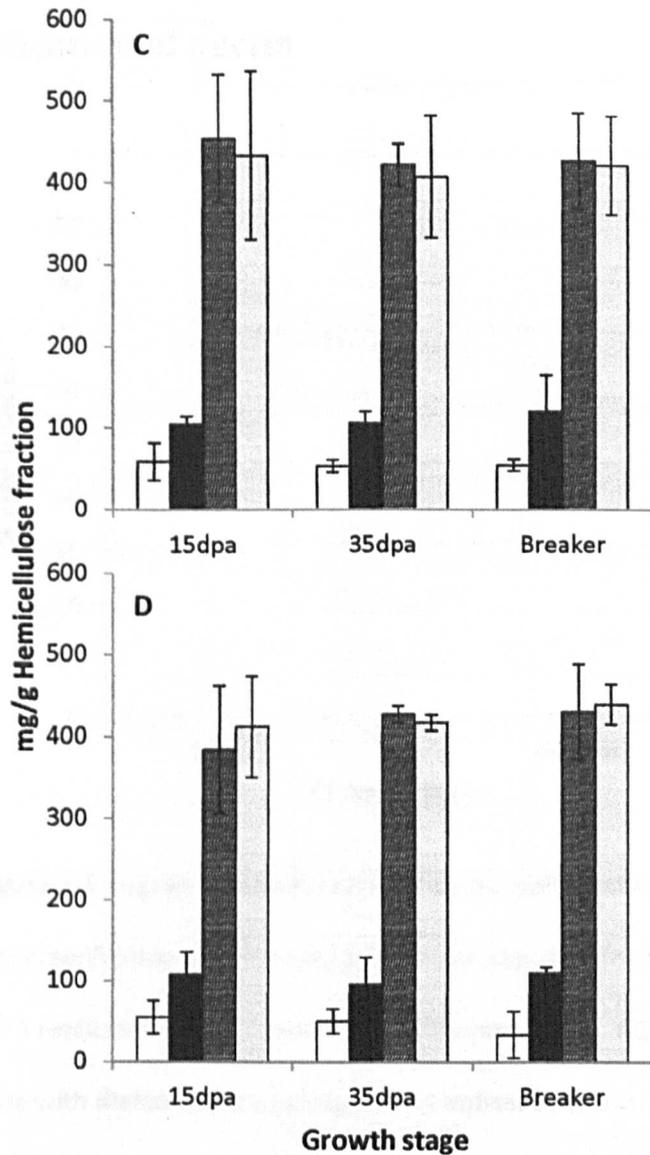
Figure 7-8 Monomer composition of the "hemicellulosic rich" fraction

Monomer composition of the "hemicellulosic rich" fraction displayed with error bars

showing the standard deviation of 3 replicates of fruit taken from 3 different plants.

Key: A) AC** B) G4 antisense. Developmental stages shown are 15 and 35 days post

anthesis and breaker.

Key = arabinose (☐), galactose (■), glucose (◥), xylose (☐).

7.3 Esterification of pectin
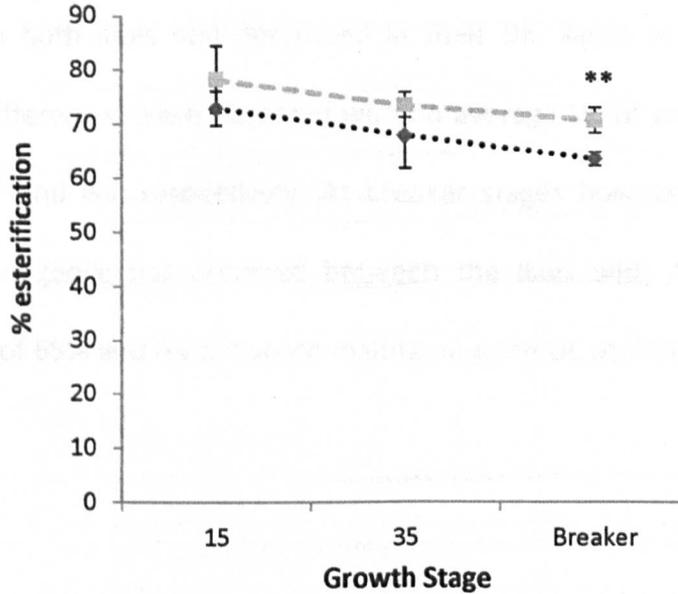
Figure 7-9 Degree of esterification of pectic polysaccharides

Percentage esterifcation of the pectic polysaccharides showing the standard deviation of 3 replicates of fruit taken from 3 different plants. AC^{++} is shown by dotted black line with diamond data points and G4 antisense shown by a long dashed grey line with square data points. Statistical significance conducted by T-test is shown by *** at the developmental stage, showing $p < 0.001$. Developmental stages shown are 15 and 35 days post anthesis and breaker.

With RabA knockouts shown to cause differences in the pectin levels in both *Arabidopsis* and tomato fruit shown it became an interesting question as to the nature of the deposited pectin. In particular the degree of esterification (DE) in tomato fruits this had only previously been conducted post breaker. To do this the DE of the total pectin from wild type and G4 antisense fruit was

determined as described in materials and methods. The results are shown in figure 7-9. From the data shown AC⁺⁺ fruit initially had a DE of around 75%, with G4 antisense having a higher average value and of around 80% at 15dpa. After 35pda both lines had decreased in their DE. Again at this point no statistical differences were observed with an average DE of around 70% and 75% in AC⁺⁺ and G4, respectively. At breaker stages however a significant (p<0.01) divergence has occurred between the lines with AC⁺⁺ having an average DE of 65% and G4 antisense maintaining the DE at 75% esterification.

8 Discussion and Conclusion

8.1 Discussion

To truly appreciate the context of the data shown in the previous chapters it is in the first instant best to refresh the overall hypothesis of the project and individual goals within its sections. On a global scale the project aimed to assess whether the use of *Rab* genes could enhance the saccharification of biomass. This global hypothesis was to be tested through addressing several component hypotheses. Firstly, could knockouts of *Rab* genes expressed in specific tissue types (stem) be identified? From here two questions were then posed, would these gene knockouts have an effect on the plant cell wall and would said gene knockouts cause a decrease in recalcitrance towards saccharification? It was also important to determine whether agronomic traits would be impacted either through changes in cell wall composition or through the absence of the gene product.

With the respect to the initial problem posed, even though there is now a substantial amount of genetic information available there are technical considerations to be made. From the data in chapter 3 it can be concluded that using publically available microarray data all the genes expressed in stem have been located. However it is in this statement that questions may arise. The stem is a complex multitude of tissues and thus expression in stem could

be considered vague. An interesting question would be whether certain *Rab* genes are only expressed in the xylem or phloem tissues for example. Not only should the spatial aspect of stem expression be considered but also a timing aspect should be considered. Changes in cell wall expression will most likely change over the life cycle of the cell, thus posing the question, when do specific *Rab* genes get expressed? For example, of the 3 *RabA4* genes does one gene get expressed during cell plate formation? Evidently through work carried out by Chow *et al.*, (2008) *RabA* proteins do localise to the cell wall but are all the genes active in the same instant. Certainly from the RT-PCR and microarray data available it is impossible to add this extra level of detail to the analysis. It can also be concluded that knockouts have been successfully isolated from all the stock lines purchased. Unfortunately all the RabA proteins expressed in stem could not be analysed with the stock materials currently available. This was most disappointing in terms of knockouts for the RabA5 and RabA6 sub-clade, which if available would have given a more complete appreciation of the entire clade. The scope for continuing the work done in this area is evident to see, with a proposal of an in depth expression analysis of the *Rab* genes highlighted in the microarray and use of insertion technologies to create single gene knockout lines in the RabA5 and RabA6. In the case of the former this would encompass the incorporation of GFP fusions for the individual genes, allowing their localisation of expression to be studied within the stem organ and expression followed over time in the cell. To create targeted insertions in the A5 and A6 sub-clade, zinc finger nucleases (Sigma

Aldrich) could be employed. These use gene specific zinc finger domains to cleave the DNA at specific sites. The DNA and zinc-finger nuclease then dissociates from the DNA with a large portion of the transcript.

With established knockout lines the next question was would *Rab* gene knockouts have an effect on cell wall deposition. Asking this question at first glance would appear to be rather speculative, because the Rab family has always been considered highly redundant (Pereira-Leal and Seabra 2001). However, these assumptions were based on sequence homology. The novel approach showed in chapter 4 looked at testing these hypotheses though quantitative analysis. The methodology used for fractionation gives basic quantitative figures of cell wall composition. Arguably the results produced by these fractionation experiments group large classes of polymers into one category. For example the "hemicelluloses" rich fraction is a grouped class of many individual polymers (Scheller and Ulvskov 2010). However, the data produced are representative of monomeric composition data in the literature (Brown *et al.,* 2007), removing the possibility of the changes in initial fractionation being due to poor separation. It is also noteworthy that the similar results shown in several related genes within sub-clade rules out the possibility of results being due to an insertion artefact or random mutation. With the limitations of the technique appreciated it is still possible to confirm that Rab gene knockouts have a downstream effect on cell wall composition. Interestingly the significance shown by individual genes implies that Rab

proteins may not be completely redundant. These data are consistent with findings of Szumlanski and Nielsen (2009) where a *rabA4a* mutant could not be rescued through complementation by an EYFP-RABA4b construct.

Through FT-IR it was hoped to have an independent, non-destructive, method for distinguishing differences in the whole cell wall. Unfortunately the results here were difficult to interpret as changes in fingerprint regions are often limited to one wavenumber and not shown across the whole set of fingerprint functional groups. The difficulties encountered here could be due to the question being addressed. We are addressing a system in which the entire cell wall of the material is being analysed; a potential problem with this is fingerprint regions are based on functional groups, many of which overlap in wavenumber and may occur in all the main pectin, hemicelluloses and cellulose polymers. This limitation in the technique could well be the reason why groups analyse particular components and try to isolate epitopic differences instead of examining general overall cell wall composition (Chen *et al.*, 1998; Coimbra *et al.*, 1999; Kačurákova *et al.*, 2000; Černá *et al.*, 2003; Fissore *et al.*, 2012; Toole *et al.*, 2013). These overlaps in the spectra may be exacerbated by only the partial reduction of cell wall polysaccharides studied. Instead a more useful interpretation may have been possible with a complete or >50% reduction of these components. Despite the limitation of the method and the results obtained, it was encouraging that through PCA analysis groups were formed corresponding to the biochemical data, adding further weight to

the original hypothesis. A reason for the PCA success was most likely due to definition of the principal components around one of the finger print regions for the cell wall components.

Lignin analysis showed a slight but significant increase in the *rabA3* line. It is difficult to attribute an increase here to biological significance; however there are two possible explanations for the data observed. First of these is the inherent problems with lignin measurement. Difficulties in spectroscopic measurement have led to direct gravimetric methods, the Klason method (Kirk and Obst 1988), or indirect absorption by substitution of free hydroxyl groups with a suitable substance, most commonly acetyl-bromide (Fukushima and Hatfield 2004). For technical reasons only the Fukushima and Hatfield method was used here; limitations of this method however is that you are measuring the number of free hydroxyl groups within the lignin structure. Thus it is possible that the increase seen in the *rabA3* line is due to a monolignol composition change and not an increase in total lignin per say. While the above hypothesis cannot be discounted, the nature of RabA3 would make a monolignol composition change difficult to explain biologically. As mentions in chapter 1 lignin contains 3 monolignols with various side chains, it would seem unlikely that a single standalone Rab protein would have affected just one subunit, especially with the data from the cell wall analysis showing distinct clades for each component. This leads onto the second hypothesis in which RabA3 protein is possibly a redundant gene within the

clade. What is certain is that *RabA3* is not the ancestral gene within the clade, because of phylogenetic data within the literature (Rutherford and Moore 2002). From the data shown it is difficult to do anything other than speculate on these two hypotheses or whether the data produced is merely an artefact.

A study of the metal ion composition was interesting to give a complete analysis of the sample. Of particular though this was interesting for *rabA1* knockouts as their impact on pectin may have correlated with reduction in calcium where the egg box structure is formed. Although this study produced significant differences statistically, but the distribution of the data and error margins was large and difficult to draw accurate conclusions from, as no obvious trends could be observed. It is highly likely that the reason for the significance is due to environmental factors over genetic makeup.

As stated in chapter 1 the literature showed that RabA2 and RabA3 proteins localised to the cell plate Chow *et al.,* (2008) and thus it was reasonable to assume their role in cell wall deposition. Work done in this study presents evidence that RabA1 and RabA4 proteins are also involved in cell wall metabolism. Furthermore *RabA1, RabA2* and *RabA4* affected pectin, cellulose and hemicelluloses, respectively and *RabA3* may have affected lignin. From these data it is possible trafficking of these cell wall polymers occurs, through a targeted process. Thus influence of vesicle disruption may be through direct trafficking of polymers; such as would be the case for pectin and

hemicelluloses which are made in the Golgi and transported to the wall (Cafall and Mohnen 2009; Scheller and Ulvskov 2010), or through indirect influence of cell wall enzymes in the case of cellulosic material (Crowell *et al.*, 2009; Gutierrez *et al.*, 2009). There are two possible reasons for the compositional reductions. Firstly that recycling has been affected, this is known to occur for pectic polysaccharides and xyloglucans (Baluška *et al.*, 2002; 2005; Dhonukshe *et al.*, 2006) however, it is difficult to provide a biological explanation of how a reduction of mobilisation from the wall, presumably since this is a loss of function, would lead to a reduction of polymer level . Another hypothesis is that the secretion of cell wall modifying enzymes may be effected as shown by Lu *et al.*, 2001 in a RabA1a orthologue antisense in tomato. A final hypothesis is direct trafficking of the polysaccharide polymers and new CESA complex components from the apoplast to the plasma membrane may have been reduced. Continuation of this work would at first focus on further analysis of the hemicelluloses fraction to investigate whether specific hemicellulosess had been impacted. This task could be easily accomplished through polysaccharide analysis by carbohydrate electrophoresis (PACE) analysis (Tryona *et al.*, 2012; Kosik *et al.*, 2012.) Current theory suggests that trafficking occurs via a bulk flow mechanism. Recently literature has been released providing mounting evidence for multiple routes from the trans-Golgi network to the PM and cell wall (Rehman *et al.*, 2008; Lanubile *et al.*, 1997; Leucci *et al.*, 2007; De Caroli *et al.*, 2011; Bottanelli *et al.*, 2011). Of particular interest is work conducted by Moore *et al.*, 1991 which indicates

that different cell wall polymers may exit the *trans*-Golgi cisternae or the *trans*-Golgi network in different vesicles and more recently where a low concentration of brefeldin A (an inhibitor of ER-Golgi traffcking) only slightly inhibited incorporation of lablled proteins into the PM and cell wall, however polysaccharides were greatly affected. Work presented here does support this growing body of evidence however to further this field would require co-localisation work. For this the use fluorescent markers and polymer specific antibodies and markers (Kieran *et al.*, 2011), combined with a labelled RabA sub-clades. However, it is important to remember that these antibodies are purpose built for specific epitopes and thus the questions being asked by such experimentation should be well defined.

Cell wall alterations characterised in chapter 4, added weight to the global hypothesis, as to whether *Rab* gene knockouts could affect cell wall composition. Now the next question was whether the impacts on cell wall composition would reduce the recalcitrant nature of the cell wall. Unfortunately at the time there had been little work conducted in *Arabidopsis* in relation to bioenergy, with a majority of studies focusing on agronomic crops (reviewed by Wang and Ge 2006.). For this reason early experiments focused on the selection of a suitable pre-treatment method. In this study we have devised a pre-treatment method for *Arabidopsis* which gives both a 95% and a 50% saccharification respectively. The pre-treatment methods selected were based on a liquid hot water pre-treatment (Allen *et al.*, 2001) and dilute

acid (Taherzadeh *et al.,* (2000). In this study 50% release was required to elucidate both an increased and decreased sugar release as possible results.

From these experiments it was shown that *rabA1, rabA2 and rabA3* knockouts had no effect on the percentage sugar released; however *rabA44* knockouts decreased the recalcitrance in the pre-treated and gave a slight increase in the untreated samples. When related to the biochemical data, these results give intriguing information on enzyme digestibility in *Arabidopsis*. To put these data into context it is first important to remember that *rabA1, rabA2,* and *rabA4* knockouts have reduced pectin, cellulose and hemicelluloses, respectively. So an important question to ask is, with changes in cell wall composition why only one group of Rab knockouts resulted in the increased digestion. There are two possible ways of interpreting these data to explain is the *rabA2* knockout group. First the data collected takes glucose release as a percentage total and thus any change in cellulose would merely adjust the total available glucose which could be released. Second and more likely is that although the cellulose digestibility of the treated residue may have changed during the other components of the cell wall have not been impacted in the initial biomass and thus the recalcitrant nature of the wall will not have changed. More interesting is the failure of pectin reduction to cause increased saccharification. This could be explained in a several ways; firstly by using stem it is difficult to assume a completely homogenous material, particularly as there would be a degree of secondary thickening, producing xylem vessels.

This would explain why pectin is a small percentage of the whole material. These questions add further weight to conducting work into the location of the pectin within the sample. Secondly within the cell wall pectin occupies the role of filling material (Caffall and Mohnen 2009). However, there is little data to suggest a direct interaction with the cellulosic material, which forms a mesh like structure in the wall. Thinking in spatial terms it is easier to understand how a reduction in pectin would affect the packing of spaces between this "mesh", however cellulose super structure would remain untouched. Without the alteration to this "mesh" problems of access of enzymes to the cellulosic material would still occur. If pectic polysaccharides do not interact with cellulose, hemicelluloses mesh, then there is also the possibility that pre-treatment is able to fully remove the pectin fraction from the sample material. The differences observed in the *rabA4* mutants reinforce the biochemical data. These data are also consistent with hemicelluloses null *ixr* mutants analysed by Brown *et al.*, 2007. The decrease in recalcitrant in the pre-treated material is likely explained by the removal of the hemicelluloses cross linking with cellulose. This hypothesis is supported by data in the literature by Ibbett and colleagues (2010), showed a correlation between extractable mass and enzyme digestibility of cellulose. Upon analysis of the extractable mass "liquor" it was found that the majority component was hemicellulosic. Unlike the pectin this would directly affect the nature of the "mesh" super structure of the wall. This could have been achieved in two ways. The first of these could be that a reduction in overall hemicelluloses

would cause the cellulose fibrils to be structurally different allowing for increase in cellulose action. However, this hypothesis can be discarded because of the X-ray diffraction data, which showed no changes in fibril length and diameter between the wild-type and the *rabA4* knockout lines, which have been shown to be crucial in enzyme accessibility (Hall *et al.*, 2010). Second, hemicelluloses reduction will allow for easier enzyme access through either making the hemicelluloses more susceptible to removal by pre-treatment, or altering the cross linking in such a way whereby the cellulosic material is more accessible. The most likely explanation is a combination of both cross linkage disruption and enzyme accessibility. This is supported by the untreated digestion data, in which the *rabA4* mutant lines all show increased saccharification compared with wild-type. However, this digestion was much reduced compared to the pre-treated data, which suggests that although the knockouts are more susceptible to digestion naturally, without pre-treatment high of sugar release was not achieved. These data are of most interest in terms of cell wall biology with a 20% digestion of little interest to industry. Thus although the *rabA4* knockout lines are consistent with the hypothesis that *rab* gene knockouts which have impacted on cell wall composition would also cause reduction in recalcitrant, there is still the need for potentially expensive pre-treatment to be overcome, although it is important to note that this may lead to novel strategies which will allow the severity of pre-treatment to be scaled back in the future. Future work in this area would undoubtedly focus on generation of a *rabA4* knockout

in an agronomic crop. However, for this purpose it may not be most useful to focus on grasses, which have a large amount of data showing lignin to be the key component for their saccharification (reviewed by Limayem and Ricke 2012). Whereas in this study using a dicot system it appears that hemicelluloses has been the key component to unlocking of glucose resources. Therefore a more closely related crop, such as oil-seed rape would be a less "risky" next step.

Phenotypic data are an important part of the project brief, as production of a high glucose yielding plants would be meaningless if the agronomic traits were compromised. The lack of a gross phenotype was not surprising; as recent literature has reported reductions in cell wall components can be made without compromising the mechanical properties of the wall (Brown *et al.* 2005; Halpin *et al.* 2007; Cavalier *et al.* 2008) yet is interesting because of the compositional differences observed. While the biochemical data in this study seem to suggest rab genes are not entirely redundant, a degree of redundancy is suggested from the phenotypic data. This is evident from minor "lagging" phenotypes in the leaf analysis, which would suggest that not all of the genes are required for normal plant function. While initially a reduction in any cell wall component producing no phenotype may seem unlikely, data in the literature has shown that a reduction in hemicellulosic material produced no gross phenotypic modification (Cavalier *et al.*, 2008). The literature may suggest that a large portion of hemicellulosic material is actually not required

from a structural stand point. As stated in the introduction, cell wall evolution has always been considered to have had two main evolutionary driving forces, one being mechanical property and the other being defences against pathogens. Neither this study, nor the work of Cavalier et al., 2008 have looked at the possibility of increased pathogen susceptibility. One area in which minor phenotypic changes were observed was leaf emergence. This "lag" was only observed in the rabA1d and rabA1i knockout lines, which were shown to cause a pectin reduction in the stem. Work conducted on pollen tubes shows by immunolocalisation that at the expanding tip, pectin is the dominant cell wall component (Chebli et al, 2012). These observations have been mirrored by biochemical data (Yashoda et al, 2005; Houben et al, 2011) and data shown in this study in fruits. While the pollen tubes and fruits are very specific structures a pectin influx during expansion is not surprising. These data may suggest an increase in expression of these particular Rab proteins during leaf emergence. Unfortunately the microarray data used for selection of the genes in this study did not include expression analysis in leaf tissue. Due to the lack of expression data, the phenotype observed could have two explanations. First that the two knockout lines showing a "lag" are the only RabA1 genes in this study expressed in both expanding leaf and primordial leaf, second if all the genes analysed are expressed that particular Rab genes have a greater influence upon pectin trafficking than others. Taking into account the data in chapter 4, showing an equal reduction in cell wall components the second conclusion would seem unlikely, however cannot be

discounted because the cell wall compositional data were not taken during a metabolically active period. To answer the question posed above, in more detailed expression analysis, using a more quantitative method than microarrays offer would be needed. Added to this real time RT-PCR data the option of immunolocalisation would be of particular interest in attempting to gauge the effect on pectin deposition in real time.

The tomato ripening phenotype reported by Lu *et al.,* in 2001 is well established, however much work can still be done to characterise this unique mutation. Further work conducted by Thanh and published in Lunn *et al,* 2013 showed that *SlRab11a* gene expression was highest in the stages pre-breaker. This implied that the phenotypic observation could be due to effects during fruit development. Surprisingly cell wall compositional data for wild-type tomato fruit was not available in the literature, with studies focusing on ripening. Of particular interest was the compositional analysis of the pectin during development. At 15dpa pectin was found to have the lowest levels of all the cell wall components studied. As development progressed pectin levels increased and pectin became the dominant cell wall polymer (Yashoda *et al,* 2005; Houben *et al,* 2011). With regards to the other components analysed, cellulose levels remained proportionally constant through development and hemicelluloses levels were reduced in the period leading to breaker. There are two possible explanations for these data: firstly, that all the components are being deposited into the wall and throughout time, but the rate of pectin

deposition increases, or secondly, that the turnover of the wall material is being differentially regulated. It is worth noting here that both xyloglucans and pectic polysaccharides are known to be remobilised after deposition (Baluška *et al*, 2002; 2005; Röckel *et al*, 2008; De Caroli *et al*, 2001). Finally it is worth noting that both hypotheses here are not completely separate and thus a mixture of the two could produce these results. The G4 antisense line showed a similar trend to the AC^{++} however the pectin influx observed was significantly reduced. In these lines pectin had not become the dominant component in the cell wall by the breaker stage. This is further evidence for the "lag" effect observed in the leaf emergence data for Arabidopsis. Again these data provide evidence of *SlRab11a* which in analogous to *AtRabA1a*, being involved in pectin trafficking. This alteration in cell wall composition may have resulted in the increase in fruit firmness observed. Finally current theory in regards to pectin trafficking suggests pectin to be made then esterified while in transit between the Golgi and cell wall, these pectin isoforms are then de-esterified by *in muro* pectinesterase activity. Data presented in this study show a similar pattern to the recently published data by de-Freitas *et al*, 2012. Both data sets report a similar decreased pattern but show a dissimilar starting esterification. These differences are likely to be explained by the difference in AIS preparation method. It is also noteworthy that neither this study nor the de-Freitas study report a full 100% esterification. However, this could be due to both studies not starting at 1dpa and thus de-esterification processes occurring, between 1 and 15dpa, or

through the action of a currently unknown pectinesterase. The degree of esterification shown in this study is consistent with the literature values (Koch and Nevins 1989). Several isoforms of pectinesterase have been identified however current literature does not give a role for all these (Tieman *et al*, 1992; Hall *et al*, 1993). These data suggest a role for a PE isoform during fruit development.

8.2 Conclusion

In conclusion the research reported in this thesis has made interesting advancements in the field of trafficking and opened up novel routes by which cell wall alteration and decomposition can occur. With regards to trafficking of vesicles these data show that trafficking may occur through a highly directed manner, not through bulk flow as previously thought. This opens up a novel mechanism of interfering with trafficking on a selective basis, which will be useful for agronomic and research purposes. With regards to bioenergy, the current obstacle to 2nd generation biofuels is the inability to create an efficient cost input to output process. For this field to succeed this is a barrier which must be overcome. In this thesis we have shown that in a model plant we can alter the cell wall composition and decrease the recalcitrant nature of the cell wall without gross impact on the organism. This work is still in its infancy and must now be scaled to an agronomic crop. However, this is an exciting development which has the capacity for real

world application in the future. Finally the ability to change cell wall composition through a directed process of deposition has huge potential in many areas of research and industry. The possibility exists through processes to create a cell wall whose composition is mathematically tailored to the process for which the crop is used, while blue sky and much research is still required their remains tantalising possibilities for future.

9 References

Allen, S. G., Schulman, D., Lichwa, J., Antal, M. J., Laser, M. & Lynd, L. R. (2001) A comparison between hot liquid and steam fractionation or corn fiber. *Industrial and engineering chemistry research*. 40: 2934-2941.

Arioli, T., Peng, L., Betzner, A. S., Burn, J., Wittke, W., Herth, W., Camilleri, C., Höfte, H., Plazinski, J., Birch, R., Cork, A., Glover, J. & Redmond, J., Williamson, E. (1998) Molecular analysis of Cellulose Biosynthsis in *Arabidopsis*.

Baluška, F., Hlavacka, A., Šamaj, J., Palme, K.,Robinson, D. G., Matoh, T., McCurdy, D. W., Menzel, D. & Volkmann D. (2002) F-actin dependant endocytosis of cell wall pectins in meristematic root cells. Insights from brefeldin A-induced compartments. *Plant Physiology*. 130; 422-431.

Baluška, F., Hlavacka, A., Šamaj, J.,. Palme, K.., Robinson, D. G., Matoh, T., McCurdy, D. W., Menzel, D. & Volkmann D. (2002) F-Actin-dependent endocytosis of cell wall pectins in meristematic root cells. Insights from brefeldin A-induced compartments. *Plant Physiology* 130: 422-431.

Baluška, F., Liners, F., Hlavacka, A., Schlicht, H., Van Cutsem, P., McCurdy, D. W. & Menzel, D. (2005) Cell wall pectins and xyloglucans are internalized into

dividing root cells and accumulate within cell plates during cytokinesis. *Protoplasma*. 255: 141-155.

Baluška, F., Liners, F., Hlavacka, A., Schlicht, P., Van Cutsem, P., McCurdy, D. W., Menzel, D. (2005) Cell wall pectins and xyloglucans are internalised into dividing root cells and accumulate within cell plates during cytokinesis. *Protoplasma* 225: 141-155.

Bianco, F. A., Meschini, E. P., Zanetti, M. E. & Aguilar, O. M. (2009) A small GTPase of the Rab family is required for root hair formation and preinfection stages of the common bean-*Rhizobium* symbiotic association. *The Plant Cell* 21: 2797-2810.

Bottanelli, F., Foresti, O., Hanton, S. & Denecke, J. (2011) Vacuolar transport in tobacco leaf epidermis cells involves a single route for soluble cargo and multiple routes for membrane cargo. *The Plant Cell*. 23: 3007-3025.

Boyes, D. C., Zayed, A. M., Ascenzi, R., McCaskill, A. J., Hoffman, N. E., Davis, K. R. & Görlach, J. (2001) Growth stage-based phenotypic analysis of *Arabidopsis*: A model for high throughput function genomics in plants. *The Plant Cell*, 13, 1499-1510.

Brett, C. & Waldron, K. (1996) Physiology and Biochemistry of *Plant Cell Walls*. Topics in Plant Functional Biology. London: Chapman and Hall.

Brett, C. T. (2000) Cellulose microfibrils in plants: biosynthesis deposition and integration into the cell wall. *International Review of Cytology* 199: 161-199.

Brodeur, G., Yau, E., Badal, K., Collier, J., Ramachandran, B. K. & Ramakrishnan, S. (2011) Chemical and physiochemical pre-treatment of lignocellulosic biomass: A review. *Enzyme Research* 2011: Article ID 787532.

Brown, D. E., Wightman, R., Zhang, Z., Gomez, L. D., Atanassov, I., Tryona, T., McQueen-Mason, S. J., Dupree, P. & Turner, S. (2011) *Arabidopsis* genes *irregular xylem* (*irx15*) and *irx15L* encode DUF579-containing proteins that are essential for normal xylan deposition in the secondary cell wall. *The Plant Journal* 66: 401-413.

Brown, D. M., Goubet, F., Wong, V. W., Goodacre., Stephens, E., Dupree, P., & Turner, S. R. (2007) Comparison of five xylan synthesis mutants reveals new insights into the mechanisms of xylan synthesis. *The Plant Journal*. 52, 1154-1168.

Brown, D. M., Zeef, L. A. H., Ellis, J., Goodacre, R. & Turner, S. R. (2005) Identification of novel genes in *Arabidopsis* involved in secondary cell wall

formation using expression profiling and reverse genetics. *The Plant Cell.* 17, 2281-2295.

Bundick, Y., Boniwell, J. M., Fletcher, J. D.,Rray, J. A., Schuch, W., Bird, C. R. & Grierson, D. (1993) Antisense inhibition of pectin esterase gene expression in transgenic tomatoes. *The Plant Journal* 2: 121-129.

Caffall, K. H. & Mohnen, D. (2009) The structure, function and biosynthesis of plant cell wall pectic polysaccharides. *Carbohydrate Research.* 344: 1879-1900.

Camacho, L., Smertenko, A. P., Pérez-Gómez, J., Hussey, P. J. & Moore, I. (2009) *Arabidopsis* Rab-E GTPases exhibit a novel interaction with the a plasma-membrane phosphatidylinositol-4-phosphate 5-kinase. *Journal of Cell Science* 122: 4383-4392.

Campbell, M. M. & Sederoff, R. R. (1996) Variation in lignin content and composition (mechanisms of control and implications for the genetics improvement of plants). *Plant Physiology* 110: 3-13.

Carpita, N. C. & Gibeaut, D. M. (1003) Structural models of primary cell walls in flowering plants: consistency of molecular structure with the physical properties of the walls during growth. *The Plant Journal* 3: 1-30.

Carrasco, J. E., Sáiz, C., Navarro, A., Soriano, P., Sáez, F. & Martinez, J. M. (1994) Effects of dilute acid and steam explosion pre-treatments on the cellulose structure and kinetics of cellulosic fraction hydrolysis by dilute acids in lignocellulosic materials. *Applied Biochemistry and Biotechnology* 45: 23-34.

Cavalier, D. M., Lerouxel, O., Neumetzler, L., Yamauchi, K., Reinecke, A., Freshour, G., Zabotina, O. A., Hahn M. G. Burgert, I., Pauly, M., Raikhel, N. V. & Keegstra, K. (2008) Disrupting two *Arabidopsis thaliana* xylosyltransferase genes results in plants deficient in xyloglucan, a major primary cell wall component. *The Plant Cell* 20: 1519-1537.

Cavalier, D. M., Lerouxel, O., Neumetzler. L., Yamauchi, K., Reinecke, A., Freshour, G., Zabotina, O. A., Hahn, M. G., Burgert, I., Pauly, M., Raikhel, N. V. & Keegstra, K. (2008) Disrupting two *Arabidopsis* thaliana xylosyltransferase genes results in plants deficient in xyloglucan, a major primary cell wall component. *The Plant Cell* 20: 1519-1537.

Černá, M., Barros, A. S., Nunes, A., Rocha, S. M., Delgadillo, I., Čopíková, J. & Coimbra M. A. (2003) Use of FT-IR spectroscopy as a tool for the analysis of polysaccharide food additives. *Carbohydrate polymers* 51: 383-389.

Chakrabortty, A. (2008) Biomass caused food crisis. *Internal World Bank Study.*

Chebli, Y., Kaneda, M., Zerzour, r & Geitmann, A. (2012) The cell wall of the *Arabiopsis thaliana* pollen tube- spatial distribution, recycling and network formation of polysaccharides. *Plant Physiology* 160: 1940-1955.

Chen, I. M., Carpita, N. C., Reiter, W. D., Wilson, R. H., Jefferies, C. & McCann, M. C. (1998) A rapid method to screen for cell wall mutants using discriminant analysis of flourier transform infrared spectra. *The Plant Journal* 16: 385-392.

Chen, L, Carpita, N., Reiter, W. D., Wilson, R. H., Jeffries, C. & McCann, M. C. (1998). A rapid method to screen for cell-wall mutants using discriminant analysis of flourier transform infrared spectra. *The Plant Journal*, 16(3), 385-392.

Chow, C..M., Neto, H., Foucart, C. & Moore I. (2008) Rab-A2 and Rab-A3 GTPases define a *trans*-Golgi endosomal membrane domain in *Arabidopsis* that contributes substantially to the cell plate. *The Plant Cell*, 20; 101-123.

Coimbra M. A., Barros, A., Rutledge, D. N. & Delgadillo, I. (1999) FTIR spectroscopy as a tool for the analysis of olive pulp cell-wall polysaccharide extracts. *Carbohydrate polymers* 317: 145-154.

Cosgrove, D. J. (2001a) Wall structure and wall loosening. A look backwards and forwards. *Plant Physiology* 125: 131-134.

Cosgrove, D. J. (2001b) Enhancement of Accesibility of Cellulose by Expansins. US Patent No. 6326470.

Crowell, E. F., Bischoff, V., Desprez, T., Rolland, A., Stierhof, Y., Schumacher, K., Gonneau, M., Höfte, H. & Vernhettes, S. (2009) Pausing of Golgi bodies on microtubules regulates secretion of cellulose synthase complexes in *Arabidopsis*. *The Plant Cell* 21: 1141-1154.

De Caroli, M., Lenucci, M. S., Di Sansebastiano, G. P., Dalessandro, G., De Lorenzo, G. & Piro, G. (2001) Protein trafficking to the cell wall occurs through mechanisms distinguishable from default sorting in tobacco. *Plant Journal* 65 295-308.

De Caroli, M., Lenucci, M. S., Di Sansebastiano, G.P., Dalessandro, G., De Lorenzo, G. & Piro, G. (2011) Protein trafficking to the cell wall occurs through

mechanisms distinguishable from default sorting in tobacco. *The Plant Journal.* 65: 295-308.

De Freitas, S. T., Hana, A., K., Wu, Q., Park, S. & Mitcham, E., J. (2012) role of pectin methylesterases in cellular calcium distribution and blossom-end rot development in tomato fruit. *The Plant Journal* 71: 824-835.

Desprez, T., Juraniec, M., Crowell, E. F., Jouy, H., Pochylova, Z., Parcy, F., Hofte, H., Gonneau, M. & Verhettes, S. (2007) Organisation of cellulose synthase complexes involved in primary cell wall synthesis in *Arabidopsis thaliana. Proceedings of the National Academy Sciences* 104: 15572-15577.

Dhonukshe, P., Baluška, F., Schlicht, M., Hlavacka, A., Šamaj, J., Friml, J., Theodorus, W. J. & Gadella, J. (2006) Endocytosis of cell surface material mediates cell plate formation during plant cytokinesis. *Developmental Cell.* 10: 137-150.

Dhugga, K. S., Barreiro, R., Whitten, B., Stecca, K., Hazebroek, J., Randhawa, G. S., Dolan, M., Kinney, A. J., Tomes, A., Nichols, S. & Anderson, P. (2004) Guar seed β-mannan synthase is a member of the cellulose synthase super gene family. *Science* 303: 363-366.

Djerbi, S., Lindskog, M., Avrestad, L., Sterky, F. & Teeri, T. (2005) The genome sequence of black cottonwood (*Populus trichocarpa*) reveals 18 conserved cellulose synthase (CesA) genes. *Planta* 221: 1407-1420.

Duchesne, L. C., Larson, D. W. (1989) Cellulose and the evolution of plant life. *Science* 39: 238-241.

Edwards, M., Bulpin, P. V., Dea, I. C. M. & Reid, J. S. G. (1989) Biosynthesis of legume-seed galactromannans in *vitroL* cooperative interactions of a guanosine 5'-diphosphate mannose-linked (1,4)-β-D-mannosyltransferase and a uridine 5'-diphosphate-galactose-linked α-D-galactosyltransferase in particulate enzyme preparations from developing endosperms of fenugreek (*Trigonella foenum-graecum* L.) and guar (*Cyamopsis tetragonoloba* L.) *Planta* 178: 41-51.

Eudes, A., George, A., Mukerjee, P., Kim, J. S., Pollet, B., Beneke, P. I., Yang, F., Mitra, P., Sun, L., Cetinkol, Ö. P., Chabout, S., Mouille, G., Soubigou-Taconnat, L., Balzergue, S., Singh, S., Holmes, B. M., Mukhopadhyay, A., Keasling, J. D., Simmons, B. A., Lapierre, C., Ralph, J. & Loqué, D. (2012) Biosynthesis and incorporation of side-chain-truncated lignin monomers to reduce lignin polymerization and enhance saccharification. *Plant Biotechnology Journal.* 10: 609-620.

European Commission (2013) Directive of the European Parliament and of the council: Amending Directive 98/70/EC relating to the quality of petrol and diesel fuels and amending Directive 2009/28/EC on the promotion of the use of energy from renewable sources.

Faik, A., Prince, N. J., Raikhel, N. V. & Keegstra, K. (2002) An *Arabiopsis* gene encoding an alpha-xylosyltransferase involved in xyloglucan biosynthesis. *Proceedings in the National Academy of Sciences* 99: 7797-7802.

Filisetti-Cozzi, T.M.C.C. & Carpia, N.C., (1991) Measurement of uronic acids without interference from neutral sugars. *Analytical Biochemistry*,197, 157-162.

Fissore, E. N., Rojas, A. M., Gerchenson, L. N. & Williams, P. A. (2012) Butternut and beetroot pectins: characterization and functional properties. *Food Hydrocolliods* 31: 172-182.

Fry, S. C., Smith, R. C., Renwick, K. F., Martin, D. J., Hodge, S. K. & Matthews, K. J. (1992) Xyloglucan endotransglycosylase a new wall-loosening enzyme activity from plants. *Biochemical Journal* 282: 821-828.

Fukushima, R. S., & Hatfield, D. S. (2004) Comparison of the acetyl bromide spectrophotometric method with other analytical lignin methods for

determining lignin concentration in forage samples. *Journal of Agricultural and Food Chemistry.* 52, 3713-3720.

Grant, G. T., Morris, E. R., Ress, D. A., Smith. P. J. C & Thom, D (1973) Biological interactions between polysaccharides and divalent cations: The egg box model. *FEBS letters* 32, 195-198.

Greetham, D., Wimalasena, T., Brindley, S., Ibblet, R. N., Linforth, R. L., Tucker, G. A., Phister, T. G. & Smart, K. A. (2012) Development of a phenotypic characterisation assay to determine ethanologenic yeast strain sensitivity to inhibitors released from lignocellulosic feedstocks. *Biotechnology for Biofuels*

Gutierrez, R., Lindeboom, J. J., Paredez, A. R., Emons, A. M. & Einhardt, D. W. (2009) *Arabidopsis* cortical microtubules position cellulose synthase delivery to the plasma membrane and interact with cellulose synthase trafficking compartments. *Nature Cell Biology.* 11: 797-806.

Haiger, C. H. & Brown, R. M. (1986) Transport of rosettes from the golgi apparatus to the plasma membrane in isolated mesophyll cells of *Zinnia elegans* during differentiation to treachery elements in suspension culture. *Protoplasma* 134: 111-120.

Hall, L. N., Tucker, G. A., Smith, C. J. S., Watson, C. F., G., Seymour, G. B., Bundick, Y., Boniwell, J. D., Flectcher, J. D., Ray, J. A., Schuch, W., Bird, C. R. & Grierson, D. Antisense inhibition of pectin esterase gene expression in transgenic tomatoes. *The Plant Journal* 3: 121-129.

Hall, M., Bansal, P., Lee, J. H., Realff, M. J. & Bommarius, A. S. (2010) Cellulose crystallinity – a key predictor of the enzymatic hydrolysis rate. *Federation of European Bioscience* 227: 1571-1582.

Halpin, C., Daly, P., Maluk, M., Kim, S. Y., McQueen-Mason, S., Gomez, L., Waugh, R. & Stephens, J. (2011) Manipulating lignin for bioenergy applications. *Aspects of Applied Biology* 110: 3-5.

Halpin, C., Thain, S. C., Tilston, E. L., Guiney, E., Lapierre, C. & Hopkins, D. W. (2007) Ecological impacts of trees with modified lignin. *Tree Genetics and Genomics* 3: 101-110.

Harris, P. J., (2005) Diversity in plant cell walls. In: Henry RJ, ed. Plant diversity and evolution: genotypic and phenotypic variation in higher plants. Wallingford, UK: CAB International Publishing, 201-227.

Houben, K., Jolie, R. P., Fraeye, I., Van Loey, A. M. & Hendrickx, M. E. (2011) Comparative study of the cell wall composition of broccoli, carrot and tomato:

sturcutral characterization of the extractable pectins and hemicellulosess. *Carboyhydrate Research* 346: 1105-1111.

I. E. A. (2009) World Energy Outlook. *International Energy Agency.*

I. E. A. (2012) Technology roadmap: Bioenergy for heat and power. *International Energy Agency.*

Ibblet, R. N., Gaddipati, S., Davie, S., Hill, S. & Tucker, G. A. (2010) The mechanism of hydrothermal deconstruction of lignocellulose: New insights from thermal analytical and complementary studies. *Bioresource Technology* 102: 9272-9278.

Jarvis, M. C. Structure and properties of pectin gels in plant cell walls, (1984) *Plant Cell Environment* 7: 153-164.

Jordens, I., Marsman, M., Kuijl, C. & Neefjes, J. (2005) Rab proteins connecting transport and vesicle fusion. *Traffic* 6: 1070-1077.

Kačurákova, M., Capek, M., Sasinková, V., Wellner, N. & Ebringerová, A. (2000). FT-IR study of plant cell wall model compounds: pectic polysaccharides and hemicellulosess. *Carbohydrate Polymers* 43: 195-203.

Kimura, S., Laosinchai, W., Itoh, T., Cux, X., Linder, C. R. & Brown, R. M. Jr. (1999) Immunogold labelling of rosette terminal cellulose-synthesizing complexes in the vascular plant *Vigna angularis. The Plant Cell* 11: 2075-2086.

Kirk, T. K. & Obst, J. R. (1988) Lignin determination. *Methods In Enzymology.* 161: 89-101.

Koch, J. L. & Nevins, D., J. (1989) Tomato fruit cell wall: Use of purified tomato polgalactuonase nd pectinmethylesterase to identify developmental changes in pectins. *Plant Physiology* 91:816-822.

Kosik, O., Bromley. J. R., Busse-Wicher, M., Zhang, Z. & Dupree, P. (2012) Studies of enzymatic cleavage of cellulose using polysaccharide analysis by carbohydrate gel electrophoresis. *Methods in enzymology* 510: 51-67.

Kumar, R. & Wyman, C. E. (2009) Effect of xylanase supplementation of cellulase on digestion of corn stover solids prepared by leading pre-treatment technologies. *Bioresource Technology* 100: 4203-4213.

Lanubile, R., Piro, G. & Dalessandro, G. (1997) Effect of brefeldin A on the synthesis and transport of cell wall polysaccharides and proteins in pea root seedlings. *Journal of experimental biology* 48: 1925-1933.

Lee, K. J. D., Marcus, S. E. & Knox P. J. (2011) Cell Wall Biology: Perspectives from cell wall imaging. *Molecular Plant* 4: 212-219.

Leucci, M. R., Di Sansebastiano, G. P., Gigante, M., Dalessandro, G. & Piro, G. (2007). Secretion marker proteins and cell-wall polysaccharides move through different secretory pathways. *Planta* 225: 1001-1017.

Li, Xu., Ximense, E., Kim, Y., Slininger, M., Meilan, R., Ladisch, M. & Chapple, C. (2010) Lignin monomer composition affects *Arabidopsis* cell wall degradability after liquid hot water pre-treatment. *Biotechnol Biofuels* 3: 27-34.

Liepman, A. H., Wilkerson, C. & Keegstra, K. (2005) Expresion of cellulose synthase-like (*Csl*) genes in insect cells reveals that *CslA* family members encode mannan synthases. *Proceedings in the National Academy of Sciences* 102: 2221-2226.

Limayem, A. & Ricke, S. C. (2012) Lignocellulosic biomass for bioethanol production: Current perspectives and potential issues and future prospects. *Progress in Energy and Combustion Science* 38: 449-467.

Loraine, A. E., Yalovsky, S., Fabry, S. & Gruissem, W. (1996) Tomato Rab1A homologues as molecular tools for studying Rab gernanyl-geranyl transferase in plant cells. *Plant Physiology* 110: 1337-1347.

Lu, C. (2000) The role of a ripening-induced RAB11A GTPase in tomato development. *PhD. Thesis University Of Nottingham.*

Lu, C., Zainal, Z., Tucker, A. G. & Lycett, W. G. (2001) Developmental abnormalities and reduced fruit softening in tomato plants expressing an antisense Rab11 GTPase gene. *The Plant Cell* 13, 1819-1833.

Lunn, D., Thanh, D. P., Tucker, G. A. & Lycett, G. W. (2013) Cell wall composition of tomato fruit changes during development and inhibition of vesicle trafficking is associated with reduced pectin levels and reduced softening. *Plant Physiology and Biochemistry* 66, 91-97.

McCann, M. & Carpita, N. C. (2008) Designing the deconstruction of plant cell walls. *Current Opinion in Plant Biology* 11: 314-320.

McIntosh, S. & Vancov, T. (2010) Enhanced enzyme saccharification of *Sorghum* bicolor straw using dilute alkali pre-treatment. *Bioresource Technology* 101: 6718-6727.

Mohen, D. (2008) Pectin structure and biosynthesis. *Current Opinion in Plant Science* 11: 266-277.

Moore, P. J., Swords, K. M., Lynch, M. A. & Staehelin, L. A. (1991) Spatial organisation of the assembly pathways of glycoproteins and complex polysaccharides in the Golgi apparatus in plants. *Journal of Cell Biology* 114: 589-602.

Nakamura, A., Furuta, H., Maeda, H., Takao, T. & Nagamatsu Y. (2002) Structural studies by stepwise enzymatic degradation of the main backbone of soybean soluble polysaccharides consisting of galacturonan and rhamnogalacturonan.

Nebenführ and Staehelin (2001) Mobile factories: Golgi dynamics in plant cells. *Trends in Plant Science* 4: 160-167.

Nielsen, E., Cheung, A. Y. & Ueda, T. (2008) The Regulatory RAB and ARF GTPases for vesicular trafficking. *Plant Physiology* 147: 1516-1526.

O'Neill, M. A., Ishii, T., Albersheim, P. & Darvill, A. G. (2004) Rhamnogalacturonan II: structure and function of a borate cross-linked cell wall pectic polysaccharide. *Annual Reviews in Plants Biology* 55: 109-139.

O'Neill, M., Albersheim, P. & Darvill, A. (1990) The pecticpolysaccharides of primary cell walls. *Methods in Plant Biochemistry* 2. Edited by Dey P. M., London: Academic Press: 415-441.

Pauly, M. & Keegstra, K. (2008) Cell wall carbohydrates and their modifications as a resource for biofuels. The *Plant Journal* 54: 559-568.

Pauly, M. & Keegstra, M. (2010) Plant cell wall polymers as precursors for biofuels. *Current Opinion in Plant Biology* 13: 1-8.

Pear, J. R., Kawagoe, Y., Schreckengost, W. E., Delmer, D. P. & Stalker, D. M. (1996) Higher plants contain homologs of the bacterial celA genes encoding the catalytic subunit of cellulose synthase. *Proceedings in the National Academy of Sciences* 93: 12637-12642.

Pereira-Leal, J. B. & Seabra, M. C. (2000) The mammalian Rab family of small GTPases: definition of family and subfamily sequence motifs suggests a mechanism for functional specificity in Ras Superfamily. *Journal of Molecular Biology* 301: 1077-1087.

Pereira-Leal, J. B. & Seabra, M. C. (2001) evolution of the Rab family of small GTP-binding proteins. *Journal of Molecular Biology.* 313, 889-901.

Perrin, R. M., DeRocher, A. E., Bar-Peled, M., Zeng,, Norambuena, I., Orellana, A., Raikhel, N. V. & Keegstra, K. (1999) Xyloglucan fucosyltransferase, an enzyme involved in plant cell wall biosynthesis. *Science* 284: 1976-1979.

Pinheiro, H.,, Samalova, M., Geldner, N., Chory, J., Martinez, A & Moore, I. (2009) Genetic evidence that the higher plant Rab-D1 and Rab-D2 GTPases exhibit distinct but opverlapping interactions in the early secretory pathway. *Journal of Cell Science* 122: 3749-3758.

Popper, Z. A. & Fry, S. C. (2004) Primary cell wall composition of pteridophytes and spermatophytes. *New Physiologist* 164: 165-174.

Preuss, M. L., Schmitz, A. J., Thole, J. M., Bonner, H. K. S., Otegui, M. S & Nielsen, E. (2006) a role for the RabA4b effector protein PI-4Kβ1 in polarized expansion of root hair cells in *Arabidopsis thaliana*. *The journal of Cell Biology* 172: 991-998.

Raven, P. H., Ray, F. E., Eichhorn, S. E., (2005) Biology of plants. New W.H. Freeman.

Regent, M., Corti-Monzón, G., Maldonado, A. M., Pinedo, M., Jorrín, J. & De la Canal, L. (2009) *Federation of European Biochemical Societies* 583: 3363-3366.

Rehman, R. U., Stigliano, E., Lycett, G. W., Sticher, L., Sbano, F., Faraco. M., Dalessandro, G. & Sansebastiano G. P. (2008) Tomato Rab11a characterization evidenced a difference between SYP121-dependent and SYP122-dependent exocytosis. *Plant Cell Physiology*. 49: 751-766.

Ridley, B. L., O'Neill, M. A. & Mohen, D. (2001) Pectins: structure, biosynthesis, and oligogalacturonide-related signalling. *Phytochemistry* 57: 929-967.

Röckel, N., Wolf, S., Kost, B., Rausch, T. & Greiner, S. (2008) Elaborate spatial patterning of cell-wall PME and PMEI at the pollen tube tip involves PMEI endocytosis, and reflects the distribution of esterified and de-esterified pectins. *Plant Journal* 53: 133–143.

Rose, J. K. C., Catalá, C., Gonzalez-Carranza, Z. H., Roberts, J. (2003) Cell wall disassembly in: Rose JKC, The plant cell wall. Boca Raton, FL: CRC Press 264-324.

Roussel, M. R. & Lim, C. (1995) Dynamic model of lignin growing in restricted spaces. *Macromolecules* 28: 370-376.

Rutherford, S. & Moore, I. (2002) The *Arabidopsis* Rab GTPase family: another enigma variation. *Current Opinion in Plant Biology*. 5: 518-528.

Sahoo, D., K., Stork, J., DeBolt, Se. & Maiti, I. B. (2013) Manipulating cellulose biosynthesis by expression of mutant *Arabidopsis* proM24::CESA3[ixr1-2] gene in transgenic tabaacco. *Plant Biotechnology journal*. 11: 362-372.

Sakanen, K. V. & Ludwig, C. H. (1971) Lignins: occurrence, formation, structure and function. *Wiley Publishing*, New York.

Sakar, P., Bosneaga, E. & Auer, M. (2009) Plant cell walls through evolution: towards a molecular understanding of their design principles. *Journal of Experimental Botany* 60: 3615-3635.

Sakar, P., Niki, T. & Gladish D. K. (2008) Changes in cellular ultrastructure induced by sudden flooding at 25°C in *Pisum sativum* (Fabaceae) primary roots. *American Journal of Botany* 95: 1-12.

Saxena, I. M., Brown, R. M. & Dandekar, T. (2001) Structure function characterisation of cellulose synthase: relationship to other glycosyltransferases. *Pytochemistry* 57: 1135-1148.

Scheller, H. V. & Ulvskov, P. (2010) Hemicellulosess. *Annual Reviews in Plant Biology.* 61, 263-2289.

Sims, R. E. H., Mabee, W., Saddler, J. N. & Taylor, M. (2010) An overview of second generation biofuel technologies. *Bioresource Technology* 101: 1570-1580.

Stenmark, H. & Olkkonen, V. M. (2001) The Rab GTPase family. *Genome Biology* 2: 3007.1-3007.7.

Sun, R., Lawther, J. M. & Bnaks, W. B. Influence of alkaline pre-treatment on the cell wall components of wheat straw. *Industrial Crops and Products* 4: 127-145.

Suzuki, S., Li, L. G., Sum, Y. H. & Chiang, V. L. (2006) The cellulose synthase gene superfamily and biochemical functions of xylem-specific cellulose synthase-like genes in *Populus trichocarpa*. *Plant Physiology* 142: 1233-1245.

Szumlanski, A. L. & Nielsen, E. (2009) The Rab GTPase RabA4d regulates pollen tube tip growth in *Arabidopsis thaliana*. *The Plant Cell* 21: 526-544.

Szumlanski, L. & Nielsen E. (2009) The Rab GTPase RabA4d regulates pollen tube tip growth in *Arabidopsis thaliana*. *The Plant Cell*. 21: 526-544.

Taherzadeh, M. J., Gustafsson, L., Niklasson, C. & Lidén, G. (2000) Inhibition effects of furfural on aerobic batch cultivation of Saccharomyces cerevisiae growing on ethanol and/or acetic acid. *Journal of Bioscience and Engineering*. 90: 374-380.

Taherzadeh, M. J., Niklasson, C. & Lidén, G. (2000) Conversion of dilute acid hydrolyzates of spruce and birch to ethanol by fed-batch fermentation. *Bioresource Technology*. 69: 59-66.

Taiz, L and Zeiger, E. (2006) Plant physiology 4th edn. Sunderland, MA: Sinaur Associates Inc.

Taylor, N. G. (2008) Cellulose biosynthesis and deposition in higher plants. *New Phytologist* 178: 239-252.

Tieman, D. M., Harriman, R. W., Ramamohan, G. & Handa, A. K. (1992) An antisense pectin methylesterase gene alters pectin chemistry and soluble solids in tomato fruit. *The Plant Cell* 4: 667-679.

Toole, G. A., Selvatico, E., Salt, L. J., Gall, G. L., Colquhoun, I. J., Wellner, N., Shewry, P. R. & Mills, E. N. C. (2013) Effect of dough mixing on wheat endosperm cell walls. *Journal of agricultural and food chemistry*. 61: 2522-2529.

Tryona, T., Liang, H. C., Kotake, T., Tsumuraya, Y., Stephens, E. & Dupree, P. (2012) Structural characterisation of *Arabidopsis* leaf arabinogalactan polysaccharides. *Plant Physiology*. 160: 653-666.

Ulvskov, P., Wium, H., Bruce, D., Jorgensen, B., Qvist, K. B., Skjot, M., Hepworth, D., Borkhardt, B. and Sorensen, S. O. (2005) Biophysical consequences of remodelling the neutral side chains of rhamnogalacturonan I in tubers of transgenic potatoes. *Planta* 220: 609-620.

Vanholme, R., Demedts, B., Morreel, K., Ralph, J. & Boejan, W. (2010) Lignin biosynthesis and structure. *Plant Physiology* 153: 895-905.

Vanzin, G. F., Madson, M., Carpita, N. C., Raikhel, N. V., Keegstra, K. & Reiter, W. D. (2002) The *mur2* mutant of *Arabidopsis thaliana* lacks fucosylated xyloglucan because of lesion in fucosyltransferase AtFUT1. *Proceedings in the National Academy of Sciences* 99: 3340-3345.

Wang, Z. Y. & Ge, Y. (2006) Recent advances in genetic transformation of forage and turf grasses. *In Vitro Cellular & Developmental Biology - Plant.* 42: 1-18.

Yang, B. & Wyman, C. E. (2008) Pre-treatment the key to unlocking low cost cellulosic ethanol. *Biofuels, Bioproducts and Biorefining* 2: 26-40.

Yashoda, H. M., Prabha, T. N. & Tharanathan, R. N. (2005) Mango ripening - Chemical and structural charactisation if pectic and hemicellulosic polysaccharides. *Carboyhydrate Research* 340: 1335-1342.

Yuan, J. S., Tiller, K. H., Al-Ahmad, H., Stewart, N. R. & Stewart Jr., C. N. (2008) Plants to power: bioenergy to fuel the future. *Trends in Plant Science* 13: 421-429.

Zeef LAH, Brown DE. (2006) MEXP-265 Transcription profiles from *Arabidopsis* stem, leaf and hypocotyls tissue. Publically available microarray data: http://www.ebi.ac.uk/arrayexpress/experiments/E-MEXP-265 accessed on 15th December 2009.

Zegzouti, H., Jones, B., Frasse, P., Marty, C., Maitre, B., Latché, A., Pech J-C. & Bouzayen, M. (1999) Ethylene-regulated gene expression in tomato fruit: characterisation of novel ethylene-responsive and ripening related genes isolated by differential display. *The Plant Journal* 18: 589-600.

Zhang, G. E. & Staehelin, L. A. (1992) Function compartmentation of the golgi apparatus of plant cell wall, immunocytochemical analysis of high-pressure freeze frozen and freeze substituted sycamore maple suspension culture cells. *Plant Physiology* 99: 1070-1083.

10 Appendix

Table 10-1 Knockout line database

Rab gene	AGI ID	Insert line	Insert code	NASC ID	Insert direction	Position
RabA1a	At1g06400	Salk	Salk_077747	N653306	Forward	Exon
RabA1c	At5g45750	Salk	Salk_145363	N679206	Reverse	Exon
RabA1d	At4g18800	Salk	Salk_088879	N588879	Forward	Intron
RabA1g	At3g15060	Salk	Salk_091906	N591906	Forward	Exon
RabA1i	At1g28550	Sail	Sail_218_C11	N810111	Reverse	5' UTR
RabA2b	At1g07410	Sail	Sail_124_F05	N806084	Forward	Exon
RabA2d	At5g59150	Salk	Salk_041182	N668131	Forward	Exon
RabA3	At1g01200	Sail	Sail_291_G02	N813511	Reverse	Exon
RabA4a	At5g65270	Salk	Salk_111140	N656868	Reverse	Intron
RabA4b	At4g39990	Salk	Salk_047016	N659845	Forward	Exon
RabA4e	At2g22390	Salk	Salk_120411	N620411	Reverse	Exon

Table 10-2 Primer database for genotyping

Rab gene	Forward primer	FP TM	Reverse primer	RP TM	Gene product	RB+RP product
A1a	GCCTGGAGAGTGGAGAGA	58.2°C	TCTCCTCTGTCTTGTCTTG	54.5°C	1174bp	753bp
A1c	ATTGCCGTAGCCATAACTGTG	57.9°C	CGATTCTTCTGTTGTTTTTGC	54.7°C	1199bp	728bp
A1d	TGCTTTCTCGATTCACCAGGAACG	57°C	TCAACATTGGTAGATTCAAGAGC	52°C	1053bp	809bp
A1i	GTGGTCTTAACCGGAGATTCC	59.8°C	TGTGTTGCACTCAAAATCTGC	55.9°C	1101bp	803bp
A2b	ACTGTGACGGTGCCTAAAGTG	59.8°C	GATTGCTCGATAACGCTCTTG	57.8°C	1191bp	823bp
A2d	TAACCAGAGCTTTACGGGTTG	57.9°C	TCACCTGAAGAGTTCTGGGTGG	59.8°C	989bp	556bp
A3	TGGTGGCCGATTAATCATATG	60°C	TACGACATTACCAAACGCCTC	63°C	1021bp	524bp
A4a	TACTGGCTCGTTATGCTAGAGACG	57°C	TCAACATTGGTTGCGTTAAATGC	52°C	1167bp	694bp
A4b	AAAACGGATCTTCCAAAATGGC	54°C	TCGTTCGATCGGATAAAAACAC	55.9°C	1013bp	560bp
A4e	AGGTGGTTCGGTAAATGGAAG	57.9°C	TCGATTTCAATACTCGAACGC	55.9°C	1182bp	653bp

209

Table 10-3 Primer database for RT-PCR

Rab Gene	Forward primer	Reverse primer	Gene product
A1a	TGCTCTCGGTTCACCAAGAACG	GCTCTAGACGCAACCAATGTTGAA	406
A1c	TGCTTTCACGATTCACGAAGAACG	GCTCTCGAAGCCACCAATGTTGAG	407
A1d	TGCTTTCTCGATTCACCAGGAACG	TGAATCTACCAATGTTGAGAACGC	406
A1i	TGTTATCTCGTTTCACCAGAAATG	GCACTTGAAGCTGTGAATGTTGAT	407
A2b	TTCTCTCGATTCACCAGAAACG	GCTTTAGAAGCGGACTAACATCGAG	407
A2d	TCTTGTCTAGATTCACAAGGAATG	GCTCTTGAAGCCACCAATGTGGAG	407
A3	GATGAGCGGTGAGTCGCCGGAGAA	GTGATCATGCTCGTCGGAAACAAA	415
A4a	TACTGGCTCGTTATGCTAGAGACG	GCATTTAACGCAACCAATGTTGAG	407
A4b	TACTTGCTCGATTCGCTAGAGACG	GCTTTAAACGCAACCAATGTCGAA	407
A4e	TACGAGCTCGGTTCACAAGAGACG	AAATTATGTAGTGATGATCACATT	414
Actin	GTTGTCCTCCTCACTTTCATCAGC	GACAAACTCTCTGGGTTTTACTT	1454

210